THE LIQUID-VAPOUR INTERFACE AND ADHESION IN FLOTATION

by

James A. Finch

A Thesis Submitted to the Faculty of Graduate Studies and Research in Partial Fulfilment of the Requirements for the Degree of Doctor of Philosophy

Department of Mining and Metallurgical Engineering
McGill University
Montreal

July 1973

To my parents for making it all possible, to my wife, Lois, for patient attention to my thoughts and writings and to Selma, the typist, for creating the end product.

Ph.D.

Mining and
Metallurgical
Engineering

James A. Finch

THE LIQUID-VAPOUR INTERFACE AND ADHESION IN FLOTATION

ABSTRACT

The dynamic surface tension of dodecylamine acetate solutions from pH 7 to 13 and concentrations 2.04×10^{-5} to 8.16×10^{-4}M has been determined. A pronounced pH dependence is observed. A maximum surface activity at pH 10 is observed and explained by assuming amine ion:molecule complexes.

The time-dependent surface tension explains the dynamic contact angles observed in the system quartz/alkaline dodecylamine; the variation in surface activity with pH is shown to correspond to the flotation response of oxides.

Wetting and transfer models of flotation have been tested. A decrease in bubble pick-up of magnetite with decreasing surface tension was observed, supporting the wetting model.

The critical surface tension of wetting, γ_c, is introduced and measured for dodecylamine-coated magnetite and quartz, varying the surface tension by controlling the bubble age. The author's opinion on the advantages of introducing γ_c is given.

The rate of adsorption is tentatively concluded as diffusion-controlled.

Ph.D.

Genie Métallurgique
et Minie

James A. Finch

L'ADHERENCE ET L'INTERFACE LIQUIDE-VAPEUR DANS LA FLOTTATION

RESUME

La tension superficielle dynamique de solutions d'acétate de dodécylamine à été déterminée dans le domaine de pH s'étendant de 7 à 13 et pour des molarités variant entre 2.04×10^{-5} et 8.16×10^{-4}. L'activité superficielle, très sensible au pH, présente un maximum pour une valeur du pH égale à 10. Ce maximum peut être expliqué en supposant l'existence de complexes molécule-ion amine.

La tension superficielle dépendente du temps permet d'expliquer les angles de contact dynamiques observés dans le système quartz-dodécylamine alcaline, il est montré que la variation de l'activité superficielle avec le pH correspond à la réponse en flottation des oxydes.

Des modèles de flottation par mouillage et par transfert ont été testés. Une diminution de l'efficacité du collectage de la magnétite par les bulles à été observée lorsque la tension superficielle décroit, étayant le modèle par mouillage.

La notion de tension superficielle critique de mouillage, γ_c, à été introduite, et cette tension à été mesuré pour de la magnétite et du quartz enduits de dodécylamine, la variation de tension superficielle étant obtenue par le controlé de l'âge des bulles. L'auteur donne son opinion sur les avantages que presente l'introduction de γ_c.

Le taux d'adsorption semble être controlé par la diffusion.

ACKNOWLEDGEMENTS

The author wishes to thank the following:

Dr. Smith of the Mining and Metallurgical Engineering Department, McGill University. for continued interest and his critical reading of the manuscript;

Dr. Bendure of the Procter and Gamble research laboratories, Miami Valley, Cincinnati, Ohio, for his encouraging remarks at the outset of this work;

Dr. Hansen of Iowa State University, Ames, Iowa, for help in understanding the adsorption kinetics, notably the derivation of the "asymptotic" solution and the limitations on its use;

Dr. Huh of the Chemistry Department, McGill, for his interest;

The other members of the Mining and Metallurgical Engineering Department, McGill for their criticism.

He is also indebted to:

The Mines Branch, Department of Energy, Mines and Resources, for personal support and for financing the practical costs of this study during 1971-73, and the Quebec Iron and Titanium Corporation for a scholarship from 1971-73.

TABLE OF CONTENTS

LIST OF SYMBOLS

L-V	liquid-vapour
S-V	solid-vapour
S-L	solid-liquid
γ_{LV}	L-V interfacial tension or surface tension, dyne cm^{-1}
γ_C	critical surface tension of wetting, dyne cm^{-1}
γ_o	surface tension of solvent, dyne cm^{-1}
γ_t	dynamic or time-dependent surface tension, dyne cm^{-1}
γ_∞	equilibrium surface tension, dyne cm^{-1}
Γ_{LV}	adsorption density at L-V interface, surface excess or surface concentration, mole cm^{-2}
Γ_t	dynamic surface concentration, mole cm^{-2}
Γ_e	equilibrium surface excess, mole cm^{-2}
Γ_m	monolayer surface concentration, mole cm^{-2}
Γ_{SV}	adsorption density at S-V interface, mole cm^{-2}
Γ_{SL}	adsorption density at S-L interface, mole cm^{-2}
$S_{L/S}$	Harkins spreading coefficient
θ	contact angle, degrees
ϕ	measure of pick-up, degrees
t	time, sec.
Z	a variable, sec.

t_∞	time to reach γ_∞, sec.
C	total amine concentration, M or mole cm^{-3}
C_o	concentration of surface active "ingredient", M or mole cm^{-3}
cmc	critical micelle concentration, M
ppt	precipitation concentration, M
C_z, C_t	dynamic sub-surface concentration, mole cm^{-3}
K'	ratio of C_o/C
K	calibration constant for bubble pressure technique, dyne cm^{-2}
r	radius of bubbling tip, cm
ΔP	excess pressure inside bubble
Δh	ΔP in cm of water
a	Langmuir constant, cm^3 $mole^{-1}$
R	gas constant, 8.31×10^7 erg $mole^{-1}$ $^oK^{-1}$
T	absolute temperature, ^oK
N	Avogadro's number,
M	molecular weight
A_1	area per adsorbed molecule, A^2
σ_1	area occupied by solute molecule or ion at the liquid surface, A^2
σ_2	average partial molecular area of solvent over the range of surface tension γ_o to γ_t, A^2
x_2	mole fraction of solvent in surface
D	diffusion coefficient or diffusivity, cm^2 sec^{-1}

LIST OF FIGURES

LIST OF TABLES

CHAPTER 1
INTRODUCTION

Flotation is a complex science involving the interaction of a liquid-vapour interface (bubble), a solid-liquid interface and the production of a solid-vapour interface. Flotation is most frequently described as the art of rendering the solid surface hydrophobic by the adsorption of low surface energy surfactants (called "collectors") which enables contact with a passing air bubble to occur (1). This places the emphasis on adsorption of collector at the solid-liquid (S-L) interface and the resulting modification of the solid surface. As a consequence, the bulk of flotation research has been directed towards understanding the adsorption of collector at the S-L interface and very little is known of the adsorption of the collector at the liquid-vapour (L-V) interface.

The literature, however, holds quite a substantial quantity of evidence which suggests that the L-V interface can play a direct role in successful bubble-particle attachment. Overbeek et al. (2) in 1954 were the first to indicate that, if the interfaces involved in developing a contact angle are assumed to be at equilibrium, the adsorption density at the solid-vapour interface (Γ_{SV}) is greater than at the solid-liquid interface (Γ_{SL}). Work by Aplan and de Bruyn (3), Somasundaran (4), Lin and Metzer (5) and Finch and Smith (6,7) on typical flotation systems, tends to support this claim;

similar observations have been made in other fields besides conventional flotation systems (8,9,10). This (i.e. $\Gamma_{SV} > \Gamma_{SL}$) is demonstrated by Finch and Smith (6,7) using the technique suggested by Smolders (8). By substituting the Gibbs adsorption isotherm into the differentiated Young equation, the following expression can be derived:

$$d\left(\frac{\gamma_{LV} \cos \theta}{\gamma_{LV}}\right) = \frac{\Gamma_{SV} - \Gamma_{SL}}{\Gamma_{LV}} \qquad \ldots\ldots\ldots\ldots 1.1$$

where γ_{LV} is the interfacial tension liquid-vapour (usually referred to as "surface tension"), Γ_{LV} the adsorption density at the L-V interface and θ is the contact angle. By plotting $\gamma_{LV} \cos \theta$ vs γ_{LV} a measure of $(\Gamma_{SV} - \Gamma_{SL})/\Gamma_{LV}$ can be made from the slope. Figure 1.1 illustrates this plot for various systems. In all cases the following observation holds;

$$d\left(\frac{\gamma_{LV} \cos \theta}{\gamma_{LV}}\right) \geq 0 \qquad \ldots\ldots\ldots\ldots\ldots\ldots 1.1a$$

Hence:

$$\Gamma_{SV} \geq \Gamma_{SL} \qquad \ldots\ldots\ldots\ldots\ldots\ldots 1.1b$$

The solid-vapour (S-V) interface is created upon bubble-particle collision. This factor alone appears to distinguish the S-V interface from the S-L interface indicating that the additional adsorption is a result of the collision.

FIGURE 1.1

$\gamma_{LV} \cos \theta$ vs γ_{LV}

(after Finch and Smith (6,7))

a)
- A Hematite, Dodecylamine, natural pH
- B Magnetite, Dodecylamine, pH 9.5
- C Barytes, Dodecylamine, natural pH

b)
- A Fluorite, Dodecylamine, natural pH
- B Quartz, Dodecylamine, natural pH
- C Hematite, Dehydroabietylamine, natural pH
- D Baddelyite, Dehydroabietylamine, natural pH

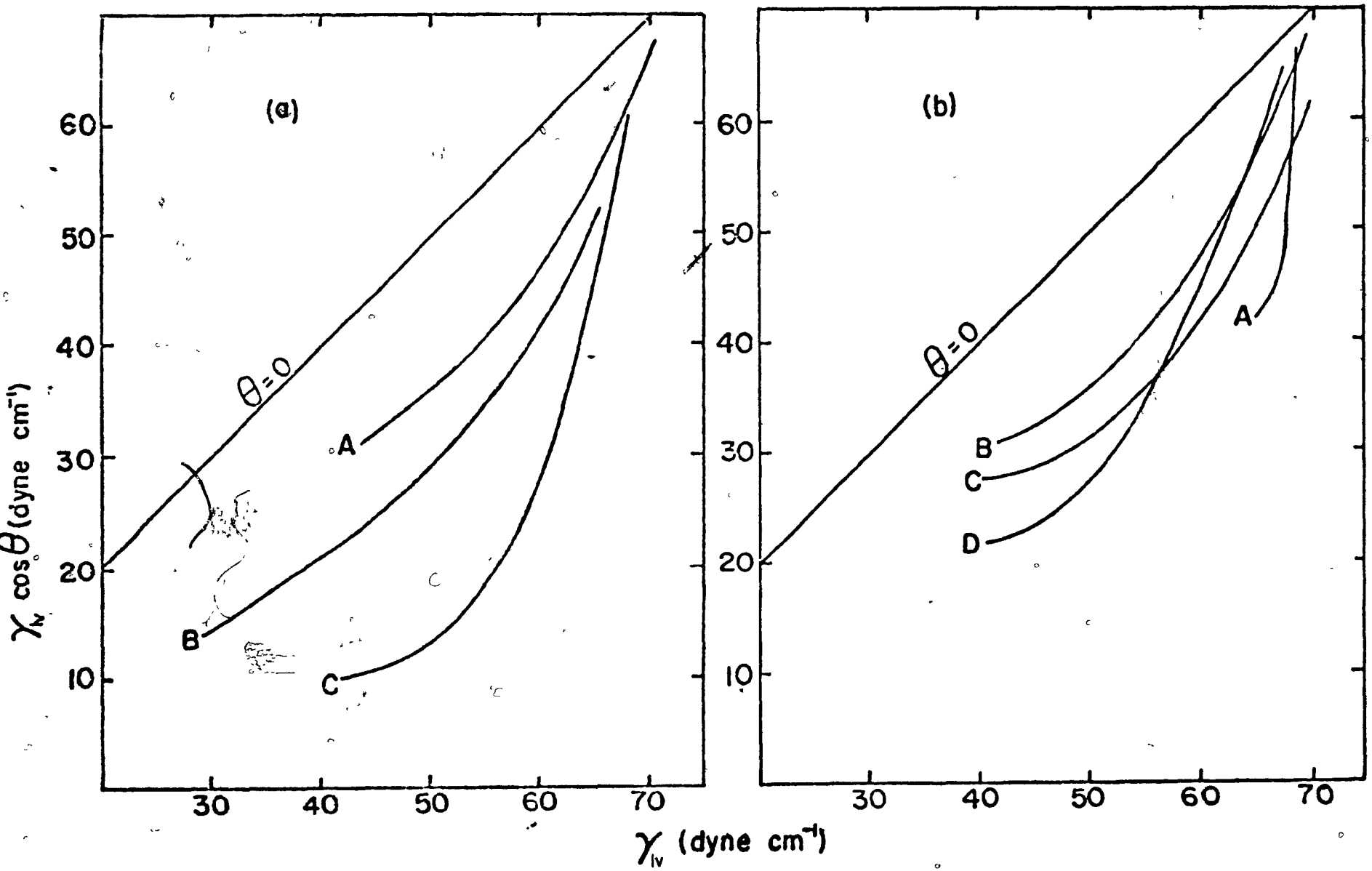
(a)
(b)
θ=0
A
B
C
D
60
50
40
30
20
10
30
40
50
60
70
γ_{lv} (dyne cm^{-1})
γ_{lv} cosθ (dyne cm^{-1})

The Γ_{SV} is, therefore, a function of both Γ_{SL} and Γ_{LV}. Somasundaran (4) and Sandvik and Digrè (11) have noted that Γ_{LV} can be greater than Γ_{SL} in the silica/dodecylamine system making the bubble an important contributor to Γ_{SV}.

The common feature noted in this work is the active role of the bubble in promoting successful bubble-particle adhesion. An important criticism, however, must be that flotation cannot be considered as an equilibrium process. The conclusions gleaned from a study of the contact angle (say as a function of collector concentration) where attaining equilibrium is a pre-requisite (12) cannot, necessarily, be applied to actual flotation. The L-V interface in particular is unlikely to reach equilibrium in all cases since flotation is a process relying on the continual creation of "fresh" bubbles in a collector solution. Adsorption of collector at the L-V interface (or, indeed, any interface) is a function not only of composition but also of time (13).

The influence of bubble "age" upon bubble-particle collision has been observed on a few occasions but has never been fully studied. Wark and co-workers (14,15) have noted that at certain concentrations of collector (e.g. sodium cetylsulphate) fresh bubbles gave good contact with the solid but bubbles allowed to age in the solution prior to contact, frequently failed to make contact at all. Observations of this

nature have also been reported by Smith (16) and Lai and Smith (17) with the system quartz/alkaline dodecylamine solutions, Rao (18) in the system caproic acid/chalcopyrite and Lee (19) working with Aerosol 22 and hematite. Smith and Lai (17) also demonstrated a time-dependent ("dynamic") contact angle. After forming a contact angle of 80° with a fresh bubble on a polished quartz specimen, it was observed that at concentrations of dodecylamine greater than 10^{-4} M and pH $\sim$ 9, the contact angle decreased as a function of time frequently resulting in zero contact angle after 100-200 sec. Wark (14) introduced the idea of bubble "armouring", the bubble building a "wetting" layer with time which eventually prevents attachment. Others have tended to agree with this explanation (15, 19,20). Under conditions where the solid is conditioned so as to be at or near equilibrium with the conditioning solution, any effect of the bubble age is reasonably interpreted as due to changes in the surface properties of the bubble.

Another effect of bubble age upon bubble particle attachment has been noted, namely a change in the induction period* (or time)(15,22). At dilute collector concentrations, a tendency for the induction time to decrease initially with bubble age was found (15,22). This observation will not be

*Induction time is the time required for the bubble and particle to attach after being brought into proximity. It reflects the kinetic stage in the attachment process; the time for thinning to rupture of the liquid film between bubble and particle.

investigated in the present work. Reference throughout to a bubble aging phenomenon will refer to the decrease in bubble-particle attachment with increasing bubble age. Attempting to explain this phenomenon should prove useful in understanding the role the bubble plays in bubble-particle attachment.

Theory

a) Bubble Aging

In order to assess the role played by the bubble in bubble-particle attachment from a study of the bubble aging effect it is first necessary to understand the processes which occur at the bubble surface as the bubble "ages" in a solution of surface-active substance. Figure 2 shows four stages in the "life" of an L-V interface freshly created in a collector solution;

a) the bulk solution with randomly distributed collector molecules/ions, prior to creating the L-V interface (i.e. $t < 0$).

b) a freshly created L-V interface at time $t = 0$ showing that the adsorption density of collector simply corresponds to the bulk concentration as insufficient time has elapsed for significant diffusion and adsorption* of collector species.

---

*The rate controlling step may be either diffusion or an adsorption (energy) barrier at the interface. For present purposes the rate controlling mechanism is of secondary importance and will be considered later (see Chapter Four).

FIGURE 1.2

Aging of an L-V Interface in
a Surfactant Solution

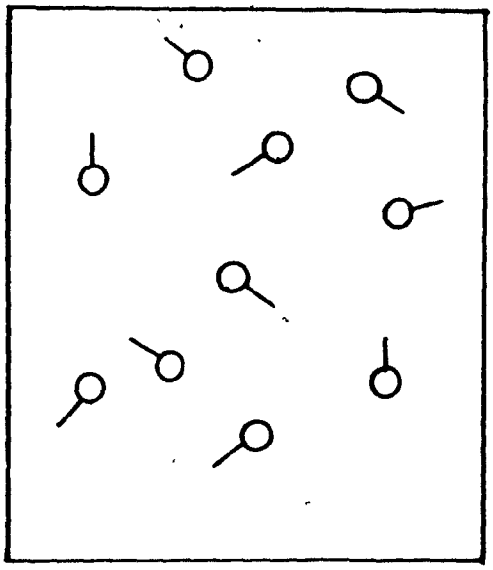

$t < 0$

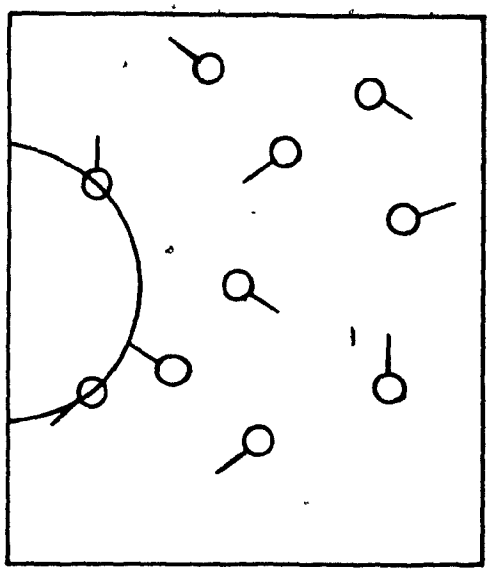

$t = 0$

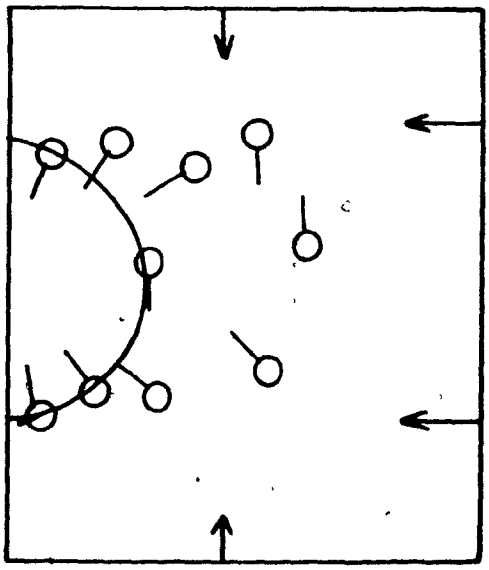

$t = t'$

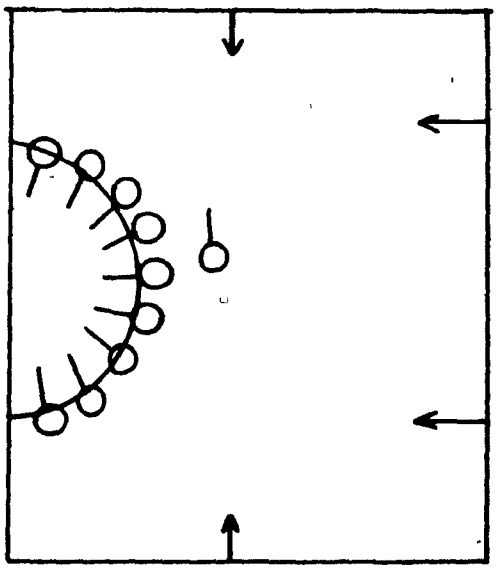

$t = t_\infty$

c) at time $t = t'$, migration of surfactant to the L-V interface causes an increase in adsorption density.

d) at time $t = t_\infty$, the L-V interface can be considered at true equilibrium with the surrounding bulk solution.

These stages result from two known properties; that surfactant species adsorb at the L-V interface since this offers a low energy region (23), and secondly this adsorption will be time-dependent since migration to the interface of the surfactant molecules/ions is not instantaneous. The extent and rate of adsorption will depend on surfactant concentration, surface activity, solute dimensions and the nature of the rate controlling step. It is quite possible for t_∞ to range from 10^{-3} sec to several hours (if not days) depending on the conditions (24).

As the adsorption density of a surface active substance increases, the surface tension, γ_{LV} of the solvent (e.g. water) decreases. The surface tension decreases with time until an equilibrium γ_{LV} is attained, at time t_∞. A reproducible surface tension value which is a non-equilibrium value is called a dynamic surface tension (25). All surfactant solutions will exhibit a dynamic surface tension to a greater or lesser degree. That γ_{LV} is a function of the age of the interface in surfactant solutions has been realized for many years (26,27).

This model of surface aging requires some modification in the turbulent conditions of a flotation cell. Relative motion of the bubble and liquid tends to increase the rate of equilibrium attainment (reduces t_∞) (28). Expansion of the rising bubble tends to retard equilibrium attainment due to creation of fresh surface. Nevertheless the principle of surface aging remains unaltered.

For the present work, other manifestations of this time-dependent adsorption (e.g. dynamic surface potentials (29)) are omitted in favour of the effect of the adsorption itself and the resulting dynamic surface tension.

b) Flotation Models

i) Wetting Models

In order for a particle to be floated, a gas phase must replace a liquid phase at the particle (solid) surface. The condition for this can be described either using the Harkins spreading coefficient (30), $S_{L/S}$, or by introducing the critical surface tension of wetting concept, γ_c, of Zisman (31). These will be referred to as the Harkins and Zisman models for convenience.

i.i) Harkins Model

The spreading coefficient, $S_{L/S}$, is defined as

$$S_{L/S} = \gamma_{SV} - \gamma_{SL} - \gamma_{LV} \quad \text{.....1.2}$$

and is illustrated in Figure 1.3

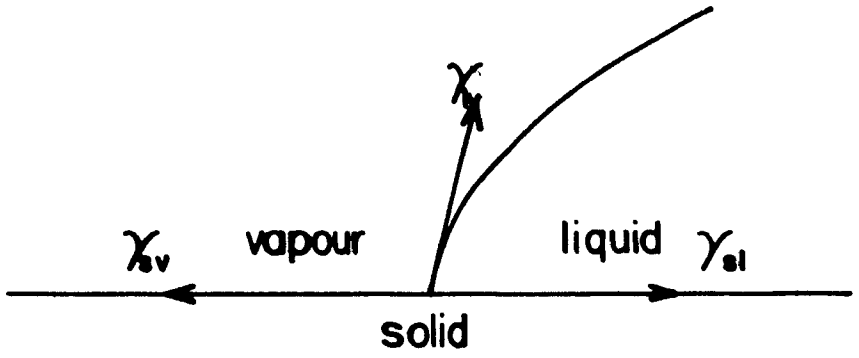

$$S_{L/S} = \gamma_{sv} - \gamma_{sl} - \gamma_{lv}$$

Figure 1.3 The Harkins Model

The terms γ_{SV}, γ_{SL} and γ_{LV} are the interfacial tensions solid-vapour, solid-liquid and liquid-vapour respectively.

When $S_{L/S}$ is greater than zero the liquid spreads to wet the solid; when $S_{L/S}$ is less than zero the liquid retreats. The second condition meets the flotation requirement. Therefore, the condition for successful flotation can be written as:

$$S_{L/S} < 0 \qquad \text{.....1.3}$$

The retreat is never complete, in the sense that vapour completely replaces the liquid at the solid surface but reaches an equilibrium state with the establishment of a contact angle, θ (measured in the liquid). This situation is described by

the Young equation (32):

$$\gamma_{LV} \cos \theta = \gamma_{SV} - \gamma_{SL} \quad \text{.....1.4}$$

i.ii) Zisman Model

This model states that in order to achieve a finite contact angle on a solid, the liquid surface tension, γ_{LV}, must be greater than some critical value, γ_C. Two conditions then become evident:

$$\gamma_{LV} - \gamma_C > 0 \text{ , dewetting} \quad \text{.....1.5a}$$

$$\gamma_{LV} - \gamma_C < 0, \text{ wetting} \quad \text{.....1.5b}$$

Expression 1.5a describes the flotation requirement.

The value of γ_C is characteristic of the solid and the condition of its surface. It can be used as a parameter to describe the "wettability" of the solid. The concept of γ_C was first introduced by Zisman and co-workers (31). Subsequent work has failed to establish the exact nature of γ_C but that it is related to the surface energy of the solid is accepted (9,33-35).

Both models indicate that a high value of γ_{LV} is advantageous in achieving the flotation condition. This is readily seen in the Zisman model. In the Harkins model it is also evident, since, regardless of the values of γ_{SL} and γ_{SV}, the larger is γ_{LV} the more likely is condition 1.3, or the

more negative is $S_{L/S}$ which implies a greater "dewetting power". Furthermore, the models include the possibility that a sufficiently low value of γ_{LV}, on its own, will prevent flotation. Again, this is readily seen in the Zisman model when γ_{LV} is less than γ_C; in the Harkins model the same is true if γ_{LV} is less than $(\gamma_{SV} - \gamma_{SL})$ because $S_{L/S}$ becomes greater than zero. This in no way is meant to imply any equivalence between γ_C and $(\gamma_{SV} - \gamma_{SL})$.

Thus the wetting model predicts that under circumstances where bubble aging produces a substantial decrease in γ_{LV}, bubble-particle attachment will decrease, and will cease entirely if γ_{LV} becomes sufficiently low. A time-dependent decrease in γ_{LV} has been suggested as the cause of the bubble aging phenomenon (15,17,36) but no work has been directed towards testing this possibility.

ii) Transfer Model

Sandvik and Digrè (11) showed that adsorption of dodecylamine (at natural pH) on quartz was greater if the adsorption tests were performed in the presence of gas bubbles than when all gas was rigorously removed. They concluded that some of the collector adsorbed at the bubble surface was transferred to the quartz upon collision. Estimates of the Γ_{LV} indicate that the bubble could be a significant source of

collector (4,11). Such a possibility would mean that correlation between Γ_{SL} measured in the absence of a gas phase (the usual procedure) and flotation recovery may be misleading. The successful flotation at low measured Γ_{SL} (e.g. Gaudin and Bloecher (37)) may be accounted for by this transfer model. The transfer model is considered to play a part (4) in the reduced reagent consumption in flotation reported by Wada (38) using aerosols to inject the collector in with the gas stream. The transfer model is compatable with Γ_{SV} being greater than Γ_{SL} (5,6,39), which was discussed earlier. Each collision creates S-V interface (even if only momentarily, in the sense that permanent bubble-particle attachment does not occur). If Γ_{SV} is greater than Γ_{SL}, it follows that after one or more collisions an increase in total adsorption will be observed. This will be true whether or not successful attachment eventually occurs so long as the measurements are made before substantial desorption of collector.

Recent work by Pope and Sutton (40) failed to verify the transfer model. A decrease in adsorption density of collector (sodium oleate, pH 9) at the solid surface (ferric oxide) after flotation was recorded in comparison with immediately prior to flotation (i.e. after the conditioning stage). This result actually implies that the bubble strips-off adsorbed collector, rather than depositing it. In addition to the work

of Pope and Sutton a particular problem associated with the transfer model is the actual mechanism of transfer. Sandvik and Digrè (11) considered a mechanism based on the retraction procedure for establishing monolayer coverage of smooth surfaces (31,41); Fowkes (42), after observing an increase in the adsorption of surfactant onto wax in the presence of gas bubbles, suggested a surface diffusion model, (diffusion along the L-V boundary to the solid) and Smolders (8) envisaged vibration of the L-V interface about the triple point resulting in deposition of surfactant at the S-V interface. The monolayer penetration model described by Leja et al (43,44), although not directly concerned with collector transfer, is another possibility. Transfer from the rear of a moving bubble, where collector tends to concentrate (45), to the solid (generally held near the rear pole (46)) might also occur. A useful contribution will be made if this transfer model is further tested.

A reasonable supposition, assuming the transfer model to be valid, is that transfer, and hence presumably flotation, will improve as the adsorption density of collector at the bubble available for transfer increases. In the system where the adsorption density at the bubble surface increases with the age of the bubble, an increase in floatability with bubble age should be recorded. A correlation should be found under these circumstances, therefore, between a decreasing surface tension and improved floatability.

With the same type of test both the wetting model and transfer model can be examined. Distinguishing between the models should be facilitated by the completely different predicted effect of increasing bubble age. In terms of a bubble pick-up technique, the wetting model predicts a decrease in pick-up with bubble age, the transfer model an increase.

Choice of System

From the literature, and from previous experience in this laboratory (47), alkaline solutions of dodecylamine acetate were chosen as the collector system. The bubble age phenomenon has been well documented for such a system (16,17) and a time-dependent surface tension was suspected (47). In addition, dodecylamine is amongst the most frequently investigated collectors and has figured prominently in experiments purporting to demonstrate $\Gamma_{SV} > \Gamma_{SL}$ (4-7) and in testing the transfer hypothesis (4,11). Alkaline dodecylamine solutions are of practical importance being employed in the flotation of oxides and silicates (48-50). However, little is known of the properties of dodecylamine solutions above pH 7. For instance, the only dynamic surface tension data available (51, 52) is for pH values less than 7.5. Extending the dynamic surface tension data for dodecylamine into the more important, practical alkaline pH region will be a valuable contribution.

The choice of the solid phase on which to test alternatively the wetting model and the bubble transfer model of flotation would appear, superficially, to be of less importance. Magnetite was chosen for the bulk of the work since its flotation response in alkaline dodecylamine solutions was known (47) for the particular flotation cell in use (53) and the same sample was still available. Quartz as a typical gangue oxide was also considered to be usefully tested. Using magnetite as one of the solid phases facilitates testing two component solid mixtures since the components can be easily separated by a hand magnet.

Aim of Thesis

The general aim is to study the role of the L-V interface in bubble-particle adhesion as related to flotation. The role will be examined in terms of a wetting model (i.e. attachment as a function of γ_{LV}) and a transfer model (i.e. attachment as a function of Γ_{LV}). Both can be examined from a knowledge of the time-dependent surface tension of a collector solution. In particular an explanation of the bubble aging phenomenon is sought.

The first part of the project (Chapter Two) is to verify the suspected pronounced dynamic surface tension of alkaline dodecylamine salt solutions. An attempt to explain the chemistry of these solutions will be made. A correlation between

the dynamic data and some literature results (notably dynamic contact angles) will be included.

In Chapter Three, the dynamic γ_{LV} data will be used to examine the wetting and transfer models of flotation. The author's opinion on the advantages of introducing the γ_C concept will be included.

The adsorption kinetics will be dealt with briefly in Chapter Four. Diffusion-control will be tested from an examination of the short and long-time solutions to the Ward and Tordai equation.

Finally, the importance of the adsorption dynamics in other surfactant systems (both in and out of flotation) will be considered in Chapter Five.

CHAPTER TWO

DYNAMIC SURFACE TENSION OF ALKALINE DODECYLAMINE ACETATE SOLUTIONS

Generally, two phenomena must be distinguished when considering dynamic surface tension (25):

a) the variation of the surface tension at constant surface area, connected with the establishment of surface equilibrium;

b) the deviation of the surface tension from the equilibrium value caused by an enlargement or diminution of the surface area.

The first group can be conveniently described as "surface aging". This refers to the time-dependence of the surface tension after formation of a fresh interface, as previously described. The second group refers to a local decrease (or increase) in surfactant concentration at the surface because of local enlargement (or diminution) of the surface area.

Of importance here is the time-dependence of γ_{LV} associated with freshly-created bubbles. This is of direct concern to the flotation process. The problems associated with the rising bubble (and consequent shape and volume changes) are not of immediate interest to this thesis. Future reference

to a dynamic surface tension will imply the surface aging phenomenon, unless otherwise stated.

Measurement of dynamic surface tension presents its own problems. Several techniques have been employed (28,54-60). Some of the simplest and most frequently employed methods are based on the maximum bubble pressure technique (52,57,60-66). The procedure used by Kuffner (57) (and later by Kragh (63)) is perhaps the most straightforward. This was the one selected.

Theory of Technique

For sufficiently fine capillaries (radius, $r < 0.01$ cm) immersed in the surface of a liquid, the excess pressure ΔP of an escaping bubble is related to the surface tension, γ_{LV} of the liquid by:

$$\gamma_{LV} = \frac{r}{2} \Delta P \qquad \ldots\ldots\ldots\ldots\ldots 2.1^*$$

This is the basis of the maximum bubble pressure technique for determining surface tension (67). In the modification for dynamic surface tension determination, ΔP is measured and the time interval between bubble generation noted. This time interval is frequently taken (57,63,65) to be the age of the bubble thus enabling the surface tension to be calculated for a surface of known age, t. Other workers (66,68) have pointed out that such a determination of surface age ignores expansion of the

*This equation holds so long as the bubbling rate is not high enough to involve air flow resistance in the capillary (69).

bubble. Austin et al (66) introduced a so-called dead-time correction for the rapid expansion of the bubble immediately prior to detachment. For $t > 1$ sec., the correction was less than 3%. Kloubek (68) has extended the work to include a correction for the slow expansion of the bubble prior to the dead-time. Such expansion will of necessity take place. The corrections only become significant for very rapid surface aging; if the aging is less than 10 dyne cm^{-1} sec^{-1} corrections are minor (< 1 dyne cm^{-1}). Work by Bendure (65) has shown that for solutions of surfactant in which the surface tension change is slow (tens of seconds) it is reasonable to take the measured time interval, t, as the age of the surface. Since the change in surface tension with time for alkaline dodecylamine solutions is believed (47) to be of the same order as found by Bendure (65) and others (57,63) the corrections outlined above were not included.

By using a manometer to measure ΔP equation 2.1 reduces to:

$$\gamma_t = K\Delta h \qquad \text{.....2.1a}$$

where K is a calibration constant, Δh is the manometer reading, and the subscript "t" employed to denote a dynamic surface tension is being recorded.

The apparatus, modelled on that described by Kuffner (57) is shown in Figure 2.1. Nitrogen gas was admitted until bubbling occurred. Tap T was closed, thus trapping nitrogen at a certain excess pressure, measured by Δh. As surfactant adsorbs at the bubble surface, γ_t reduces until equation 2.1a is temporarily satisfied, denoted by the generation of a bubble. Consequently Δh drops and adsorption again proceeds to a fresh interface. Longer and longer times will be required to satisfy equation 2.1a as Δh continually reduces. By measuring Δh and the time, t, between bubble generation, γ_t calculated from equation 2.1a, can be determined as a function of t.

The technique requires the adjustment of the level of test solution such that the bubbling tip (r) "just touches" the surface. This can lead to error by introducing a hydrostatic head component into the measured ΔP. However, if r is small, ΔP will be correspondingly large and hence the error resulting from slight variations in the depth of the tip becomes negligible.

Apparatus

Shown diagrammatically in Figure 2.1, the apparatus consisted of a nitrogen tank with a regulator and screw-valve for adjusting to low flow rates; a bubbling unit B with isolating tap T and bubbling tip r ($r < 0.01$ cm) sheathed for

FIGURE 2.1

Dynamic Surface Tension Apparatus

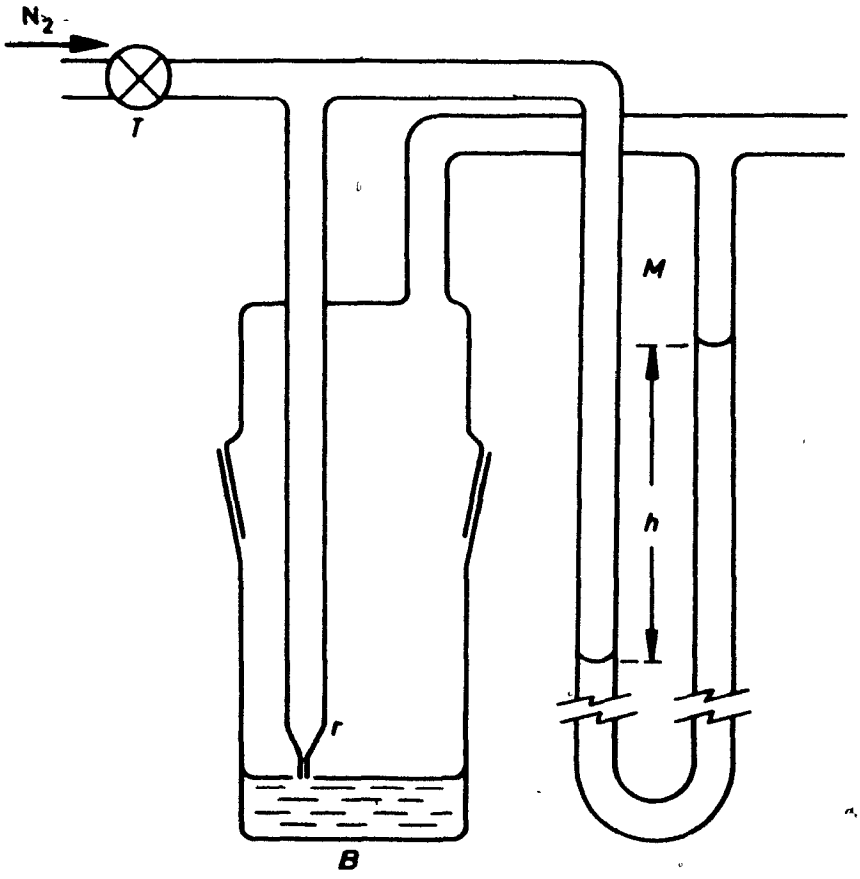
N2
T
M
h
r
B

protection; a water manometer, M, with centimetre scale and two stopwatches to determine the time interval between bubble generation. The centimetre scale was read to $\pm$ 0.25 mm, the stop watches to $\pm$ 0.1 sec. The error in Δh involved in adjusting the tip position was estimated at less than $\pm$ 0.5 mm. Connections were made with Tygon tubing. Later in the work a metal burette tip similar to that employed by Bendure (65) was also used in the determinations. This enabled a reproducible bubbling rate to be achieved, thus extending the measurable bubble age down to $\sim$ 0.5 sec (cf Bendure (65) and Kragh (63)). The experiments were performed in an air conditioned room with a temperature of 23°C $\pm$ 2°C.

Materials

The bulk of the work was performed on dodecylamine acetate. This was prepared (70) from a sample of amine supplied by Aldrich Chemical Co. An initial purification of the amine was carried out by recrystallization at 28°C. The amine acetate was then prepared according to the method of Harwood and Ralston (71). The melting point of the acetate was determined as 68.4 $\pm$ 0.2°C compared with the published value (71) of 68.5-69°C. The phase transition was sharp indicating a high purity product. The dodecylamine hydrochloride tested was purchased from Fisher Scientific as was the sample of free amine.

Both were the highest purity obtainable and were used without further purification.

The pH was adjusted using sodium hydroxide solutions made up from low-carbonate sodium hydroxide pellets ("Baker Analyzed" 98.7% NaOH). Buffering, where required, was by the addition of sufficient standard buffer as supplied by Fisher Scientific. The sodium acetate employed to test the role of the sodium ion and excess acetate ion was certified A.C.S. grade (Fisher Scientific) with < 0.002% stated impurities.

Nitrogen-flushed, double-distilled water (pH 6.5-7.0) was used for the calibration and preparation of solutions. The stock solution of amine (4.08×10^{-3} M) was freshly prepared every two weeks. High purity nitrogen, Canadian Liquid Air Grade L (99.99%) was used to generate the bubbles.

Procedure

The calibration constant for both tips was determined assuming a surface tension of 72.0 dyne cm^{-1}. The calibration equations are:

$$\text{glass tip:} \quad \gamma_t = 4.43\ \Delta h \pm 0.8 \text{ dyne cm}^{-1} \quad \ldots 2.2a$$

$$\text{metal tip:} \quad \gamma_t = 6.44\ \Delta h \pm 1.2 \text{ dyne cm}^{-1} \quad \ldots 2.2b$$

The errors (see Appendix I) represent the maximum error i.e. corresponding to the lowest values of γ_t.

To determine the dynamic surface tension, a sample solution was placed in the bubbling unit, the level adjusted so that the tip "just touched" the liquid surface and bubbling commenced. At a convenient juncture, T was closed and timing initiated from the emergence of the first bubble. By using two stopwatches, each decrement in excess pressure and corresponding time interval, t, was recorded, at least for $t > 10$ sec. A suitable end-point was difficult to adjudge, generally the experiment was carried out until no further bubble generation occurred after a five minute wait. Each test was repeated at least three times to determine the consistency of each individual experiment. Individual experiments were usually repeated once. The pH was recorded prior to and after each individual experiment.

When using the metal burette tip, a modification of the procedure was employed. A reproducible bubble rate was generated and the bubble life-time estimated from a measure of the number of bubbles per second. With the original glass tip, only bubble surges could be obtained, probably because of the conical shape of the tip (57,63).

Standard buffer solutions (pH 10, 9, 8 and 7) were required to achieve pH stability during prolonged tests at concentrations less than $\cdot 10^{-4}$ M and pH less than 10.

All glassware was cleaned using acid-dichromate solution. Final washing of the bubbling unit was with a sample of test solution.

Results

The bulk of the data was determined using dodecylamine acetate (DAA) and the glass tip. Figure 2.2 indicates that essentially the same result is obtained for both tips. Figures 2.3a and b demonstrate that the hydrochloride salt (DAC) gives a dynamic surface tension similar to the acetate.

Figures 2.4a and b illustrate the beneficial effect of pH adjustment using buffer solutions. The attempt to repeat the dynamic surface tension after a 30 min. wait in the absence of buffer failed. This failure was universally accompanied by a pH drift to acid. Buffering prevented the pH drift giving a reproducible dynamic surface tension equivalent to that obtained in the absence of buffer prior to any pronounced pH drift. Figure 2.4c gives further support for equivalence of the data with and without buffer present. At 4.08×10^{-4} M pH 9.85, no appreciable pH drift occurred permitting a more complete comparison of the data.

The reproducibility was generally better than $\pm$ 1 dyne cm^{-1}, corresponding to the expected range. Temperature fluctuations from 21°C to 25°C did not affect the reproducibility within this tolerance. Not all the data points available

FIGURE 2.2

Dynamic Surface Tension of Dodecylamine Acetate Solutions; Comparison of Bubbling Tips

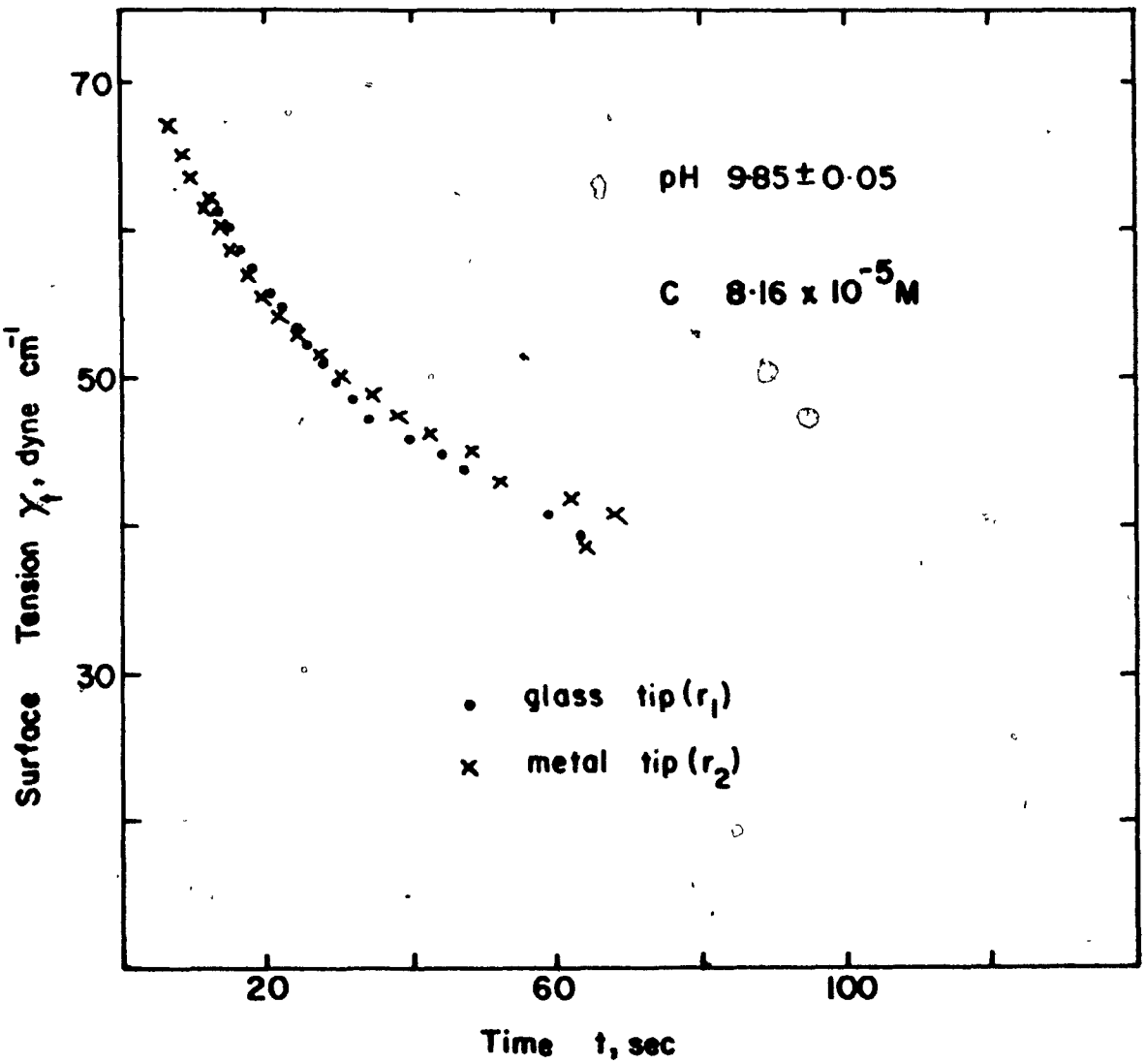
70
50
30
20
60
100
Surface Tension γ_t, dyne cm^{-1}
Time t, sec
pH 9·85 ± 0·05
C 8·16 x 10^{-5} M
glass tip (r_1)
metal tip (r_2)

FIGURE 2.3

Dynamic Surface Tension; Comparison of Dodecylamine Acetate and Hydrochloride Solutions

a) 4.08×10^{-4}M, pH 9.85 ± 0.05

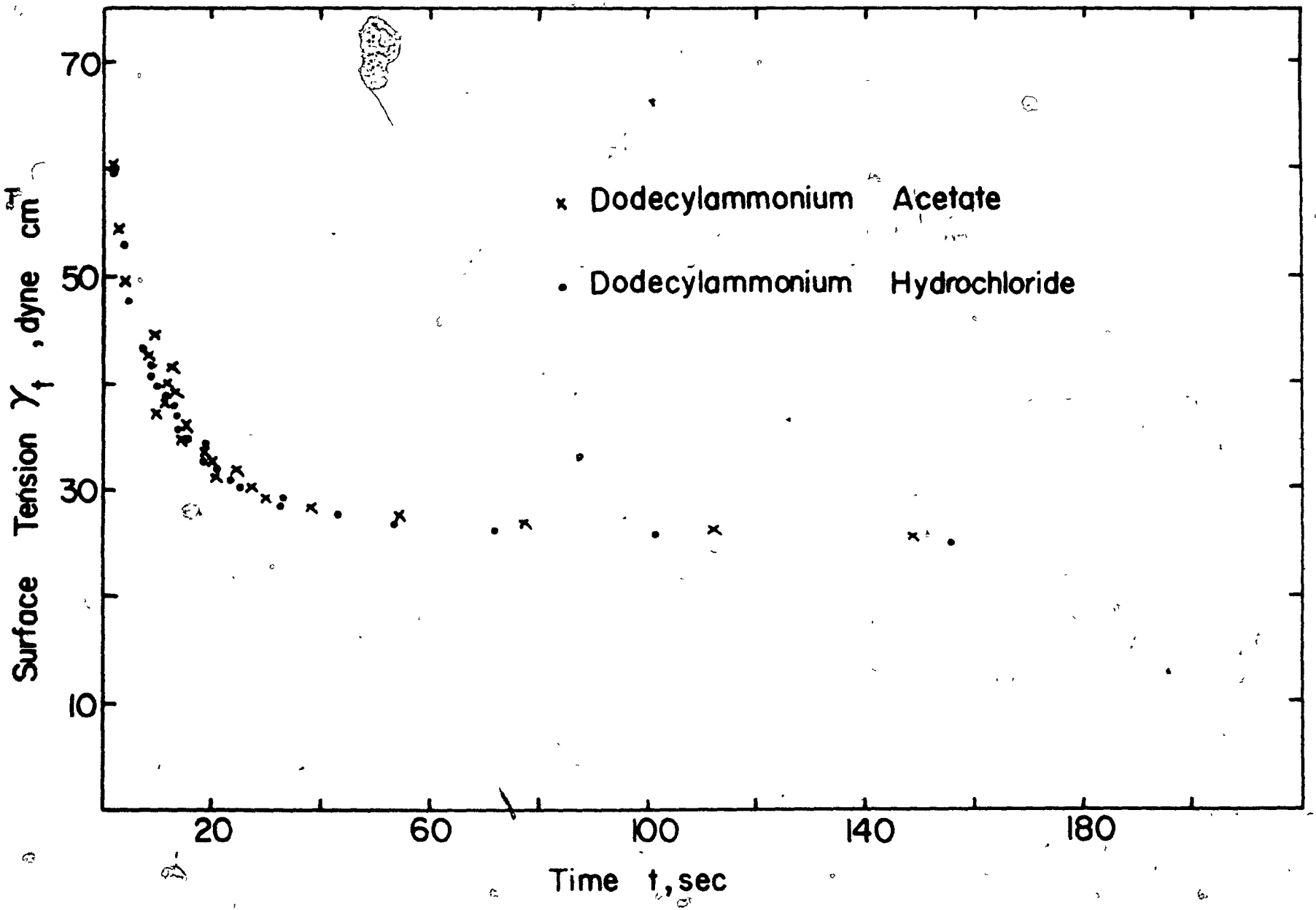
70
50
30
10
Surface Tension γ_t, dyne cm
× Dodecylammonium Acetate
• Dodecylammonium Hydrochloride
20
60
100
140
180
Time t, sec

b) 8.16×10^{-4}M, pH 9.85 ± 0.05

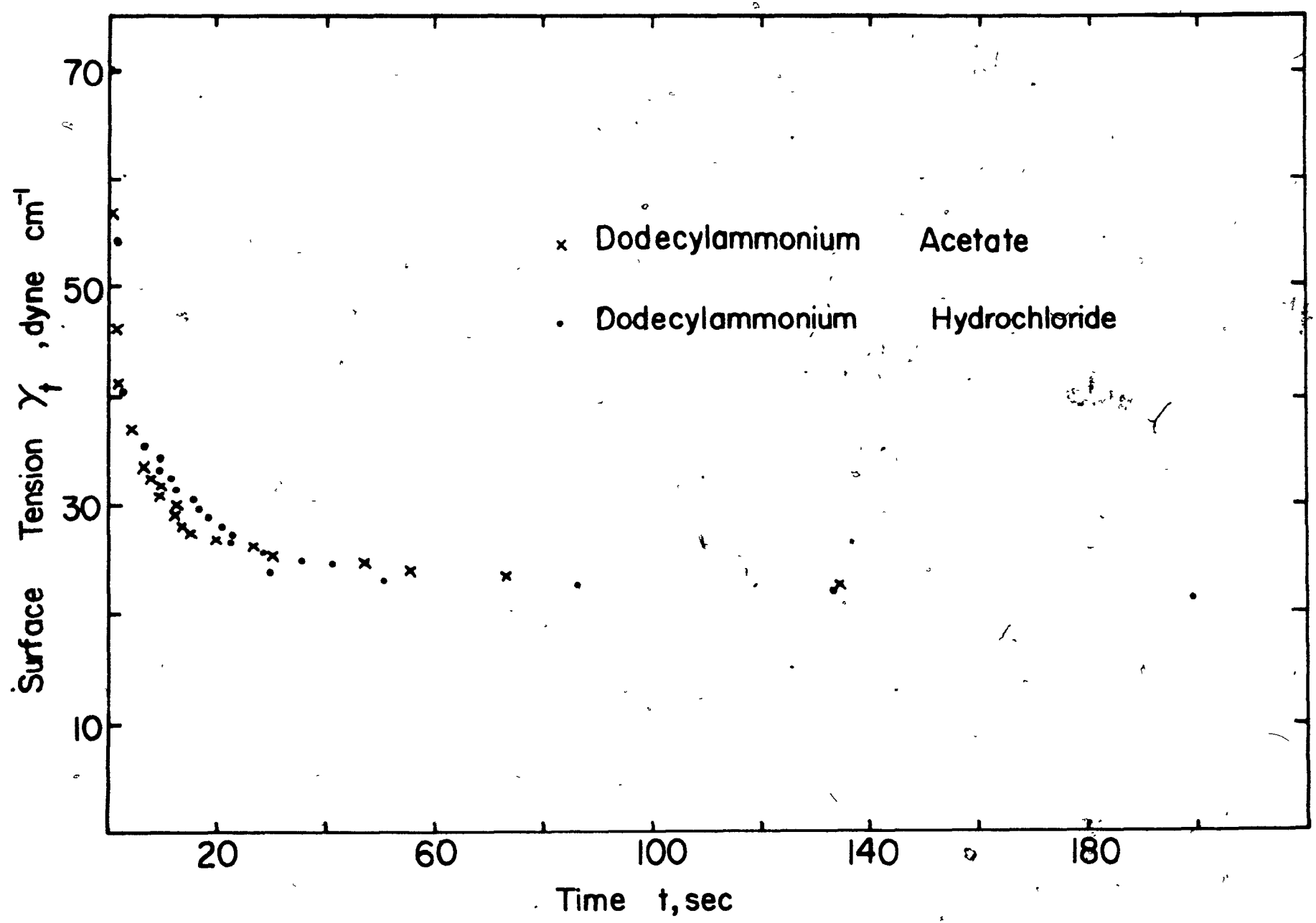
70
50
30
10
Surface Tension γ_t, dyne cm^{-1}
× Dodecylammonium Acetate
• Dodecylammonium Hydrochloride
20
60
100
140
180
Time t, sec

FIGURE 2.4

Dynamic Surface Tension of Dodecylamine Acetate Solutions; Effect of Buffering

a) 4.08×10^{-5}M, pH 9.85

b) 8.16×10^{-5}M, pH 9.5

pH_i initial pH

pH_f final pH

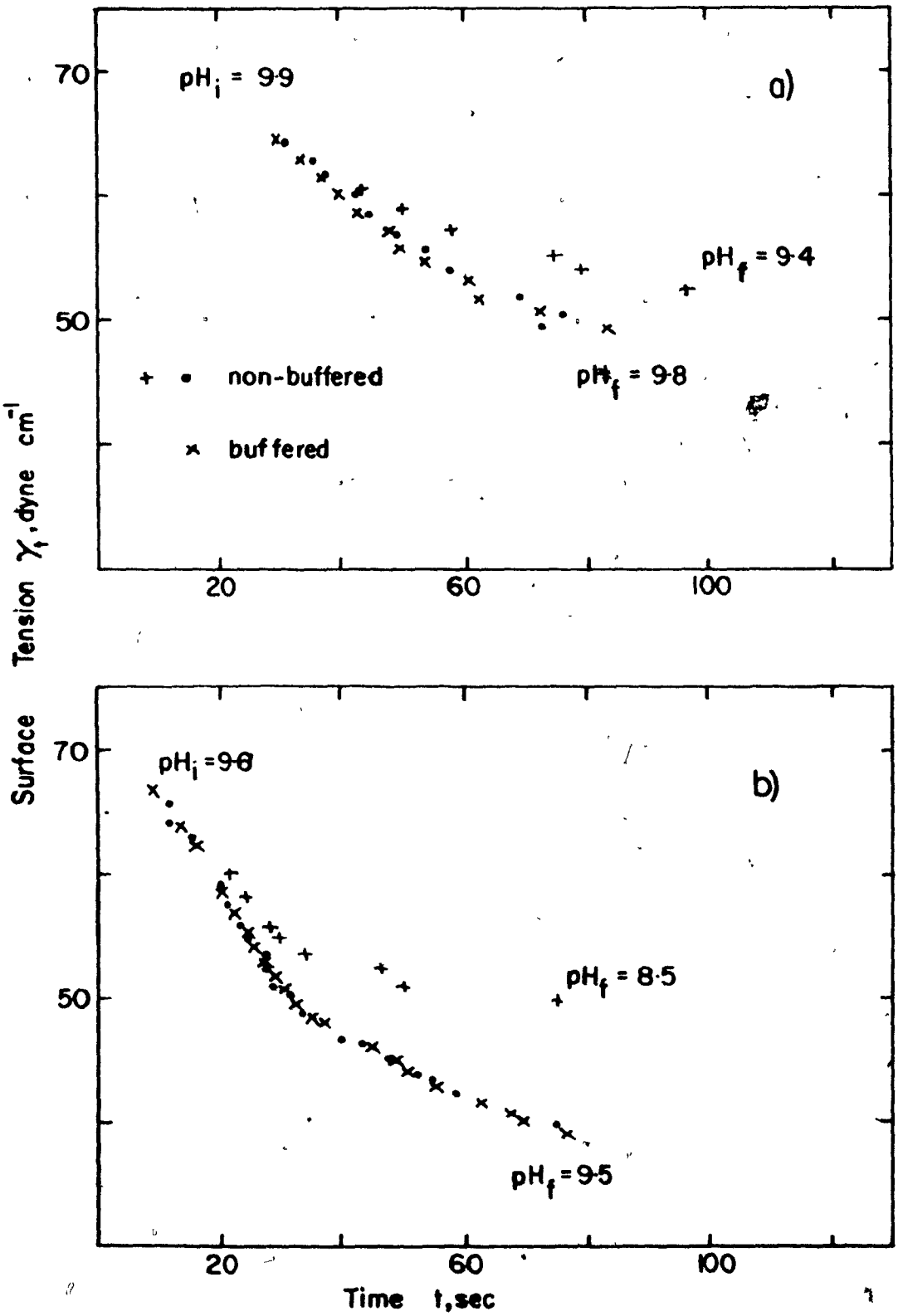
70
50
pH$_i$ = 9·9
a)
pH$_f$ = 9·4
pH$_f$ = 9·8
non-buffered
buffered
20
60
100
Surface Tension γ_t, dyne cm^{-1}
70
50
pH$_i$ = 9·6
b)
pH$_f$ = 8·5
pH$_f$ = 9·5
20
60
100
Time t, sec

c) 4.08×10^{-4}M, pH 9.85

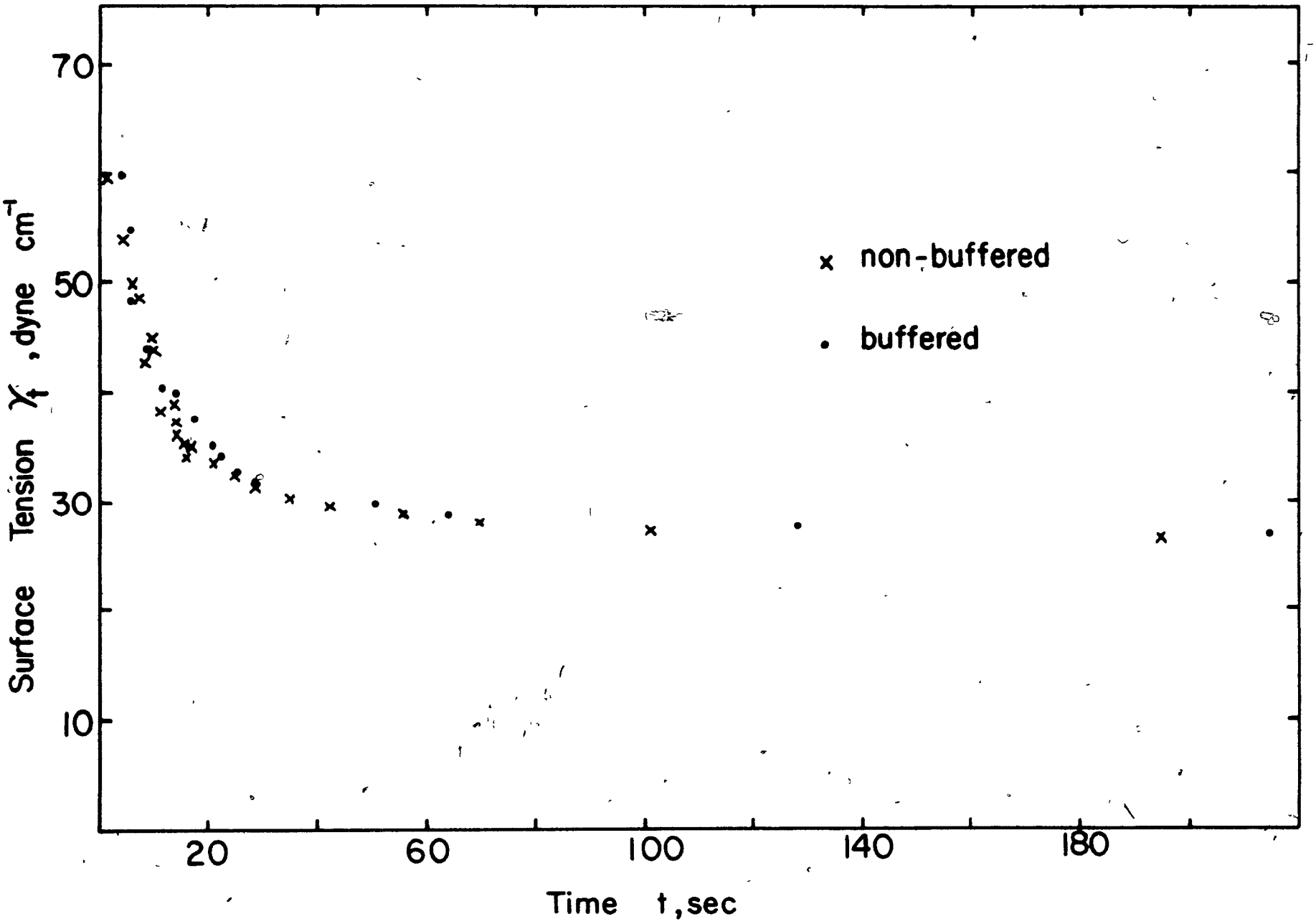
70
50
30
10
Surface Tension γ_t, dyne cm^{-1}
20
60
100
140
180
Time t, sec
× non-buffered
• buffered

are included on the figure to preserve clarity; the data points shown are from individual runs.

Figures 2.5 and 2.6 show the effect of pH on the dynamic surface tension of 4.08×10^{-5}M and 4.08×10^{-4}M solutions of dodecylamine acetate. As the pH is increased, two distinct regions are apparent. Upto pH 10, the time, t_∞, to reach the equilibrium surface tension, γ_∞, increased while γ_∞ decreased. At pH > 10, the trend reversed until at pH 12 the value of γ_∞ was similar to that at pH 7, although surface aging was not so rapid. Table 2.1 summarizes these findings.

TABLE 2.1

Approximate Values of t_∞ and γ_∞ as a Function of pH

$C \times 10^{-5}$ (M)	t_∞ (sec)		γ_∞ (dyne cm^{-1})	
pH	4.08	40.8	4.08	40.8
6.9	< 1	< 1	70	65
7.85	< 1	30	69	46
8.85	90	60	58	31
9.5	140	--	49	--
9.85	>240	100	<40	24
10.85	>240	100	<43	30
11.65	5	80	69	62
12.5	--	5	--	68

FIGURE 2.5

Dynamic Surface Tension of Dodecylamine Acetate Solutions at C = 4.08×10^{-5}M; Effect of pH

A	8.85 ± 0.05
B	9.5 ± 0.1
C	9.85 ± 0.05
D	10.8 ± 0.1
E	11.7 ± 0.01

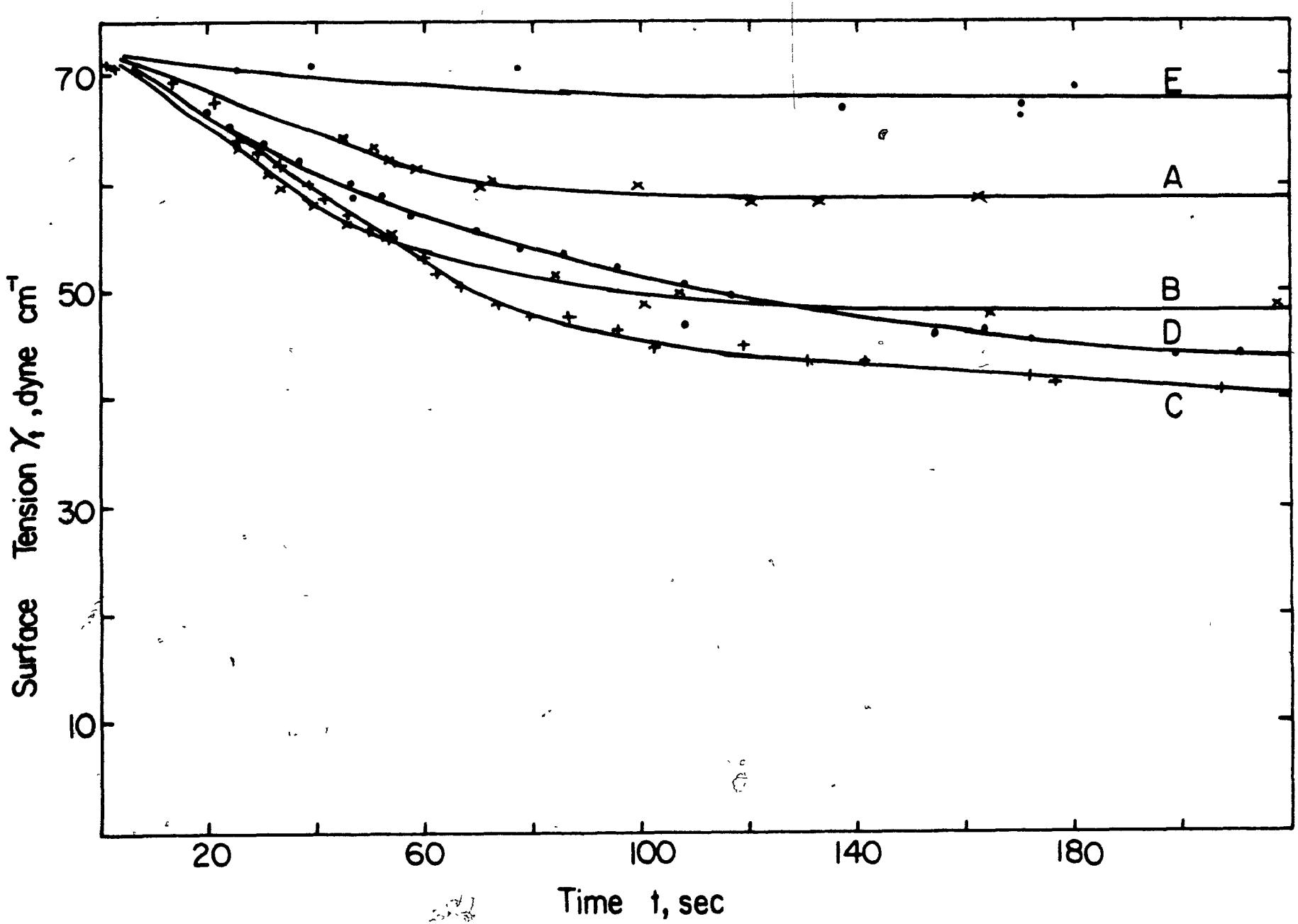
70
50
30
10
Surface Tension γ_t, dyne cm^{-1}
20
60
100
140
180
Time t, sec
E
A
B
D
C

FIGURE 2.6

Dynamic Surface Tension of Dodecylamine Acetate Solutions at C = 4.08×10^{-4}M; Effect of pH

A	7.85 ± 0.05
B	8.85 ± 0.05
C	9.85 ± 0.05
D	10.85 ± 0.05
E	11.6 ± 0.05
F	12.5 ± 0.05

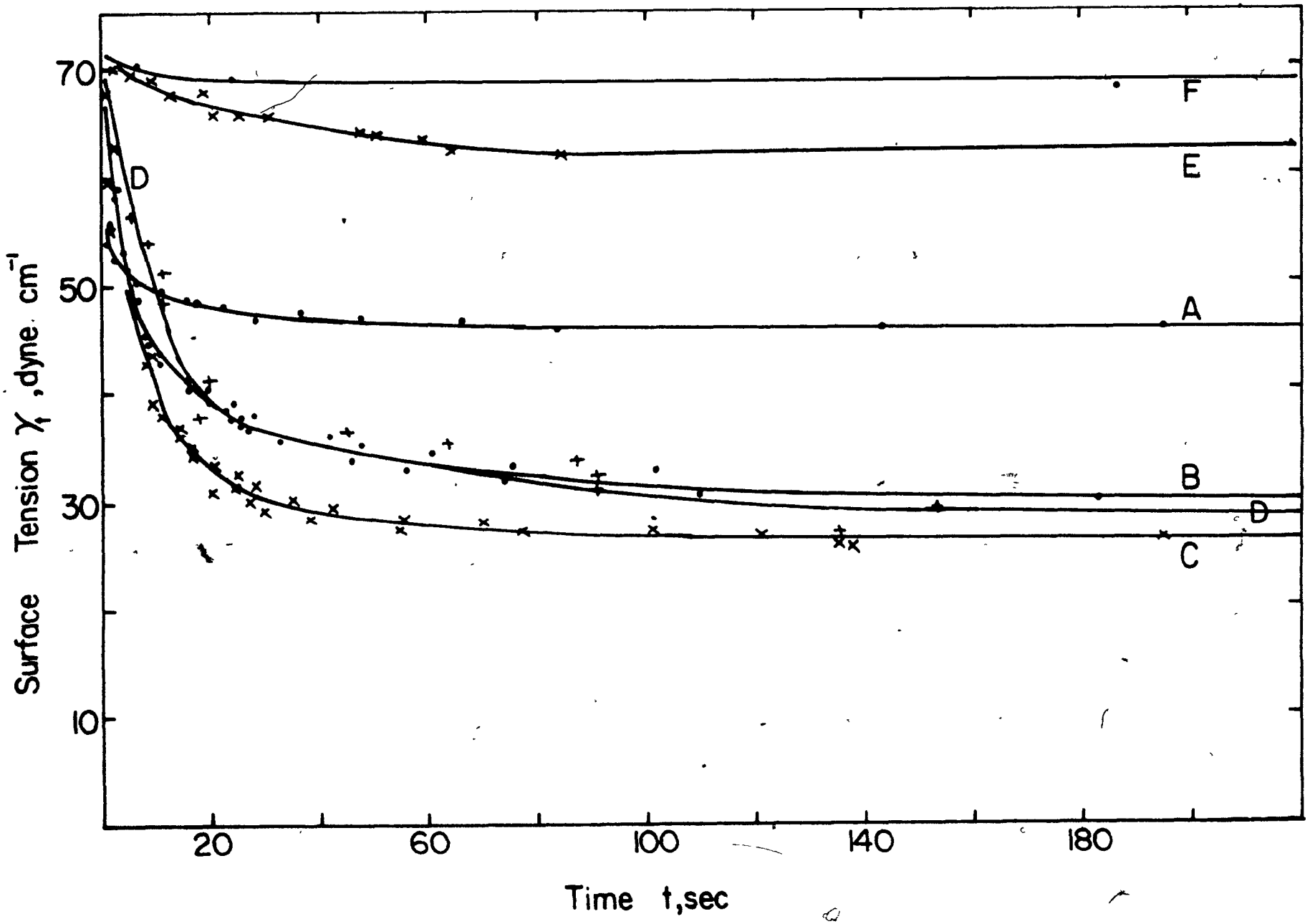
70
50
30
10
Surface Tension γ_t, dyne cm^{-1}
20
60
100
140
180
Time t,sec
F
E
D
A
B
D
C

Figure 2.7 shows that 10^{-2}M sodium acetate has no effect on the dynamic surface tension of 4.08×10^{-4}M solutions at pH 9.85. Thus the Na^+ ion does not contribute materially to the observed effect of changing the pH, supporting the reference to "pH-dependence".

Figures 2.5 and 2.6 indicate that the surface activity of the surfactant increases with pH upto pH 10 and thereafter decreases. One measure of surface activity is $\lim_{C \to 0} (\partial\gamma/\partial C)$, the slope of the surface tension vs. concentration curve at infinite dilution; another measure is to take the values of γ_∞. Neither method can be satisfactorily employed here so γ_{100}, the surface tension of a surface 100 sec. old, as an approximation to γ_∞, was selected. Figure 2.8 shows how γ_{100} varied with pH. Solutions of 8.16×10^{-5}M are also included. In 4.08×10^{-4}M solutions, γ_{100} at pH 10 is some 40 dyne cm^{-1} less than the value at pH 7 and 12, illustrating the pronounced pH-dependence of the surface activity.

A change in the appearance of the 4.08×10^{-4}M solution with pH was noted. At pH 9.85 and 10.85, a surface "scum" was visible which was absent at higher and lower pH.

The dependence of the dynamic surface tension on dodecylamine salt concentration is shown in Figure 2.9 at pH 9.85 ± 0.05 (the pH near that giving the extreme values of t_∞ and γ_∞). As the concentration increased, t_∞ decreased, the surface aged more rapidly and γ_∞ decreased. Table 2.2 illustrates these findings.

FIGURE 2.7

Dynamic Surface Tension of Dodecylamine Acetate Solution at C = 4.08×10^{-4}M, pH 9.85 $\pm$ 0.05 in the Presence of 10^{-2}M Sodium Acetate

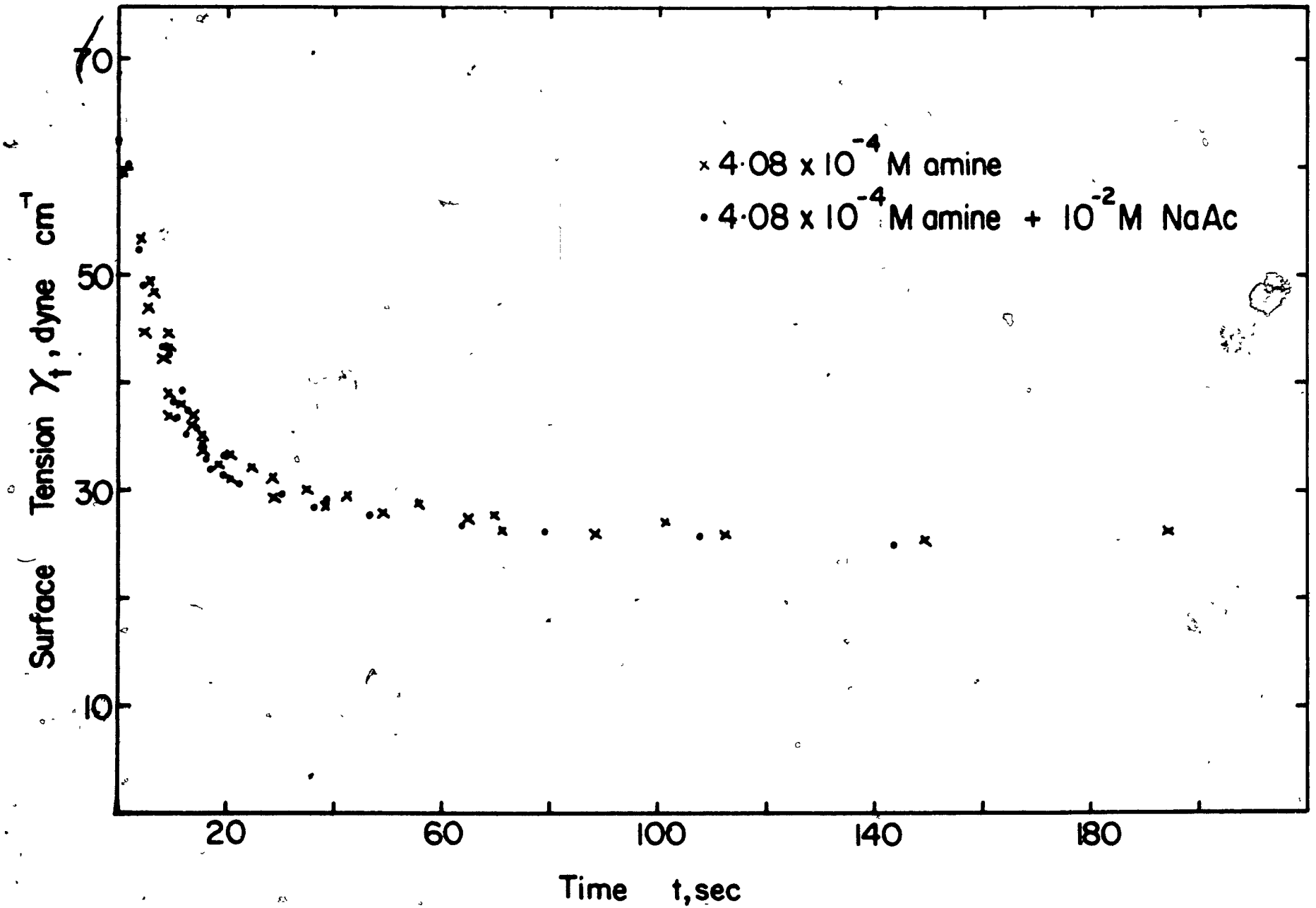
70
50
30
10
20
60
100
140
180
Surface Tension γ_t, dyne cm^{-1}
Time t, sec
× 4·08 x 10^{-4} M amine
• 4·08 x 10^{-4} M amine + 10^{-2} M NaAc

FIGURE 2.8

Surface Activity (Measured by γ_{100}) as a Function of pH

Concentration, C

A 4.08×10^{-5} M

B 8.16×10^{-5} M

C 4.08×10^{-4} M

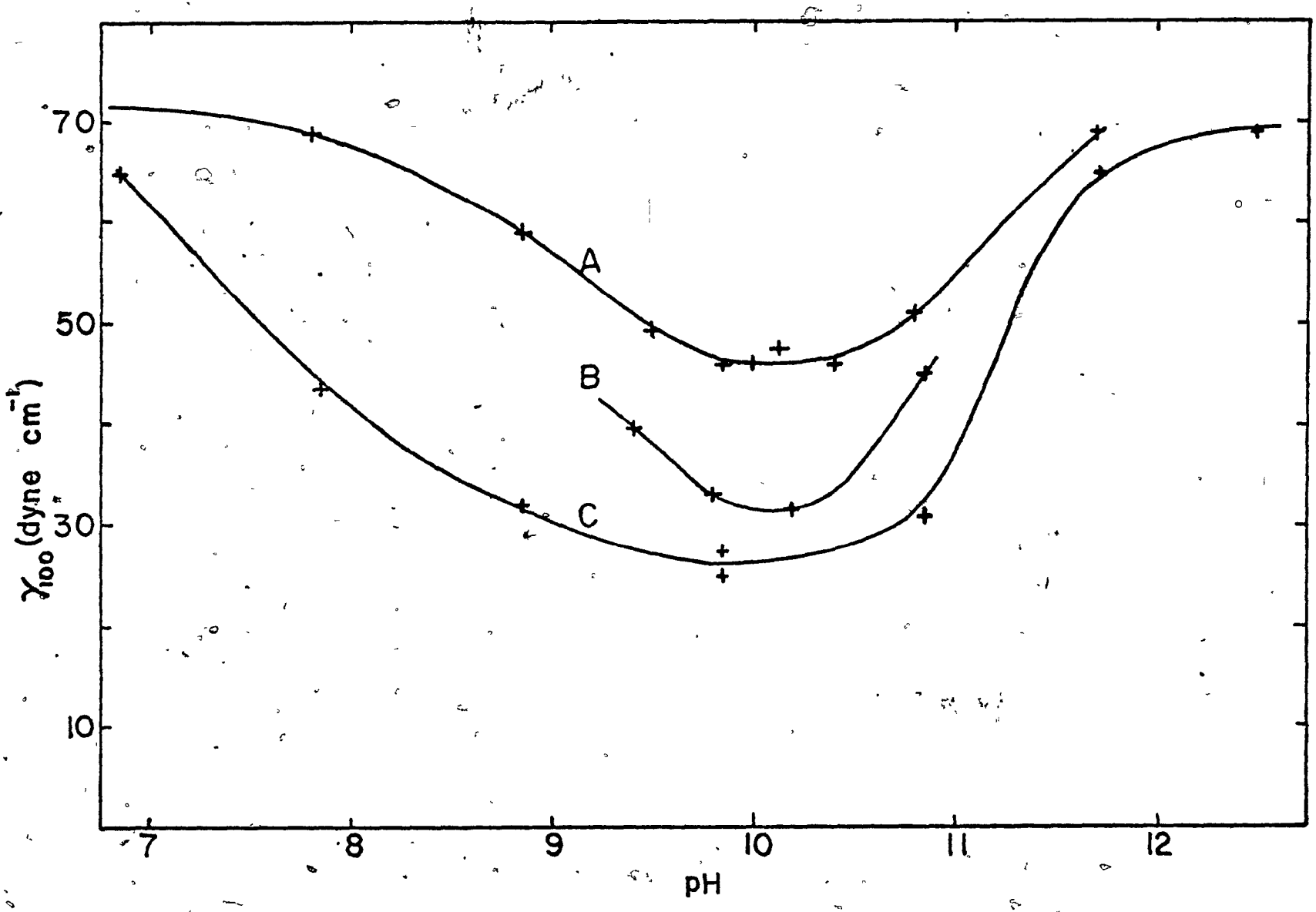
70
50
30
10
A
B
C
7
8
9
10
11
12
pH
γ_{100} (dyne cm^{-1})

FIGURE 2.9

Dynamic Surface Tension of Dodecylamine Acetate Solutions at pH 9.85 ± 0.05; Effect of Total Amine Concentration

Concentration, C

A	2.04×10^{-5} M
B	4.08×10^{-5} M
C	8.16×10^{-5} M
D	2.04×10^{-4} M
E	4.08×10^{-4} M
F	8.16×10^{-4} M

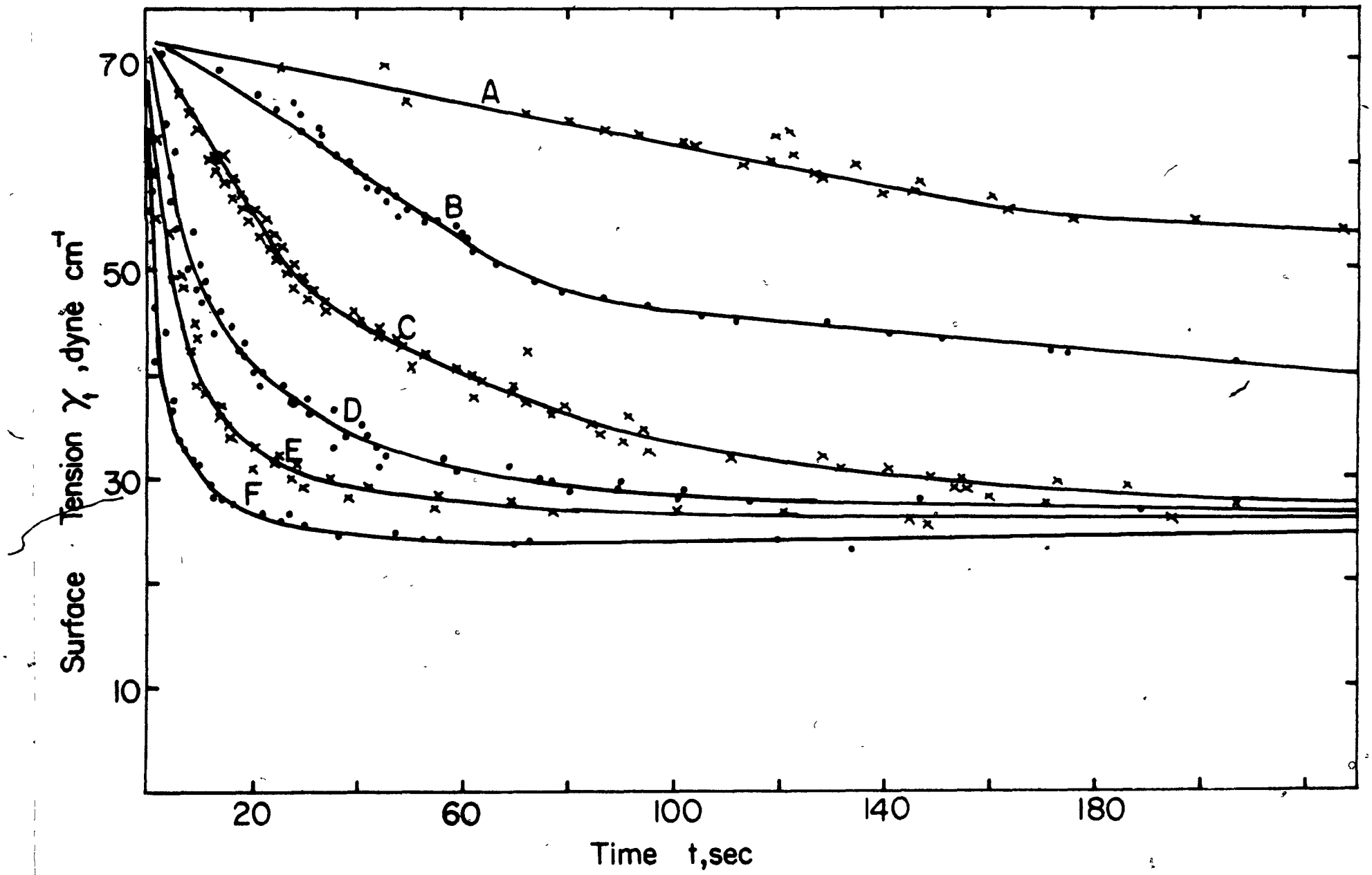
70
50
30
10
A
B
C
D
E
F
Surface Tension γ_t, dyne cm^{-1}
20
60
100
140
180
Time t,sec

TABLE 2.2

Dynamic L-V Properties as a Function of Total Concentration C at pH 9.85 ± 0.05

Concentration $C \times 10^5$(M)	t_∞ (secs)	γ_∞ (dyne cm^{-1})	$\lim_{t \to 0} (\frac{\partial \gamma}{\partial t})$ (dyne $cm^{-1} sec^{-1}$)
2.04	> 240	< 54	- 0.1
4.08	> 240	< 40	- 0.4
8.16	200	28	- 0.8
20.4	120	27	- 2
40.8	100	24	- 5
81.6	100	23	- 10

The general shape of the time-dependent surface tension curves is that of a straight line through 72 dyne cm^{-1} (γ_o, the surface tension of water) followed by a curve assymptotically approaching γ_∞.

Finally, solutions of dodecylamine as the free amine were tested (Figure 2.10). The solutions were visibly saturated (saturation concentration $\sim 2 \times 10^{-5}$ M (72). Natural pH was 10 ± 0.1 and the resulting dynamic surface tension was comparable to 8.16×10^{-4}M at pH 9.85. The same marked decrease in surface activity at elevated pH (pH 11.6) was found.

FIGURE 2.10

Dynamic Surface Tension of Free Dodecylamine Solutions at Saturation; Effect of Increasing pH

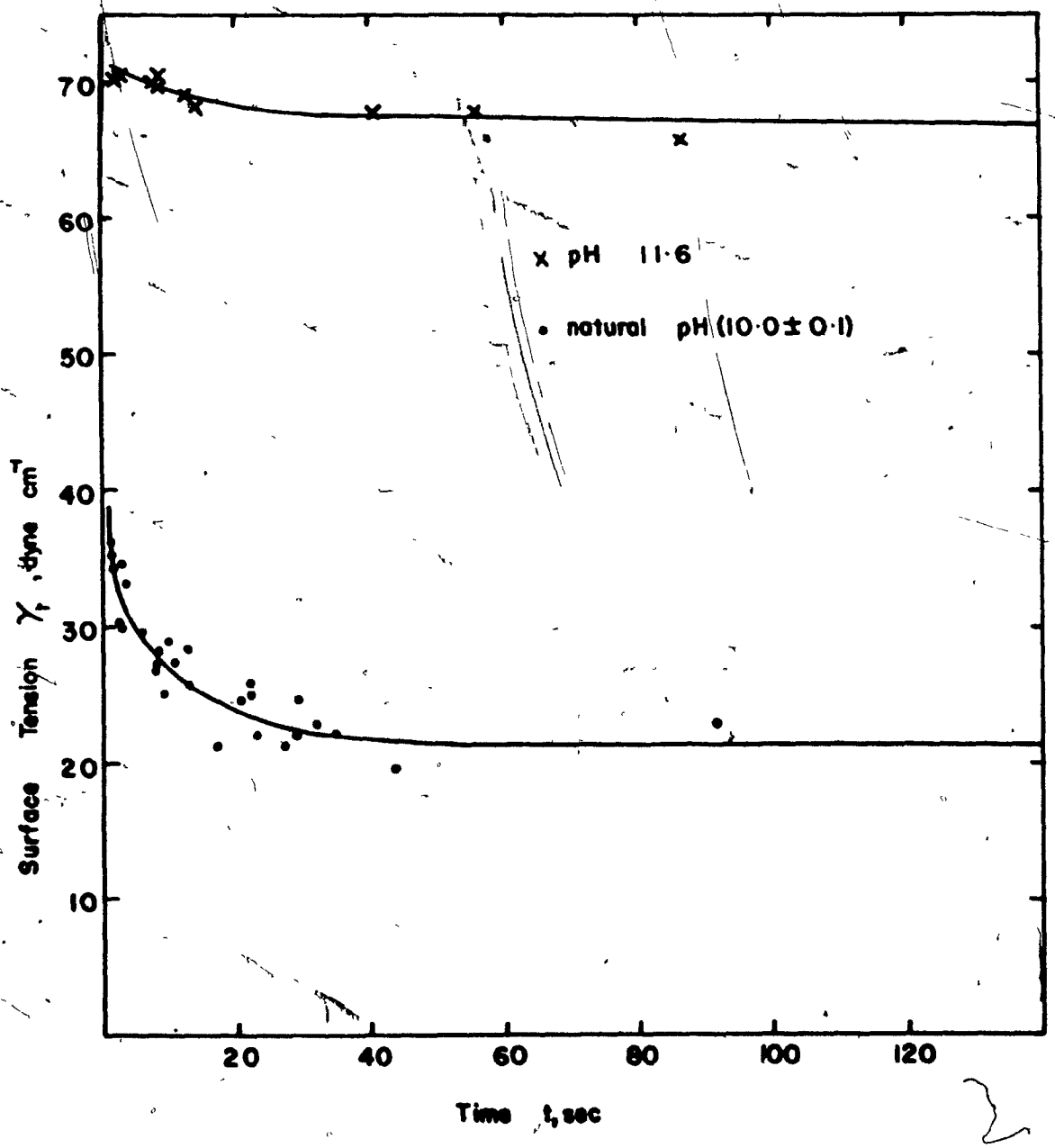
70
60
50
40
30
20
10
x pH 11·6
• natural pH (10·0 ± 0·1)
Surface Tension γ_t, dyne cm^{-1}
20
40
60
80
100
120
Time t, sec

Figure 2.10 shows that the reproducibility was not as good as for amine salt solutions, a spread of as much as 4 dyne cm^{-1} being observed.

Discussion

Clearly the suspected pronounced dynamic surface tension of alkaline dodecylamine salt solutions has been confirmed. The data deserves attention from three standpoints: the adsorption kinetics, solution chemistry and significance to flotation. The latter two will be dealt with here and in Chapter Three, the former will be the subject of Chapter Four.

a) Solution Chemistry

The dynamic surface tension has been shown to depend on amine concentration and more importantly upon solution pH. The passive role of the buffering ions, sodium ions and excess acetate (see Figures 2.4 and 2.7) strongly indicate that the pH-dependence is the result of interaction of amine ions with hydroxyl ions alone.

As the pH is increased hydrolysis of the RNH_3^+ to RNH_2 is promoted:

$$RNH_3^+ + OH^- \rightleftharpoons RNH_2 + H_2O \quad \ldots\ldots 2.3$$

Figure 2.11 shows the concentration of RNH_2 (dissolved), RNH_3^+ (dissolved) and RNH_2 (precipitated) for dodecylamine as a

FIGURE 2.11

Concentration of RNH_3^+, RNH_2 (in solution) and RNH_2 (precipitated) as a Function of pH

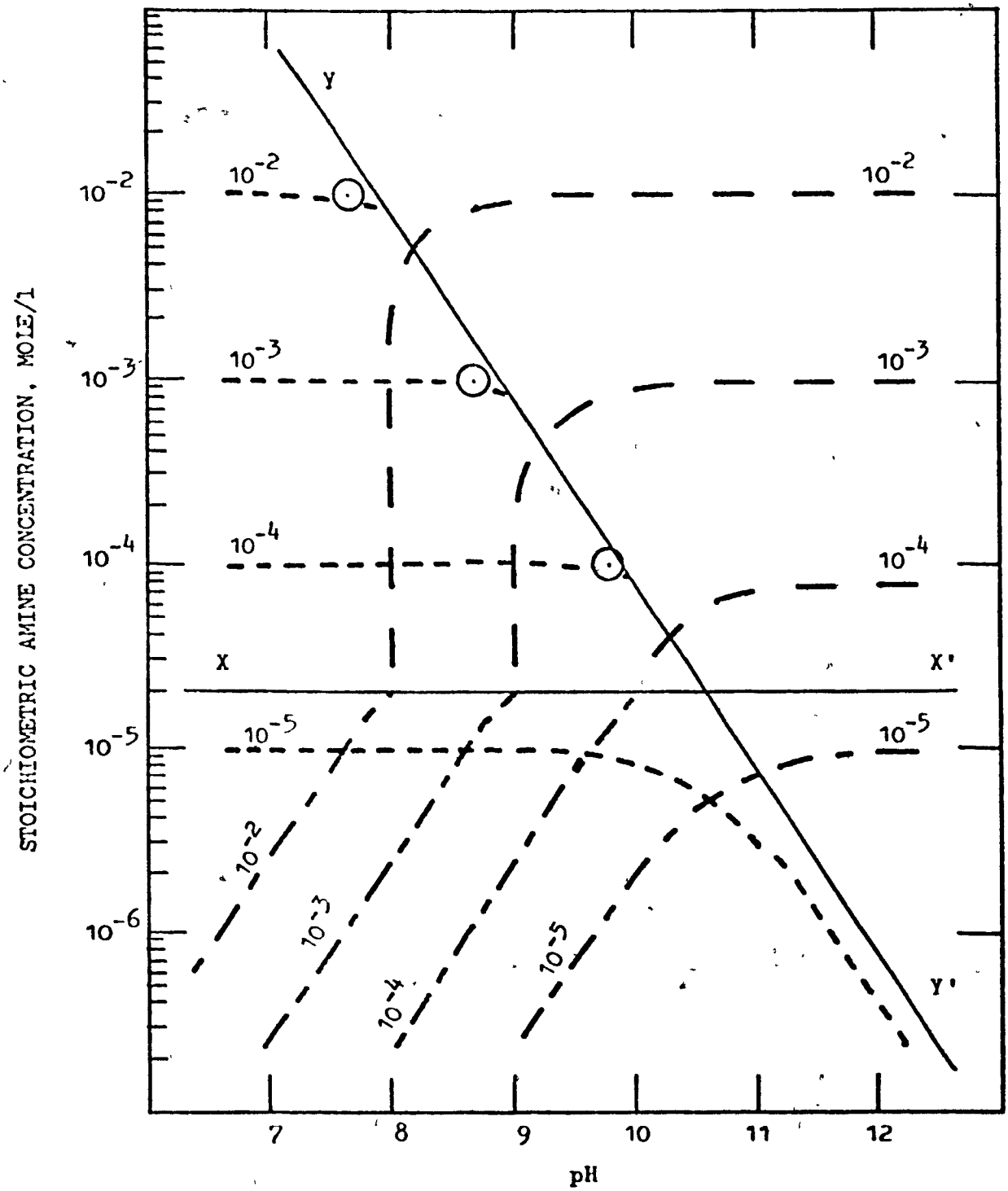

FIGURES ON CURVES INDICATE MOLARITY OF PARENT SOLUTION

X - X' MAXIMUM RNH_2 soln.

Y - Y' SOLUBILITY LIMIT of RNH_3^+

RNH_2 ppt. — RNH_2 soln. — RNH_3^+ - - - EXPERIMENTAL ⊙

function of pH and total amine concentration (72). The surfactant becomes progressively non-ionic with increasing pH. Non-ionic surfactants exhibit strong surface activity at much lower concentrations than do ionic surfactants having an equivalent hydrocarbon chain-length (25). This corresponds to the present observations as the pH is increased to 10. High surface activity at low concentration means that a proportionately greater volume of bulk solution behind the interface is required to supply the equilibrium surface excess requirements. The resulting extended diffusion path will tend to increase t_∞ (25). This corresponds with the present data upto pH 10.

Explaining the pH dependence by the generation of non-ionic RNH_2, upto pH 10, superficially at least is reasonable. It also offers an explanation of the inert nature of added electrolytes; Burcik (73), for instance, shows that the presence of electrolytes did not alter the dynamic surface tension of non-ionic surfactant solutions. The passive role of the electrolyte may not be so significant, however, in the light of recent work (74) which shows that the dynamic surface tension even of ionic surfactant solutions can be independent of the presence of electrolytes. Clearly the decrease in surface activity demonstrated at pH greater than 10 does not fit this model since the concentration of RNH_2 either continues to increase with pH or else is constant at the saturation level. Consider also 4.08×10^{-5}M at pH 8.85 and 4.08×10^{-4}M at pH 7.85. Both

are calculated to yield ~ 7×10^{-7}M RNH_2 in solution. Inspection of Figures 2.5 and 2.6 reveals little similarity in the dynamic surface tension. Figure 2.9 includes data for total amine concentrations of 2.04, 4.08 and 8.16×10^{-4}M at pH 9.85. All three are calculated to be saturated with RNH_2 but a steadily increasing rate of surface tension depression is observed. Simple dependence of the surface activity on the RNH_2 concentration in solution is insufficient.

The change in surface activity with pH can be accommodated by introducing an amine ion-molecule complex reaction:

$$xRNH_3^+ + yRNH_2 \rightleftharpoons x(RNH_3^+).y(RNH_2) \quad .....2.4$$

Two assumptions are required: 1) that the x/y ratio has a more or less fixed value and 2) the complex, $x(RNH_3^+).y(RNH_2)$ is the dominant surface active species. With these assumptions, it follows that at a certain pH (called here the "optimum" pH) the ratio of RNH_3^+ to RNH_2 will be x/y resulting in a maximum production of complex which will be manifested by a minimum in the surface tension (by virtue of assumption 2). The surface tension will increase at pH less than and greater than the optimum pH, reflecting a limiting supply of RNH_2 and RNH_3^+ respectively. The optimum pH, from Figure 2.8, is 10 ± 0.2. A similar argument (75,76) has been proposed to account for the minimum in the surface tension of sodium laurate solutions as a function of pH. In that case, the minimum was associated with the acid-soap which was assumed to be the dominant surface

active species. The correlation shown here between the optimum pH and the natural pH of free dodecylamine solutions may also be in response to complex formation. Modifying species are absent from natural solutions of free dodecylamine so the ratio of RNH_3^+ to RNH_2 can shift to satisfy the equilibrium requirements of the complexing reaction (equation 2.4). This shift will be monitored by the solution pH, according to equation 2.3. Consequently, the natural pH and optimum pH will be the same.

From Figure 2.10, the optimum pH corresponds to an RNH_3^+ to RNH_2 ratio from 2:1 to 5:1 i.e. $2 < x/y < 5$. This result must be treated with caution. Bringing more than two reactants together is unfavourable statistically. This must be coupled with the observation that all the reactants, bar one, bear a mutually repulsive positive charge. Also, this estimate (of x/y) involves the unproven assumption that the complex reaction does not modify the simple hydrolysis reaction (equation 2.3). In addition, it is possible, because of the cationic nature of the complex that hydroxyl ions will be attracted to the interface thus locally raising the pH at the surface. There is some evidence for such an occurrence from work on the surface potential of bubbles in alkaline dodecylamine hydrochloride solutions (77). Replotting Figure 2.8 on the basis of interfacial pH would shift the optimum pH to greater than 10. At pH 10.6, the x/y ratio would be given as 1:1. A possibility which arises from a 1:1 complex is that

the ion-molecule association is the result of hydrogen-bonding, utilizing the lone pair of electrons on the nitrogen atom of RNH_2. A micelle-type structure cannot be ruled out, however, which could accommodate a larger ratio.

Indirect evidence in support of amine ion-molecule complexes is substantial. The pH-dependence of flotation recovery (4,17,78), zeta potential (77,79,80), contact angle (17,81) and adsorption density on solids (17,79,82) in dodecylamine salt solutions has been attributed to ion-molecule interaction. The discrepancy between the theoretical and measured interfacial tension of the water-iso-octane system in the presence of dodecylamine has also been attributed to amine ion-molecule aggregation (83). Complexing between dodecylamine ions and alien molecules, such as alcohol (78,84,85), starches (86-88) and polymers (89,90) has been suggested to explain the properties of the mixed solutions.

Amine ion-molecule complexes appear to be a reasonable explanation of the pH-dependence of the surface activity. The long hydrocarbon chain (+ 24 carbon atoms) will impart strong hydrophobic characteristics to the complex i.e. the surfactant properties will tend to non-ionic. This is in accord with the reasoning given for the increase in t_∞ as the pH is increased to 10. Furthermore, the increase in size of the complex (in comparison with the free ion or molecule) will lead to a decrease in diffusivity, further promoting an increase in t_∞.

However, two problems are raised from the introduction of complexes.

First, if the complexes are formed in the bulk solution, as is assumed in accounting for the increase in t_∞ (i.e. reference to an "increasing diffusion-path" and "decreased diffusivity") then the hydrolysis model (equation 2.3) is oversimplified since no account is taken of the equilibrium requirements of equation 2.4. This possibility did not arise in the previous situations where amine ion-molecule complexes were considered since the complexing was tacitly assumed to occur at the adsorption interface not in the bulk. It is possible, although unlikely, that the present observations reflect the reaction kinetics of ion-molecule association at the L-V interface. Otherwise, the hydrolysis model represents only one of the results of increasing the pH. This may have some bearing on flotation studies where the RNH_3^+/RNH_2 ratio in alkaline amine solutions is calculated assuming the validity of equation 2.3 (16,20,72).

The second problem is concerned with a closer examination of the assumption that the complex is the dominant surface active species. That the complex is more surface active than the RNH_3^+ ion is not questioned, but that the surface activity of the complex is so much greater than that of the free RNH_2 is debated. From Figure 2.8, clearly the surface activity at elevated pH is decreased. The hydrolysis model, even in

conjuncture with the complex reaction, indicates that at pH 12, for example, over 95% of the amine is present in solution as free RNH_2. At total amine concentrations greater than 2×10^{-5}M, a saturated solution of RNH_2 is present. Comparison with non-ionic surfactants of similar chain-length (to RNH_2), decanoic acid (56,57) and decyl alcohol (56,57), suggests that at saturation a large decrease in the surface tension of water should occur. Either the RNH_2 for some reason is a poor surfactant or else at elevated pH the amine is not present as RNH_2. According to Sidgwick (91), aliphatic amines can exist in solution as the hydrate, R_3NHOH. This is the result of hydrogen bonding between the nitrogen of the amine and the oxygen of water;

$$R_3N + H_2O \rightleftharpoons R_3\overset{+}{N}\text{--H-}\overset{-}{O}H \text{ or } R_3\overset{+}{N}\text{--H--}\overset{-}{O}H \quad \ldots 2.5a$$

and presumably;

$$RNH_2 + H_2O \rightleftharpoons RH_2N\text{--H-OH or } RH_2\overset{+}{N}\text{-H--}\overset{-}{O}H \quad \ldots 2.5b$$

Being hydroxylic such hydrates will be readily soluble in water (91) and only poorly surface active. If under the present conditions the equilibrium is well to the right in equation 2.5b then at elevated pH when RNH_2 should be formed, the hydrate will be produced instead. This explanation must be treated as speculative. Fuerstenau et al (92) have postulated that the hydrate is responsible for the flotation of salts observed at pH > 10.

Figure 2.12 shows how the percent of amine present as RNH_3^+, complex and RNH_2 (or $RNH_2.H_2O$) may vary with pH. The assumptions used in the calculations for Figure 2.12 are: 1) no precipitation occurs (i.e. concentrations less than 2×10^{-5}M); 2) the complex is 3:1 ion:molecule; 3) the maximum possible complex formation is achieved (i.e. complex, RNH_3^+ and RNH_2 do not coexist in solution); 4) the ionization constant for dodecylamine determined by Ralston, Hoerr and Hoffman (93) is valid for calculation of percent complex formation. Details are given in Appendix I.

The surface activity of amines is believed to increase with increasing solution pH (20). The present work has shown this to be only partly true, since at pH > 10 the surface activity decreases. Nowhere in the literature (excluding the the author's own publications) has the pronounced surface aging at alkaline pH been demonstrated. This raises the need to investigate more fully the solution chemistry at alkaline pH. The simple hydrolysis model cannot furnish sufficient information. The possible formation of complexes and the nature of the amine at pH > 10 (i.e. RNH_2 vs $RNH_2.H_2O$) should be considered. Such knowledge (of the solution chemistry) should aid the understanding of the flotation response observed in alkaline dodecylamine salt solutions.

FIGURE 2.12

Possible Variation in Percent Amine Present as RNH_3^+, $3RNH_3^{3+}.RNH_2$ and RNH_2 (or $RNH_2.H_2O$)

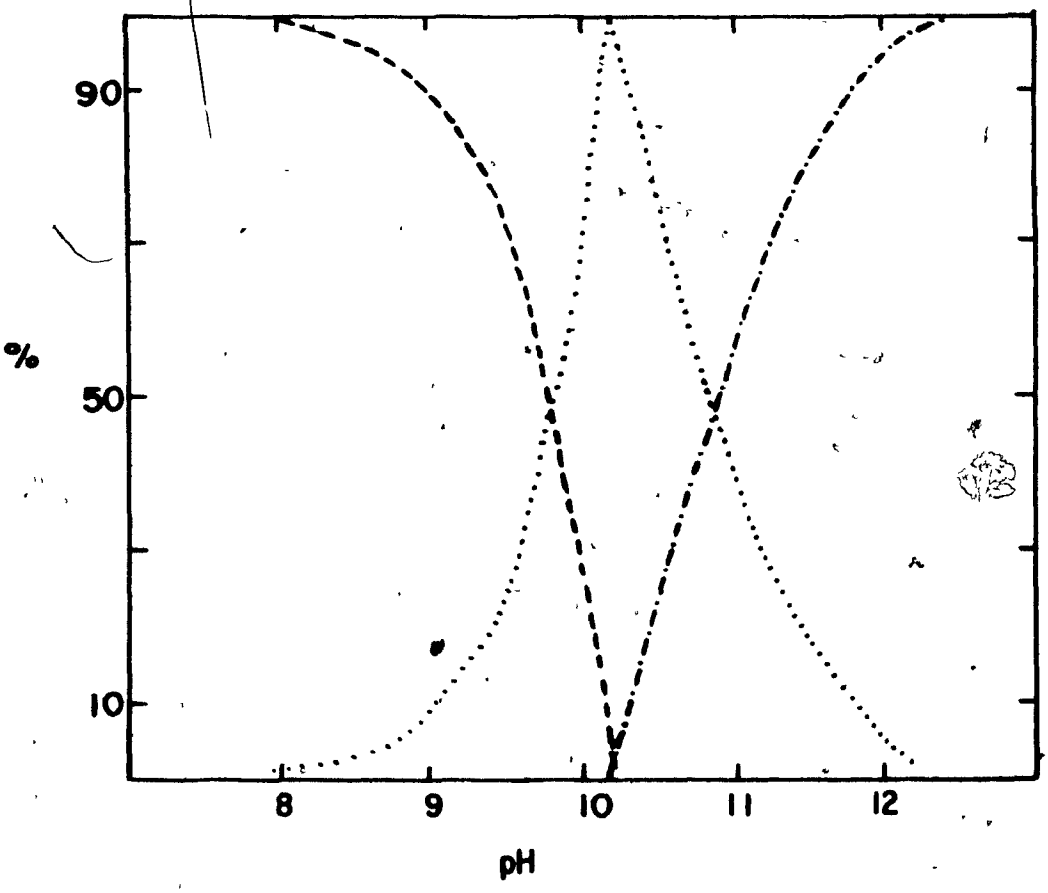
90
50
10
%
8
9
10
11
12
pH
$3RNH_3^{3+}\cdot RNH_2$
RNH_3^+
RNH_2 or $RNH_2 \cdot H_2O$

In a study by Manser (94) of the variation of the critical micelle concentration (cmc) with pH for dodecylamine salt solutions, it is evident that at pH > 9, the observed "cmc" is greater than the calculated saturation concentration (47). This apparent lack of accord with the hydrolysis model and accepted RNH_2 solubility corresponds with the observation made here. Work by Somasundaran (4) showed that the adhesion tension of dodecylamine salt solutions against glass declined with pH upto pH 10 and increased sharply at pH > 10. This is also in agreement with the data presented here.

b) Significance to Flotation

It is possible from the data presented to reconsider some of the known flotation results using dodecylamine as a collector, notably for oxides.

Figure 2.13 shows the flotation recovery vs. dodecylamine acetate concentration for magnetite at pH 9.5 (47,95). The observed contact angle over the same concentration range is also given (47,95,96). Clearly, at concentrations greater than $\sim 1.2 \times 10^{-4}$ M, the excellent flotation recovery is not predicted by the contact angle data. A similar lack of correlation is also reported by Iwasaki et al (97) for goethite and Smith (16) and Lai and Smith (17) for quartz.

FIGURE 2.13

Contact Angle and Flotation Recovery of Magnetite as a Function of Total Amine Concentration at pH 9.5

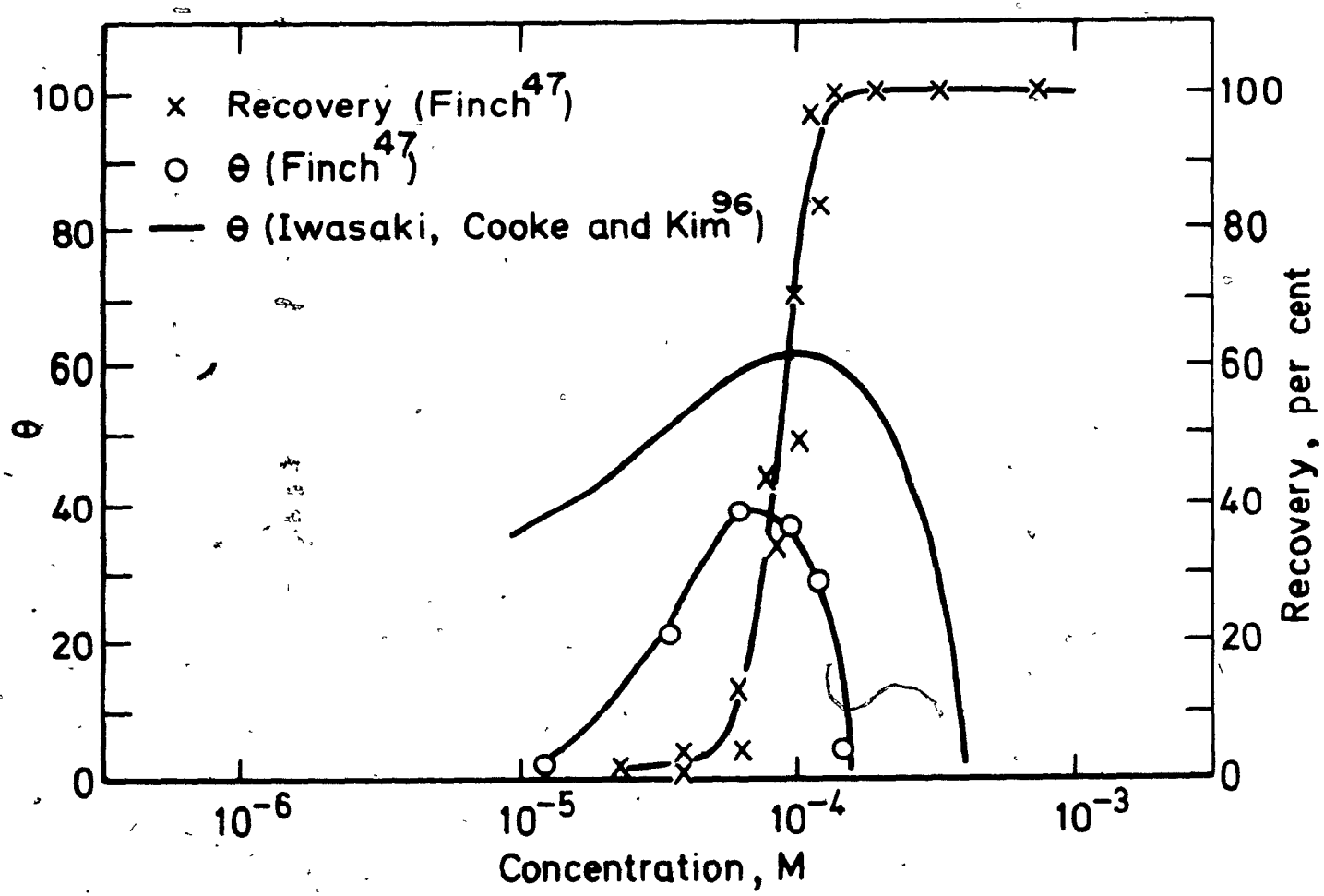
x Recovery (Finch[47])
o θ (Finch[47])
— θ (Iwasaki, Cooke and Kim[96])
θ
Recovery, per cent
Concentration, M
0
20
40
60
80
100
10^{-6}
10^{-5}
10^{-4}
10^{-3}

A major difference between flotation tests and contact angle tests is that the former is a dynamic process, whilst the latter approaches equilibrium. Indeed, equilibrium is considered a pre-requisite for contact angle tests (12). This difference manifests itself particularly with respect to the age of the bubble at bubble-particle collision. In the flotation cell with fresh bubbles being created continuously and with a bubble residence time from ~2 sec. (Hallimond tube) to ~11 sec (industrial cells (98,99)) the surface tension exerted by the bubble upon collision can be considerably greater than the equilibrium value. This is demonstrated in the present results. At concentrations greater than 1.2×10^{-4}M, pH 9.85, the value of γ_∞ is the lowest measured, about 24 dyne cm^{-1}. This low value of the surface tension predicts a small contact angle (see equation 1.2b), supporting the contact angle curve in Figure 2.13. On the other hand, in the flotation cell with $\gamma_{t\to 0} >> \gamma_\infty$, a larger contact angle is predicted, supporting the flotation result. Knowledge of the time-dependent nature of the surface tension of alkaline dodecylamine solutions enables the apparent contradiction in Figure 2.13 to be resolved.

More direct evidence of the role played by the dynamic surface tension is to be found in the dynamic contact angle phenomenon reported by Smith (16) and Lai and Smith (17) and mentioned briefly in Chapter One. Table 2.3 summarizes the dynamic contact angle data.

TABLE 2.3

pH > 9, C > 10^{-4}M: Dynamic Contact Angle

(After Smith and Lai (17))

Time (sec)	Contact Angle (degrees)
0	80
30	55
60	43
90	28
120	20
150	Nil

The present results show that a pronounced decrease in surface tension can occur under the same conditions in which dynamic contact angles were observed. Consider 4.08×10^{-4}M amine at pH 9.85, the surface tension decreases from ~ 72 dyne cm^{-1} (γ_o) to ~ 24 dyne cm^{-1} (γ_∞) over a similar time interval of 150 sec. At pH less than 9 and greater than 11 the dynamic surface tension and dynamic contact angle become less pronounced. The wetting model predicts such a correlation between a time-dependent γ_{LV} and a time-dependent θ. The observation that zero contact angle is obtained with bubbles under certain conditions, always coincides with a low value of the surface tension. According to the Zisman model, this means γ_{LV} has reduced below the critical value, γ_c, for the solid surface under the given conditions. Overall, the

dynamic surface tension data, coupled with the wetting model, explain the dynamic contact angle phenomenon and the pH and concentration limits over which it was observed.

Sandvik and Digrè (11), in discussing the transfer model of flotation, noted that a time-dependent adsorption of collector at the bubble could be a controlling factor in the flotation recovery achieved. Finch and Smith (95,100), taking the rate of surface tension depression as a measure of the rate of adsorption of collector, showed that the recovery of magnetite at pH 9.5 using dodecylamine as collector, improved with the rate of adsorption (see Figure 2.14). This ostensibly is in accord with the transfer model. However, to increase the rate of adsorption required an increase in the total amine concentration, C. Such an increase will also modify the surface chemistry of the solid which was not considered. Figure 2.14 does not, therefore, necessarily constitute support for the transfer model.

Experience with the flotation of oxides using dodecylamine salt collectors indicates that flotation is highly pH-dependent with optimum conditions between about pH 9 and 11. This coincides with the maximum in the surface activity of amine solutions shown in Figure 2.8. The correlation is illustrated in Figure 2.15. The flotation recovery data is taken from Fuerstenau (101) (quartz) and Iwasaki, Cooke and Kim (96) (magnetite). This correlation has never been

FIGURE 2.14

Flotation Recovery of Magnetite as a Function of the Rate of Surface Tension Depression at pH 9.5

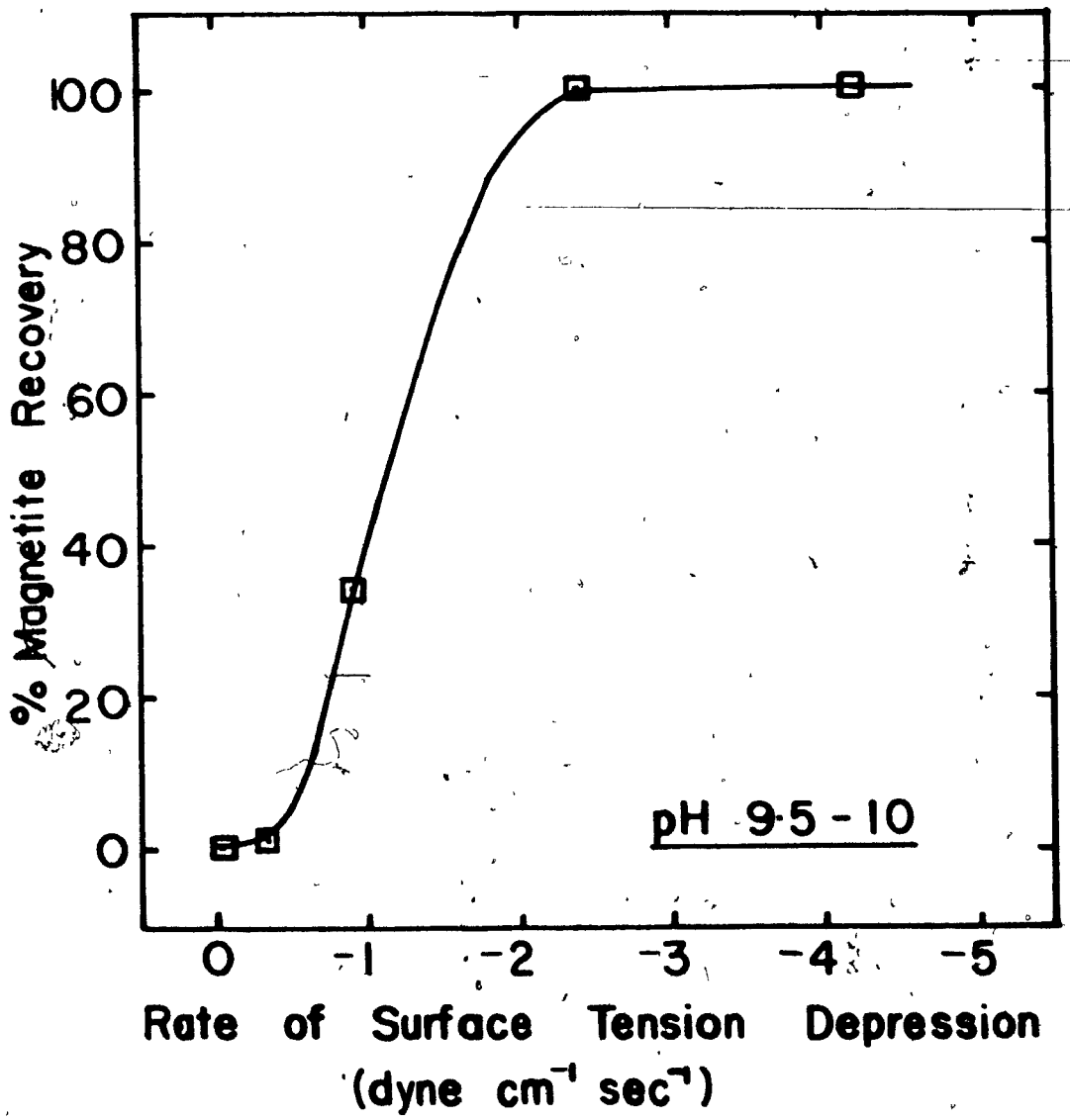
100
80
60
40
20
0
% Magnetite Recovery
pH 9·5 - 10
0
-1
-2
-3
-4
-5
Rate of Surface Tension Depression
(dyne cm⁻¹ sec⁻¹)

FIGURE 2.15

Flotation Recovery and Surface Activity (Measured by γ_{100}) as a Function of pH

a) 4×10^{-5}M, quartz (after Fuerstenau (78))

b) 4×10^{-4}M, magnetite (after Iwasaki, Cooke and Kim (96))

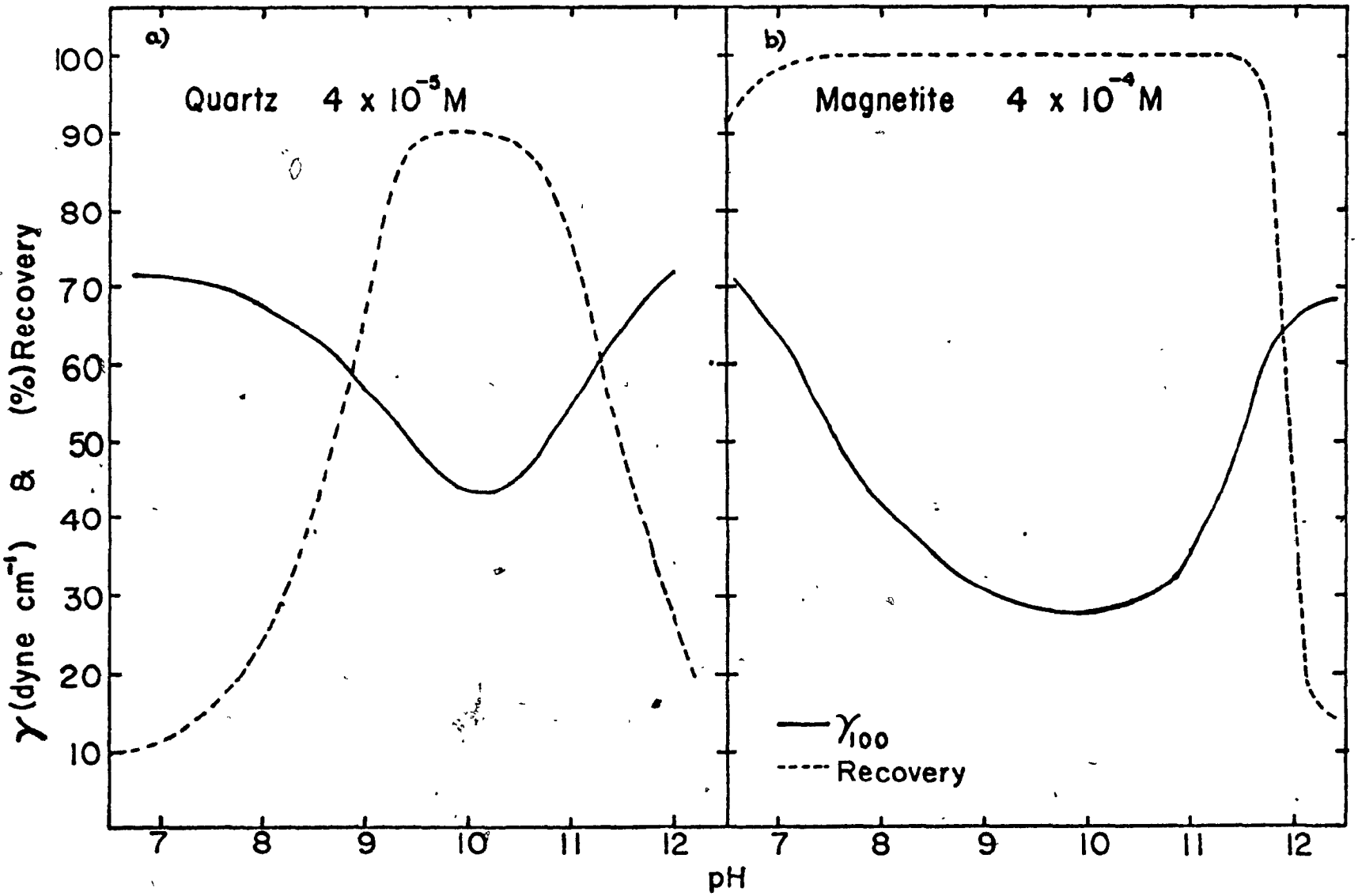
a)
Quartz 4 x 10⁻⁵M
b)
Magnetite 4 x 10⁻⁴M
γ (dyne cm⁻¹) & (%) Recovery
100
90
80
70
60
50
40
30
20
10
7
8
9
10
11
12
pH
γ100
Recovery

demonstrated before, primarily due to a lack of surface tension data.

The highly surface active form of the amine present at around pH 10 may also be capable of greatly lowering the surface energy of any solids suspended in the solution, thus promoting flotation. This will be true only if positive adsorption occurs at the solid surface. The highly surface active form is considered to be an amine ion-molecule complex. The complex will exert a positive charge in comparison with the, generally, negatively charged oxides at basic pH. Electrostatic attraction between collector and oxide is frequently considered responsible for adsorption in amine/oxide systems (20) and such attraction is retained in the case of these complexes. The complexes will adsorb and as a result of the extended hydrocarbon chain will create a solid surface amenable to flotation. At pH outside the range 9-11.5 the highly surface active complex is "lost" (see Figure 2.11) suggesting that solid surface energy will not be so significantly lowered. There is also evidence that the total adsorption of amine at the solid surface also declines outside this pH range (86,102), further lessening the lowering of the solid surface energy. The generally higher adsorption on oxides inside the pH range 9-11 may also be due to the presence of ion:molecule complexes. Adsorption density (16,101) and zeta potential (77,79,101,103) measurements suggest that the amount

of amine actually adsorbed at a quartz surface in this pH range is greater than would be expected from electrostatic attraction between the oxide and the simple RNH_3^+ ion. If instead of simple ions, complexes are adsorbing, then the available surface sites on the quartz will be occupied by, possibly, as many as four or five ions and molecules. This may explain the high adsorption density; the fact that these complexes may contain more ions than molecules may account for the zeta potential of quartz becoming positive between about pH 9.8 and 11.5 at concentrations greater than 4×10^{-5}M (77,79,101). Smith (16) describes amine ions "capturing" molecules and MacKenzie (80) considers chain-chain interaction between the ion and molecule in order to explain the adsorption density and zeta potential versus pH curves respectively. This is in broad agreement with the proposal of amine ion-molecule complexes.

In the pH range 9-11 exists an ideal set of conditions to promote flotation due to the presence of this highly surface active form of the amine; conditioning of the solid results in a considerable lowering of the solid surface energy (hence a lowering of γ_C), whilst in the flotation cell, the fresh bubbles, due to the adsorption kinetics, exert a high surface tension at collision. The low γ_C and high γ_{LV} combine to yield successful flotation.

CHAPTER THREE

BUBBLE-SOLID ATTACHMENT AS A FUNCTION OF BUBBLE AGE

The theoretical section of Chapter One described two flotation models, a wetting model based on the work of Harkins and later Zisman, and a transfer model based on the work of Sandvik and Digrè and Somasundaran. The predicted effect of increasing bubble age (i.e. an increase in Γ_{LV} and a decrease in γ_{LV}) are totally different in each model. Referring to a bubble pick-up test, the predicted results of increasing bubble age are:

a) wetting model - decreased pick-up

b) transfer model - increased pick-up

Chapter Two has shown how γ_{LV} as a function of bubble age could be determined and gave results for alkaline dodecylamine solutions. Examination of these results in the light of available (i.e. published) data lent considerable support to the wetting model. The aim of this Chapter is to further test the wetting and transfer models by performing bubble-solid contact experiments. The bubble properties are varied by controlling the bubble age. Bubble pick-up and some captive bubble tests were employed.

Theory of Technique

By pre-conditioning the solid sample, the necessary changes can be wrought in the solid surface chemistry to render the solid floatable. In terms of the Zisman model, γ_c is decreased to less than 72 dyne cm^{-1}. The solid surface chemistry remains constant during the bubble aging experiments, as indicated by repeated testing of one set of conditions. In this way, only the bubble properties are varied, a unique opportunity afforded by the dynamic properties of alkaline dodecylamine solutions.

Method and Apparatus

A standard captive bubble contact angle testing apparatus similar to that used by Mahne and Lovell (104) was employed for the bubble pick-up experiments (see Figure 3.1). In the present design the bubble was generated by tightening a screw-clip on a piece of rubber tubing attached to the bubble holder. The sample holder cell was constructed of Lucite.

The procedure adopted was to condition approximately one gramme of -65+100 mesh mineral sample in 50 ml vials for 30 min. The vials were stoppered with rubber serum caps protected by "Saran wrap". The vial contents were thoroughly mixed by rotation about the short vial axis at 60 rpm. Conditioning was performed with and without the presence of gas

FIGURE 3.1

Bubble Pick-Up Apparatus

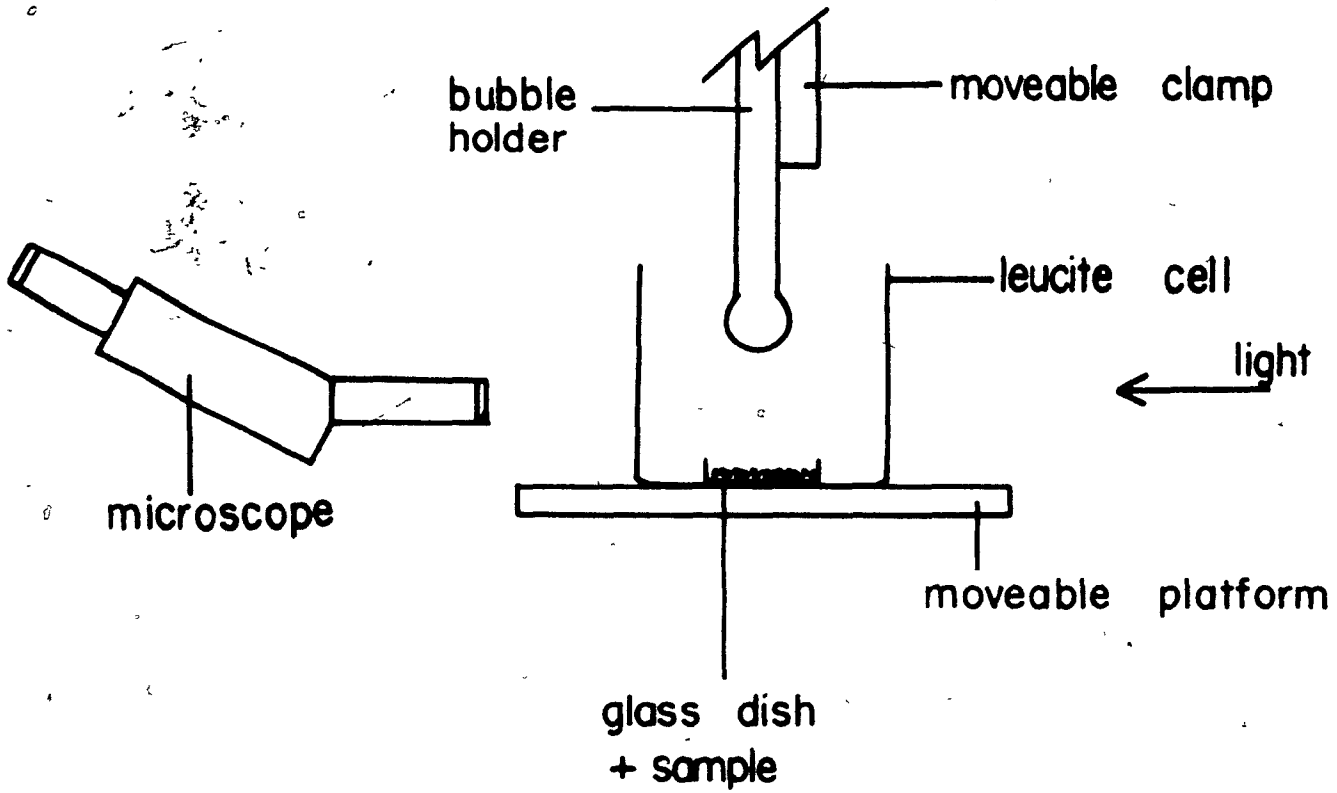
bubble
holder
moveable clamp
leucite cell
light
microscope
moveable platform
glass dish
+ sample

bubbles. The solid plus solution were than transferred to the Lucite cell. To improve sample placement, the solids were directed into a 3/4 in. diameter glass dish (approx. 1/4 in. high). This prevented the solids from being scattered over the Lucite cell. By gently tapping the glass dish, the particles could be fairly evenly distributed.

Two variations of this procedure were also used; 1) after testing the bubble pick-up response in the presence of the conditioning solution, the excess solution was decanted from the Lucite cell and distilled water added; 2) after conditioning in the vial, the excess solution was decanted, distilled water added and 30 min desorption performed. The distilled water in each case was either at natural pH or adjusted to the pH of the conditioning solution.

The bubble was generated at a thin-walled glass capillary tip of approximately 1/4 in. O.D. (referred to as the "bubble holder"). With the bubble at the desired age after formation (measured by a stop-watch), bubble-particle collision was effected by moving the particle bed up to the bubble. Contact was maintained for 2-3 sec. before the particles were withdrawn. A slight modification was incorporated to obtain bubbles of less than one second age; the particles were brought into contact with a bubble already formed and a fresh bubble generated directly into the particle bed. The

resulting bubble load was either viewed directly through the eyepiece (magnification X4) or else projected onto a ground glass screen and a photographic record made. Before performing a second bubble pick-up test, the present load was dumped outside of the glass dish. In this way bubble ages from ~ 1 sec. to 300 sec. were tested. When employing the apparatus for conventional captive bubble tests, the only modification to the procedure was to pre-condition the solid in situ for 30 min. Each set of conditions was repeated at least three times. Measurement of the pH was made before and after each experiment.

The time-dependent surface tension data was determined for each of the solutions tested after contact with the solid. The procedure was as outlined in Chapter Two. The concentration levels specified refer to the measured concentration prior to conditioning.

Flotation data was determined using an all-glass version of the cell designed by Partridge (53,70) (see Figure 3.2). The drive mechanism was replaced by a gear system to give greater reliability. Nitrogen was used to generate the bubbles at a flow rate of 100 ml/min. corrected to room pressure. The same sample conditioning procedure was employed; flotation time was 30 sec.

FIGURE 3.2

Flotation Cell (After Partridge (53,70))

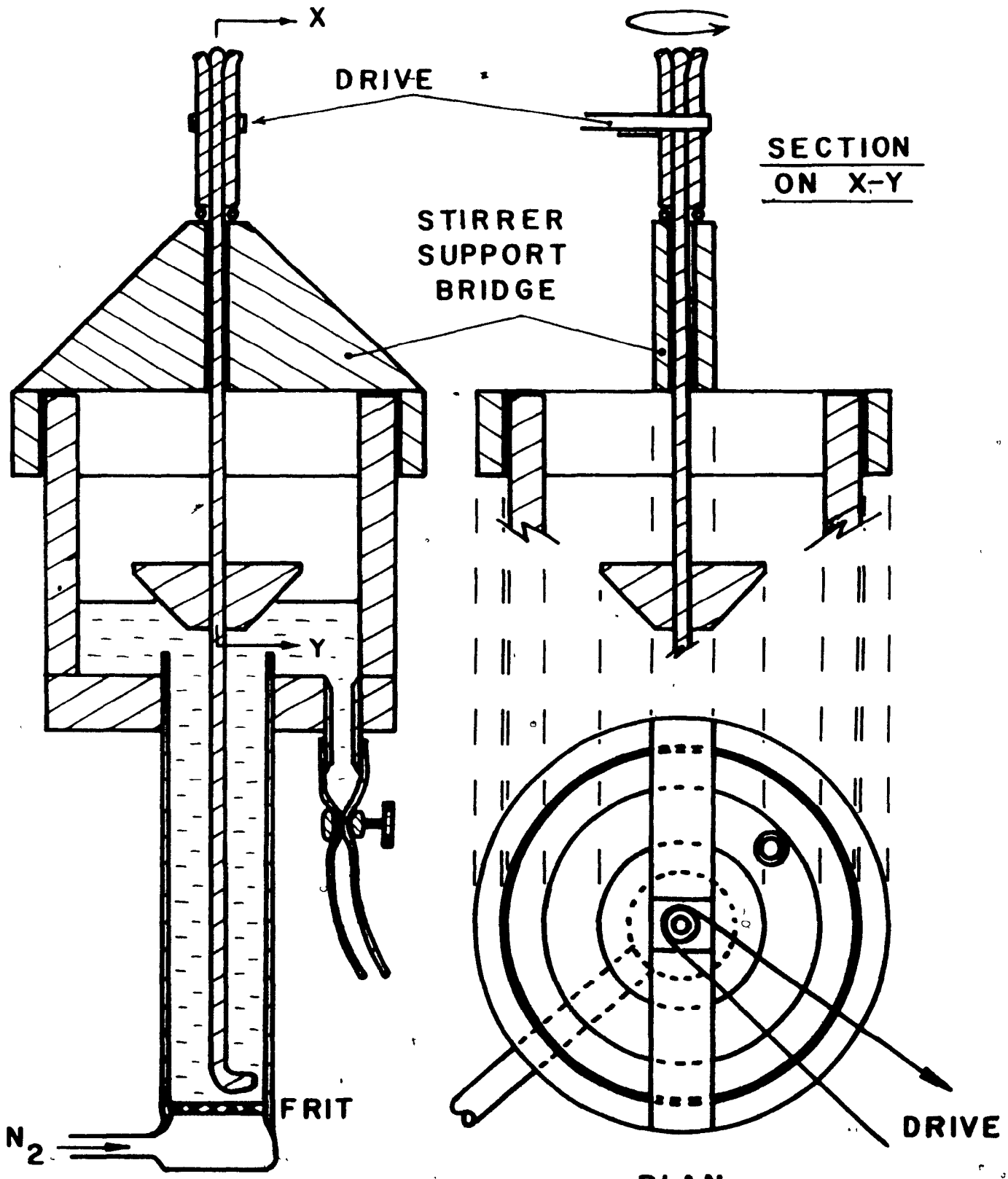

SECTION THROUGH CELL ASSEMBLY

All the glassware was cleaned using acid-dichromate cleaning solution. The Lucite cell was washed with copious quantities of tap and distilled water and allowed to stand for several hours between tests employing different collector strengths. All appropriate equipment was finally washed in a sample of the collector solution being tested.

Materials

a) Minerals

Magnetite

This mineral was tested most extensively. A sample of -65+100 mesh material was prepared (47) from a California beach sand by magnetic separation (using the "Ding" separator) followed by stage grinding in an agate mortar under distilled water.

Quartz

"Water-Clear" rock crystal from Arkansas was passed through a cone crusher and the -14+28 mesh fraction retained. Stage-grinding in an agate mortar under distilled water was used to reduce the sample to -65+100 mesh. Part of this sample was acid-leached for 12 hours in 10% HCl.

Both the magnetite and quartz samples were stored under distilled water in sealed containers. The water was frequently changed.

Hematite

A fresh surface of micaceous hematite from Michigan was prepared by cleaving under distilled water. Testing was performed immediately.

Glass

The glass dish (see Figure 3.1) was used as a representative glass. Composition is unknown.

The mineral samples were supplied by Ward's Natural Science Establishment, Inc.

b) Solutions

Dodecylamine acetate solutions were made up using single distilled and nitrogen-flushed, double distilled water. Concentration and pH levels employed were those covered in Chapter Two. No buffering was needed since the relatively short duration of the tests precluded the pronounced pH drift to acid described previously.

Gas

The bubble pick-up and contact angle tests employed atmospheric air. High purity nitrogen was again used in the dynamic surface tension determination (cf. Chapter Two).

Results

Several methods of recording bubble pick-up data have been proposed (19, 105, 106). Cooke and Digrè (105) weighed the bubble load, Sun and Troxell (106) counted the number of particles picked-up and Lee (19) recently outlined a technique for determining the cross-sectional area occupied by the bubble load. All are tedious in one respect or another. For the present purposes, it proved sufficient to estimate the angle, ϕ, subtended by a continuous load of particles on the bubble. This was done either by using a protractor graticule placed in the eyepiece or later by taking measurements of any photographic record made. Figure 3.3 illustrates a "typical" view of a loaded bubble.

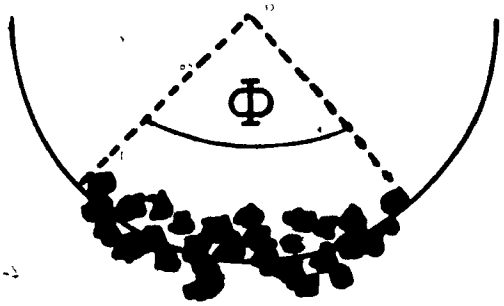

Figure 3.3 'Typical' Loaded Bubble

FIGURE 3.4

Pick-Up of Magnetite as a Function of Bubble Age and Total Amine Concentration at pH 9.7±0.1

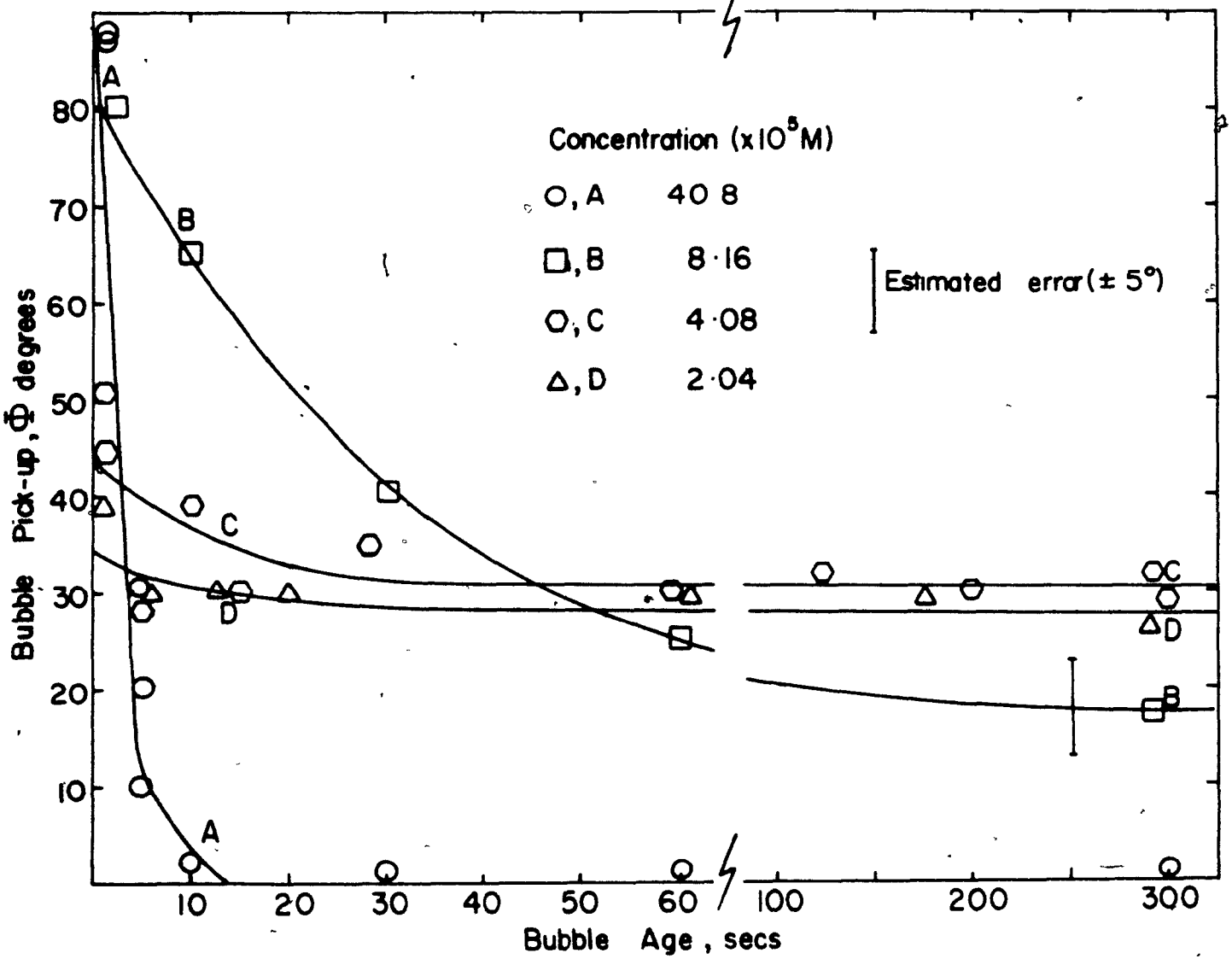
Concentration (x10⁵M)
O, A 40 8
□, B 8·16
O, C 4·08
△, D 2·04
Estimated error (± 5°)
Bubble Pick-up, Φ degrees
Bubble Age, secs
A
B
C
D
10
20
30
40
50
60
70
80
100
200
300

Angles greater than 90^{o} were arbitrarily taken as 90^{o} (representing a fully loaded bubble). Angles less than 10^{o} were taken as zero. In the latter case such a pick-up (amounting to 2 or 3 particles) could be obtained in the complete absence of collector, a frequent observation in bubble pick-up studies (107, 108). This poor pick-up was characterized by the particles being easily dislodged on tapping the bubble holder. A particular advantage of this method of recording data (i.e. "ϕ"), especially in the case of magnetite, is that particles held mechanically, magnetically or by flocculation to other particles are ignored. That is, only particles held at the L-V interface are measured.

Figure 3.4 shows the pick-up of magnetite particles as a function of bubble age for amine concentrations 2.04×10^{-5} M to 4.08×10^{-4} M at pH 9.7 ± 0.1. The pH range corresponds to the pH measurement made prior to and upon completion of each experiment. In all cases, some decrease with bubble age was recorded, the decrease becoming more pronounced with increasing amine concentration. At 2.04×10^{-5} M the decrease is almost non-existent whilst at 4.08×10^{-4} M, zero pick-up was recorded after only 10 sec.

Figures 3.5 to 3.11 give the dynamic surface tension exerted by the dodecylamine acetate solutions after conditioning of the solid under various conditions. Included is the photo-

graphic record to illustrate the bubble pick-up as a function of bubble age.

Figure 3.5 shows the result at 2.04×10^{-5} M pH 9.7 ± 0.1. Negligible change in surface tension or pick-up with bubble age occurred. The surface tension was constant at approximately 69 dyne cm^{-1}, the pick-up was about 30°.

Figure 3.6 gives the result at 4.08×10^{-5} M, pH 9.7 ± 0.1. A detectable dynamic surface tension was apparent, along with a slight decrease in pick-up with bubble age. From t = 0 to t = 300 sec. ϕ decreased from 45° to $\sim 30^{\circ}$ and γ_{LV} from ~ 72 dyne cm^{-1} to ~ 62 dyne cm^{-1}.

The result at 8.16×10^{-5} M, pH 9.7 ± 0.1 is illustrated in Figure 3.7. There was a pronounced decrease in both surface tension and bubble pick-up with time. γ_{LV} and ϕ decreased from ~ 72 dyne cm^{-1} and $\sim 80^{\circ}$ respectively, to ~ 52 dyne cm^{-1} and $\sim 20^{\circ}$.

Figure 3.8, curve A, demonstrates a dramatic decrease in both γ_{LV} and ϕ with time at 4.08×10^{-4} M, pH 9.7 ± 0.1. At $t < 1$ sec. ϕ was greater than 90° (taken as 90° on Figure 3.4) and by extrapolation γ_{LV} was greater than 65 dyne cm^{-1}. At t = 10 sec., ϕ was zero and γ_{LV} at about 45 dyne cm^{-1}. At $t > 10$ sec, ϕ remained zero, and γ_{LV} further reduced to slightly less than 30 dyne cm^{-1} (after 150 sec). Curve B illustrates the result if the conditioning solution was removed

FIGURE 3.5

Dynamic Surface Tension and Pick-Up of Magnetite After 30 Min. Conditioning in 2.04×10^{-5}M Dodecylamine Acetate Solutions, pH 9.7 ± 0.1

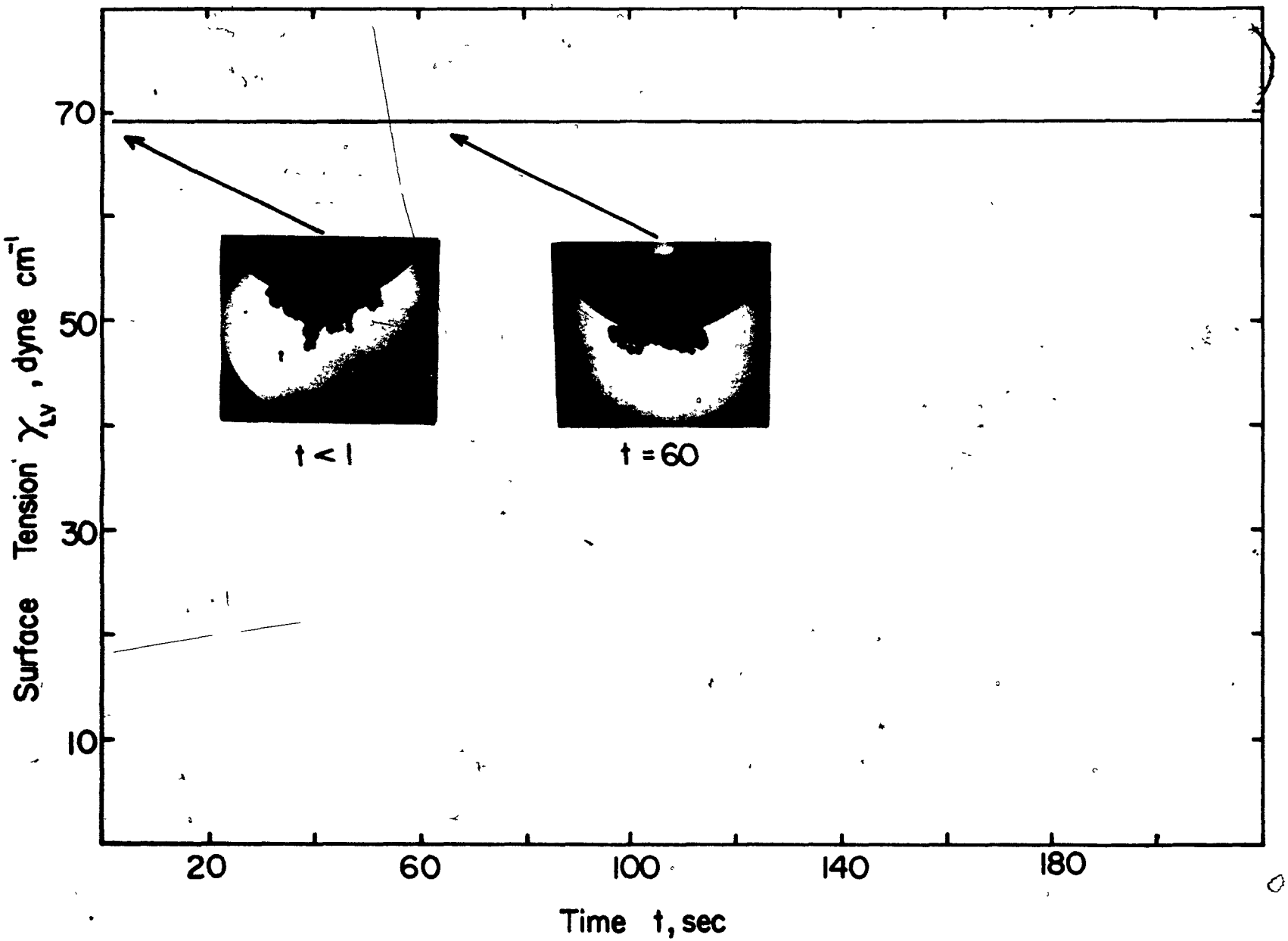
70
50
30
10
Surface Tension γ_{Lv}, dyne cm^{-1}
t < 1
t = 60
20
60
100
140
180
Time t, sec

FIGURE 3.6

Dynamic Surface Tension and Pick-Up of Magnetite After 30 Min. Conditioning in 4.08×10^{-5}M Dodecylamine Acetate Solutions, pH 9.7 ± 0.1

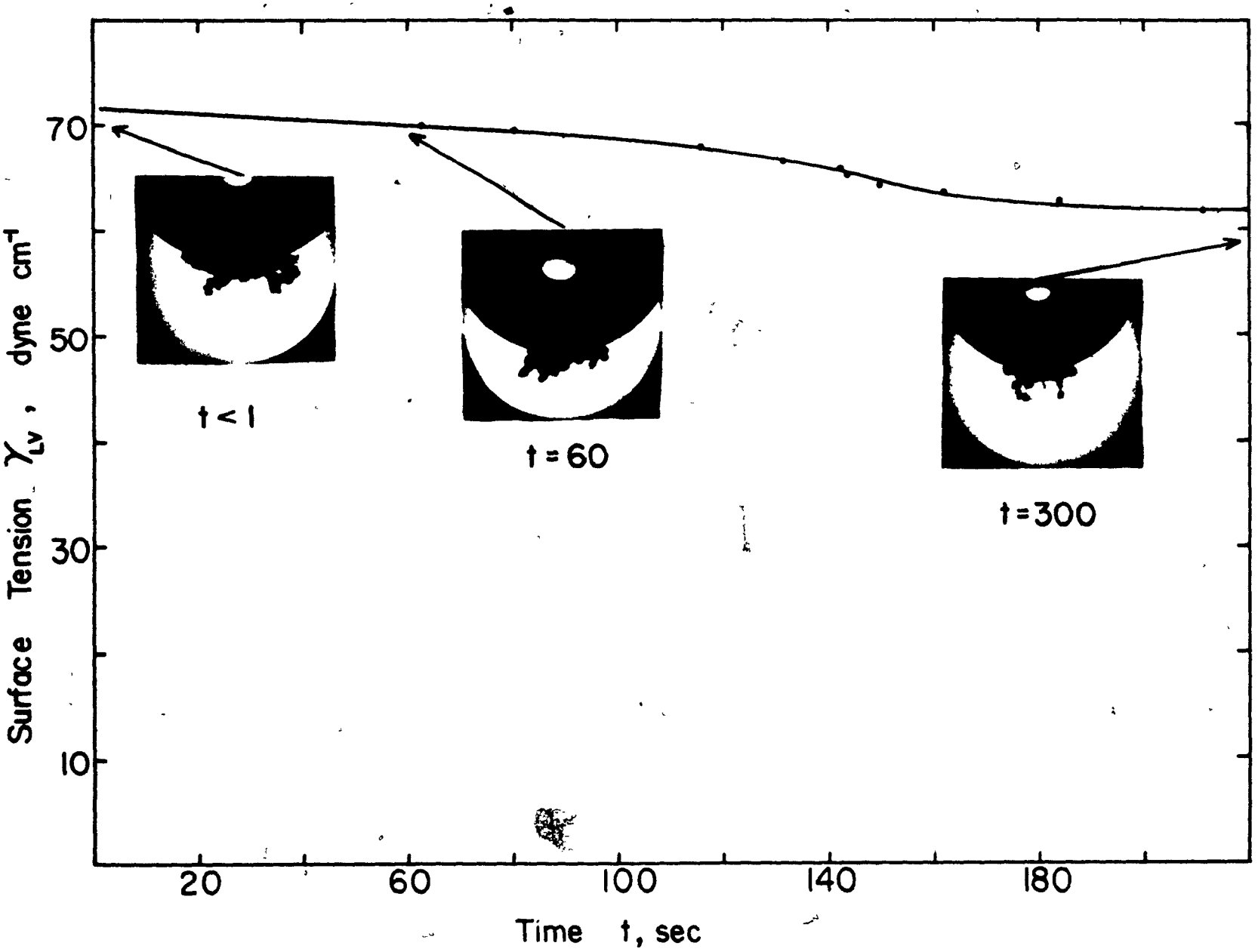
70
50
30
10
Surface Tension γ_{Lv}, dyne cm^{-1}
t < 1
t = 60
t = 300
20
60
100
140
180
Time t, sec

FIGURE 3.7

Dynamic Surface Tension and Pick-Up of Magnetite After 30 Min. Conditioning in 8.16×10^{-5}M Dodecylamine Acetate Solutions, pH 9.7 $\pm$ 0.1

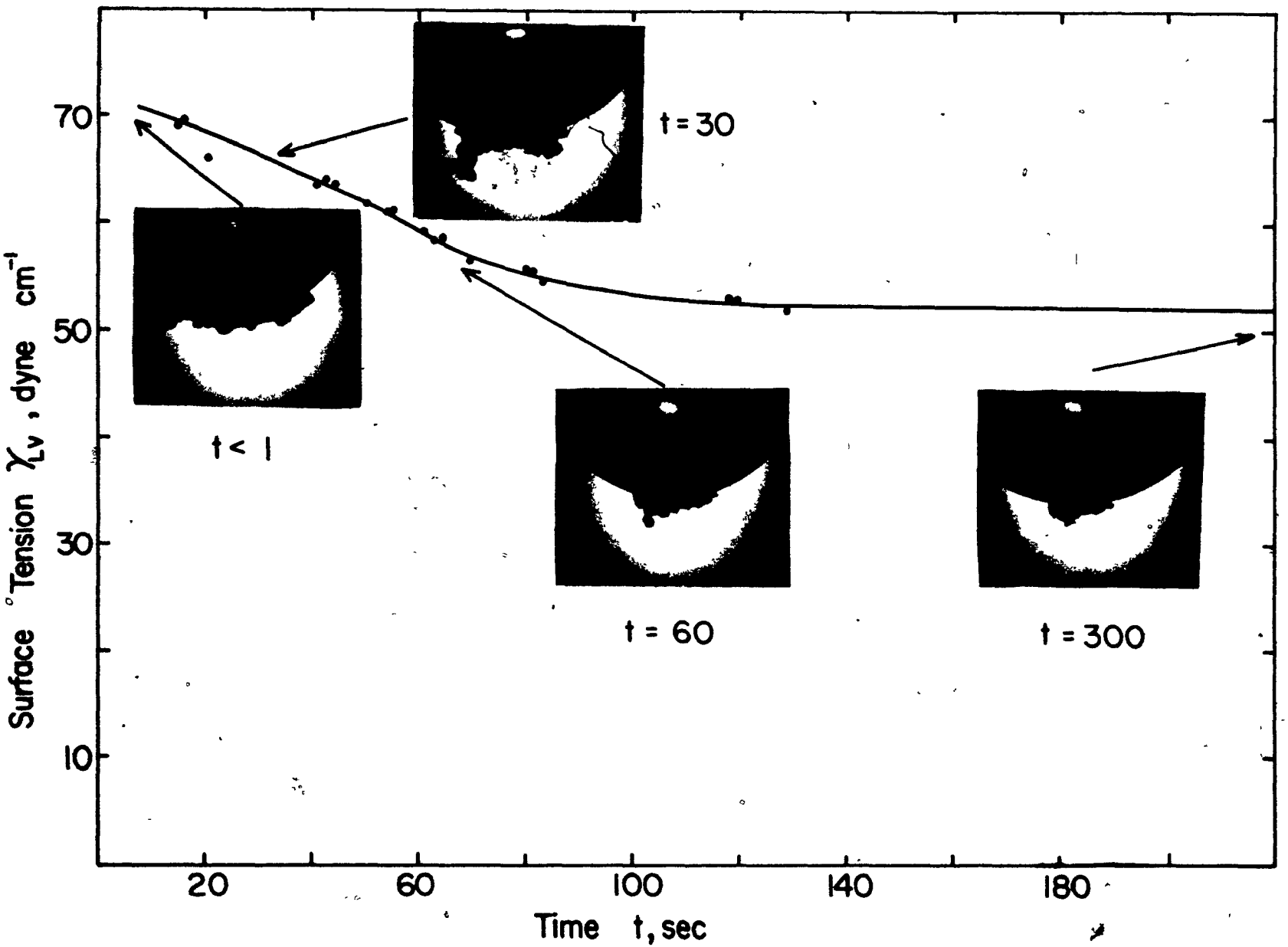
70
50
30
10
Surface Tension γ_{Lv}, dyne cm^{-1}
t = 30
t < 1
t = 60
t = 300
20
60
100
140
180
Time t, sec

FIGURE 3.8

Dynamic Surface Tension and Pick-Up of Magnetite After 30 Min. Conditioning in 4.08×10^{-4}M Dodecylamine Acetate Solutions

A pH 9.7 ± 0.1

B as A but solution replaced by distilled water (pH 6.1)

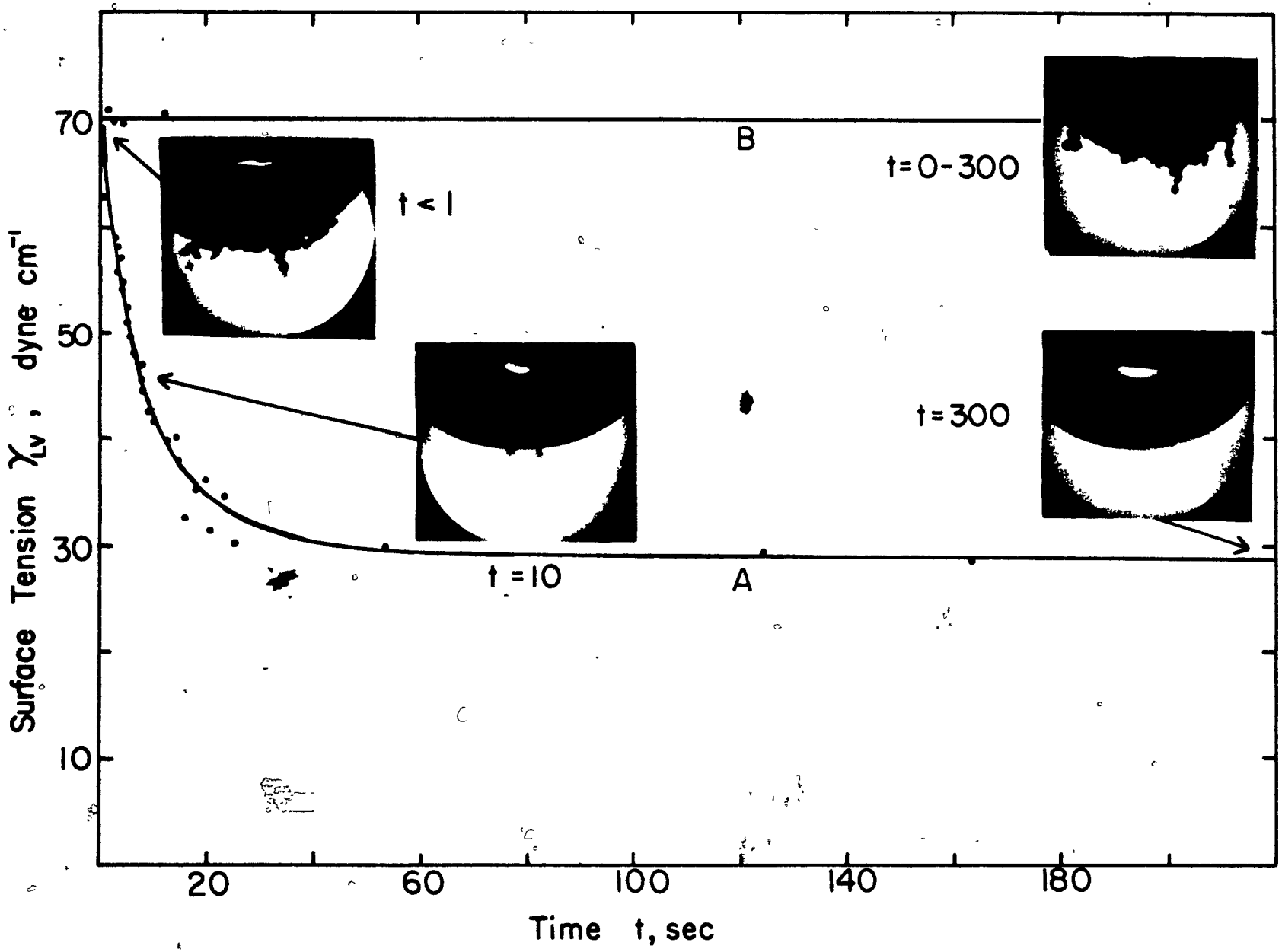
70
50
30
10
20
60
100
140
180
Surface Tension γ_{Lv}, dyne cm^{-1}
Time t, sec
B
A
t < 1
t = 10
t = 0-300
t = 300

and distilled water at natural pH added. Excellent pick-up is demonstrated at all bubble ages, and no dynamic surface tension was measured, γ_{LV} remaining constant at close to 70 dyne cm^{-1}. This result was the same whether the conditioning solution was replaced in the Lucite cell or the conditioning vial and a 30 min. desorption performed.

If instead of desorbing in distilled water at natural pH, distilled water at pH 9.7 was used and 30 min desorption performed, the result was as shown in Figure 3.9. A steady decrease in γ_{LV} and pick-up with bubble age was observed. γ_{LV} reduces from ~ 72 dyne cm^{-1} to ~ 50 dyne cm^{-1}, while ϕ decreases from 90^{o} to $\sim 15^{o}$ over a time interval of 300 sec. Figure 3.10 compares the dynamic surface tension obtained by desorption at pH 9.7 with that obtained by desorption at natural pH, with the latter subsequently adjusted to pH 9.7.

Figures 3.11 and 3.12 detail 4.08×10^{-4} M solutions at pH 12.2 and 6.1 (natural pH) respectively. At pH 12.2, no pick-up was registered; the surface tension declined slowly to yield ~ 68 dyne cm^{-1} after 100 sec. The result at pH 6.1 shows successful pick-up ($\phi \sim 45^{o}$) at all bubble ages. The surface tension was constant at ~ 67 dyne cm^{-1}.

The state of the bubbles in the vials after conditioning was also noted. In 4.08×10^{-4} M solutions, pH 9.7, the bubbles were completely barren after 30 min. conditioning, but

FIGURE 3.9

Conditions as for Figure 3A, Then Solution in Vial Replaced by Distilled Water at pH 9.7 and 30 Min. Desorption Performed

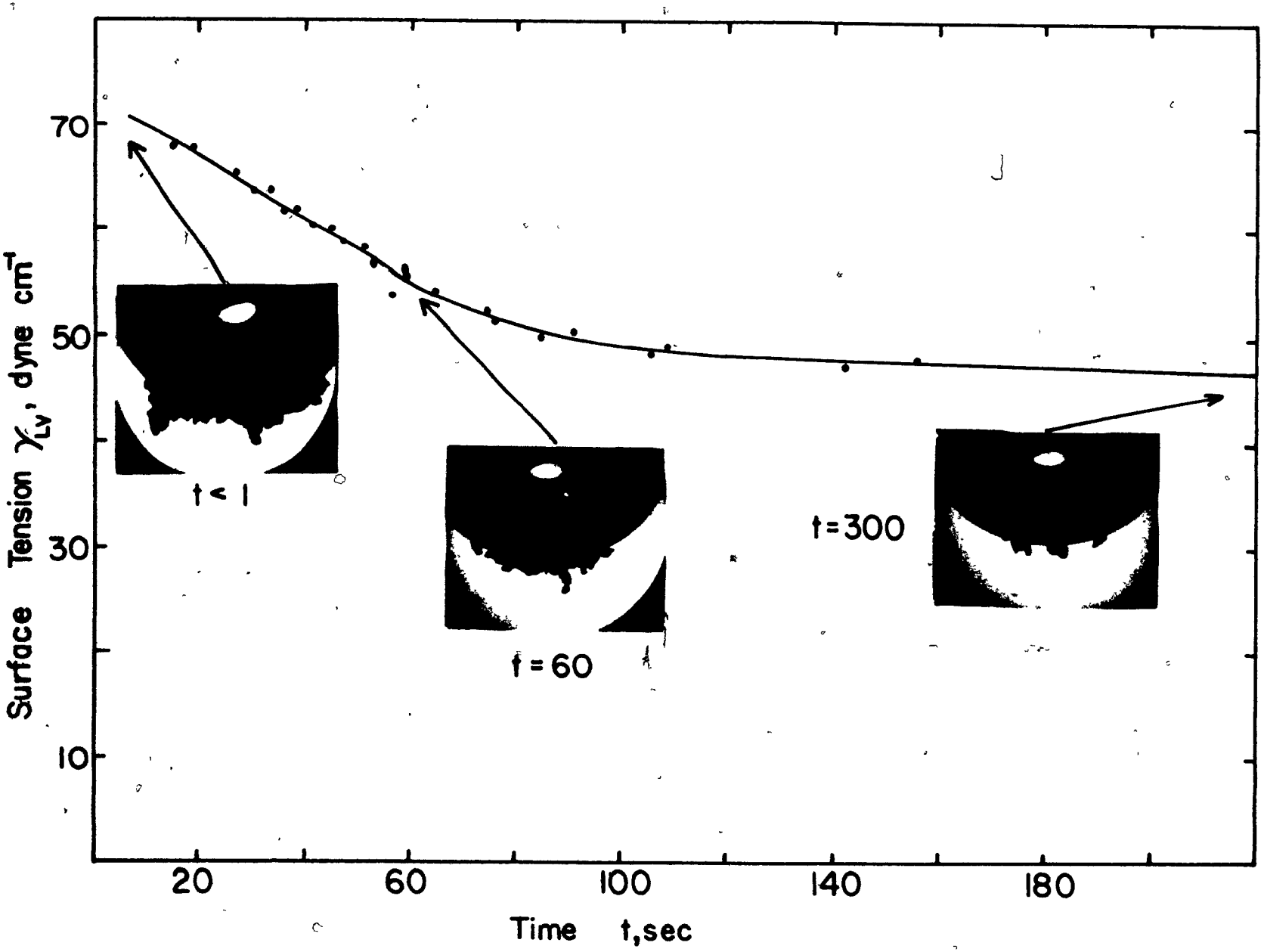
70
50
30
10
Surface Tension γ_{Lv}, dyne cm^{-1}
t < 1
t = 60
t = 300
20
60
100
140
180
Time t, sec

FIGURE 3.10

Dynamic Surface Tension Exhibited by Distilled Water After Desorption from Magnetite Conditioned at 4.08×10^{-4} M Amine, pH 9.7 for 30 Min. Using:

A) Distilled Water at pH 9.7

B) Distilled Water at pH 6.1, Subsequent Adjustment to pH 9.7

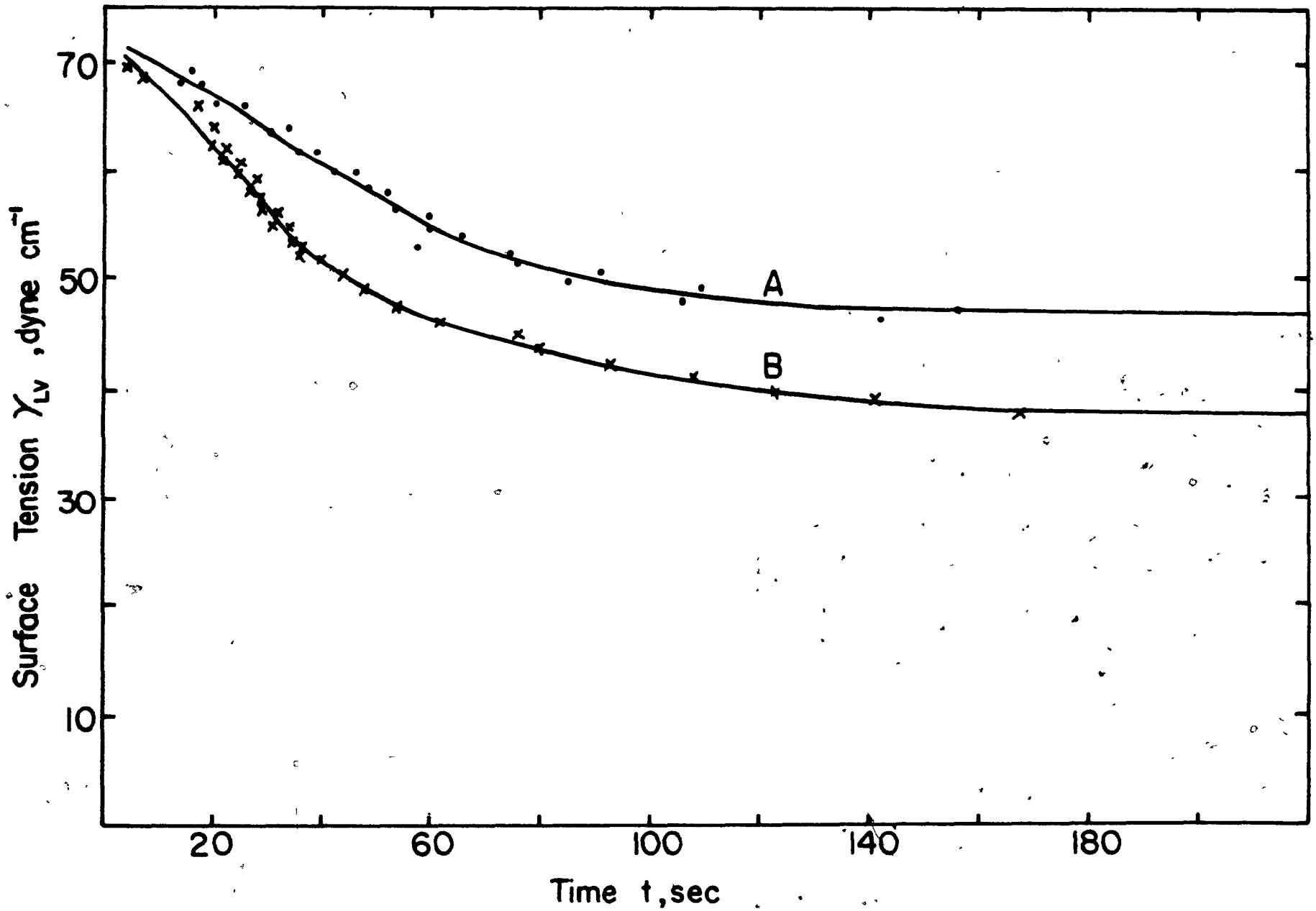
70
50
30
10
Surface Tension γ_{Lv} , dyne cm^{-1}
A
B
20
60
100
140
180
Time t, sec

FIGURE 3.11

Dynamic Surface Tension and Pick-Up of Magnetite After 30 Min. Conditioning in 4.08×10^{-4}M Dodecylamine Acetate, pH 12.2

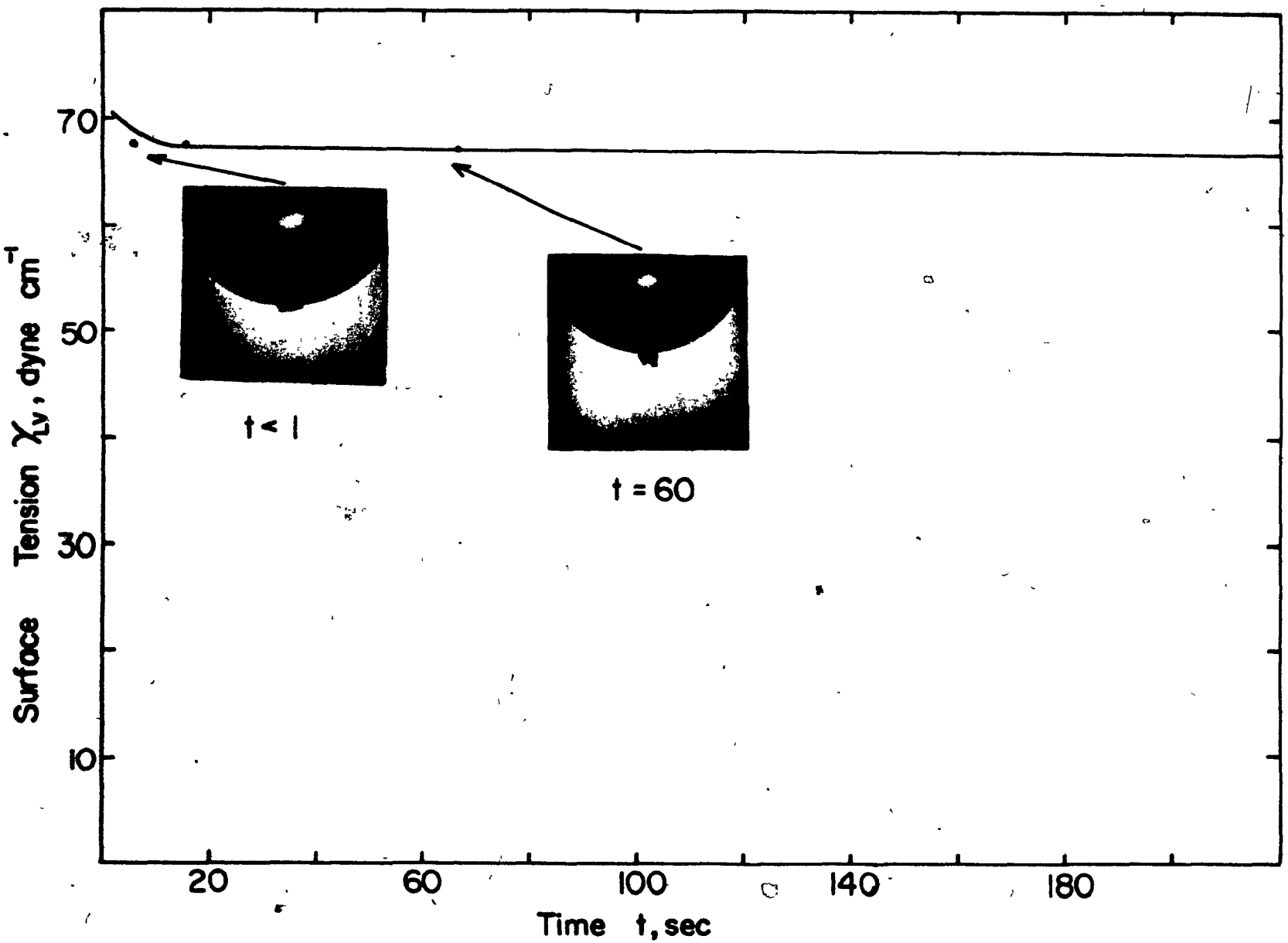
70
50
30
10
Surface Tension χ_{Lv}, dyne cm^{-1}
t < 1
t = 60
20
60
100
140
180
Time t, sec

FIGURE 3.12

Dynamic Surface Tension and Pick-Up of Magnetite After 30 Min Conditioning in 4.08×10^{-4} M Dodecylamine Acetate Solutions, pH 6.1

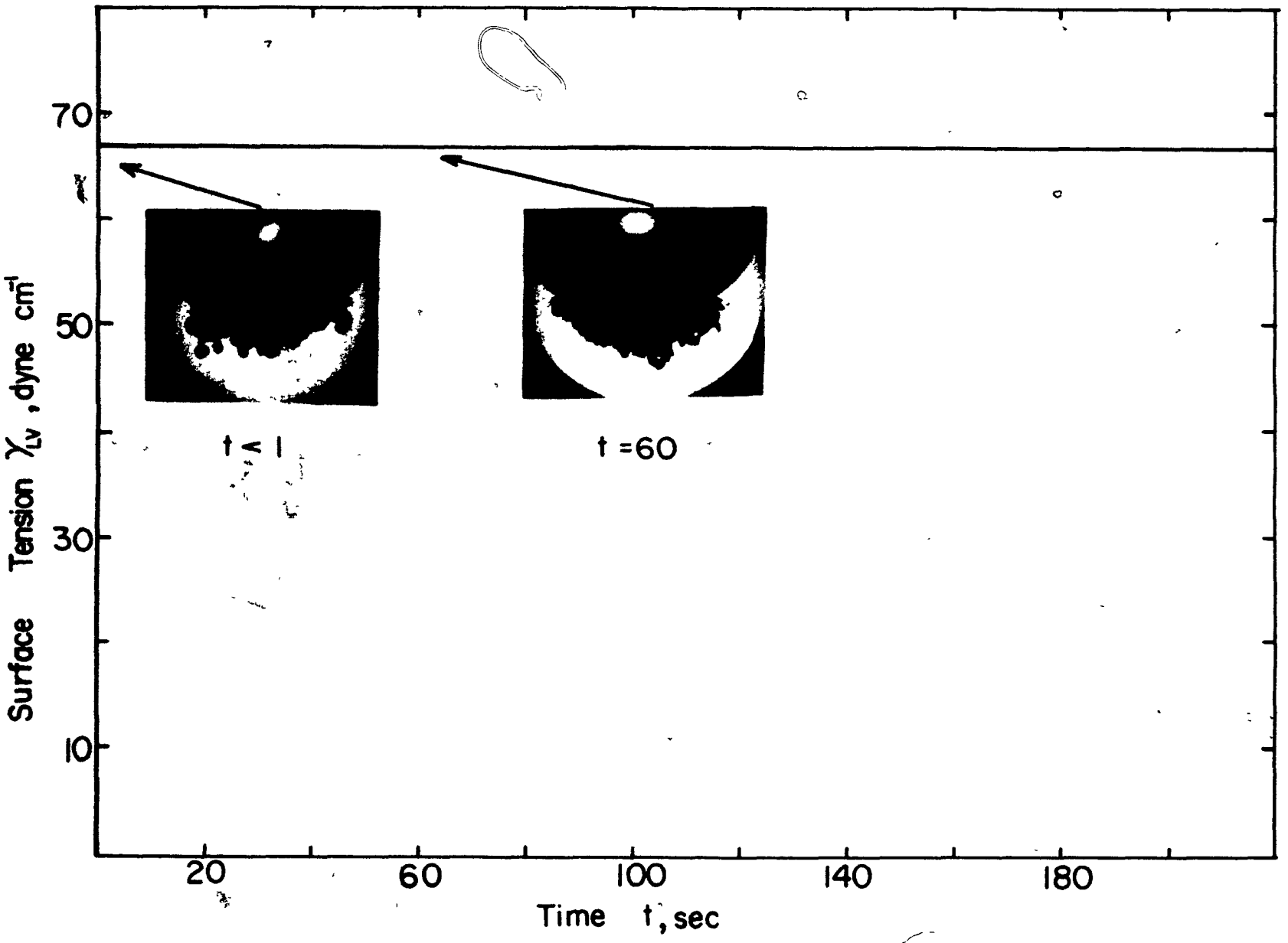
70
50
30
10
Surface Tension γ_{Lv}, dyne cm^{-1}
t < 1
t =60
20
60
100
140
180
Time t, sec

fully loaded at amine concentrations less than 8.16×10^{-5} M at the same pH.

Bubble pick-up tests were performed on the -65 + 100 mesh quartz sample at 4.08×10^{-4} M and pH 9.7 $\pm$ 0.1. No decrease in bubble pick-up with bubble age occurred with either the "as prepared" or acid-leached material (see Figure 3.13). A decrease in stability was suspected, at 300 sec some of the load could be easily dislodged by tapping the bubble holder, but this was far from satisfactorily demonstrated. The dynamic surface tension after conditioning was the same as for the magnetite sample (see Figure 3.14). Figure 3.13 shows the different effect of bubble age on the quartz and magnetite at 4.08×10^{-4} M, pH 9.7 $\pm$ 0.1.

Captive bubble tests on glass and hematite were carried out at 4.08×10^{-4} M amine solution, pH 9.7 $\pm$ 0.1. Both materials revealed a sharp decrease in tenacity of bubble attachment with increasing bubble age; at $t > 5$ sec attachment was virtually impossible. Replacing the solution in the Lucite cell with distilled water (natural pH or pH 9.7) eliminated the bubble age effect, adhesion being excellent at all bubble ages tested.

In all the examples involving a bubble age effect, once attachment had been achieved no further time effect was observed.

FIGURE 3.13

Pick-Up of Magnetite and Quartz in 4.08×10^{-4} M Dodecylamine Acetate Solutions, pH 9.7 $\pm$ 0.1 as a Function of Bubble Age

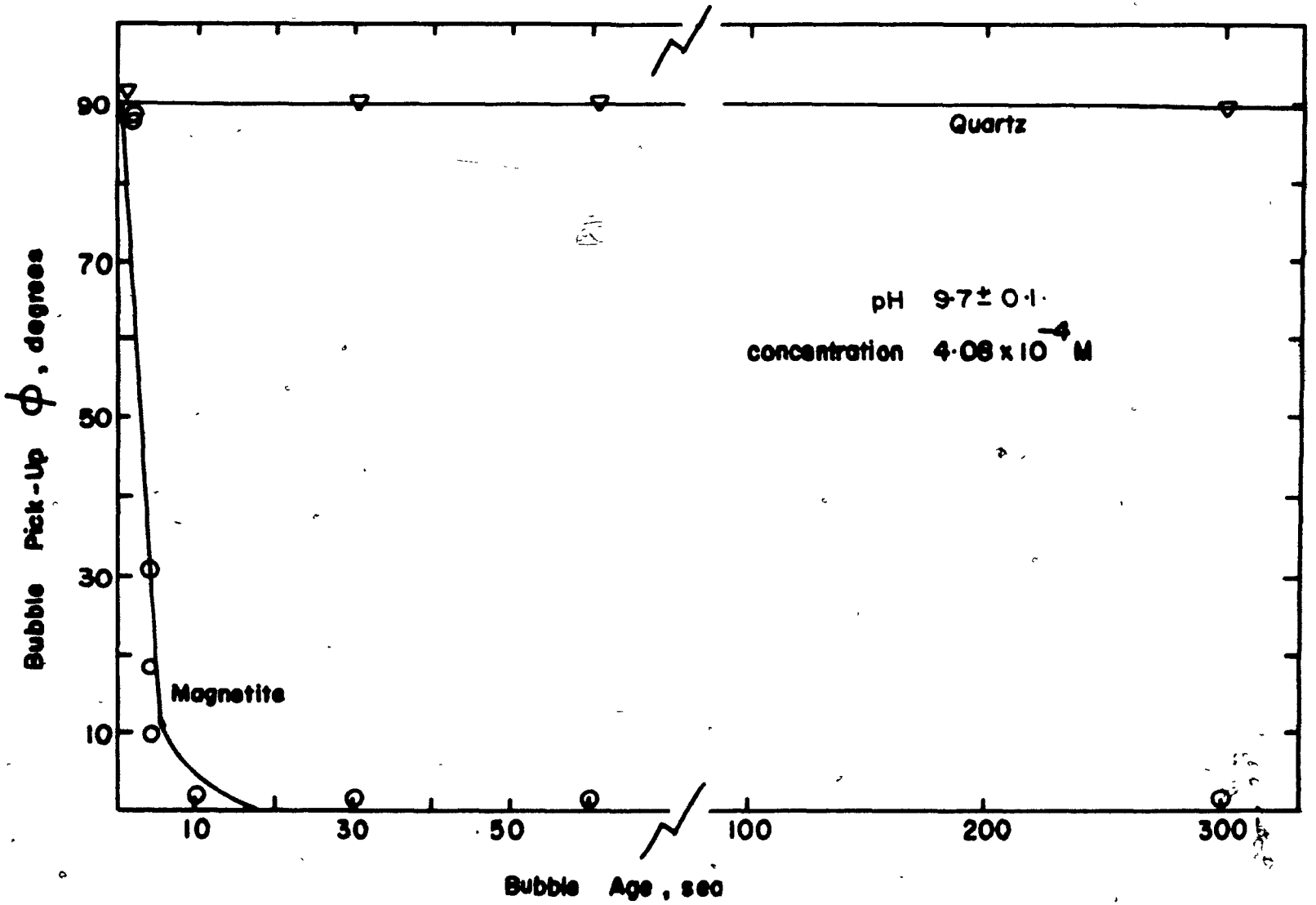
Quartz
pH 9·7 ± 0·1
concentration 4·08 x 10⁻⁴ M
Magnetite
Bubble Pick-Up ϕ, degrees
90
70
50
30
10
10
30
50
100
200
300
Bubble Age, sec

FIGURE 3.14

Comparison of Dynamic Surface Tension of Dodecylamine Acetate Solutions, pH 9.7 ± 0.1 After Conditioning a Quartz and Magnetite Sample

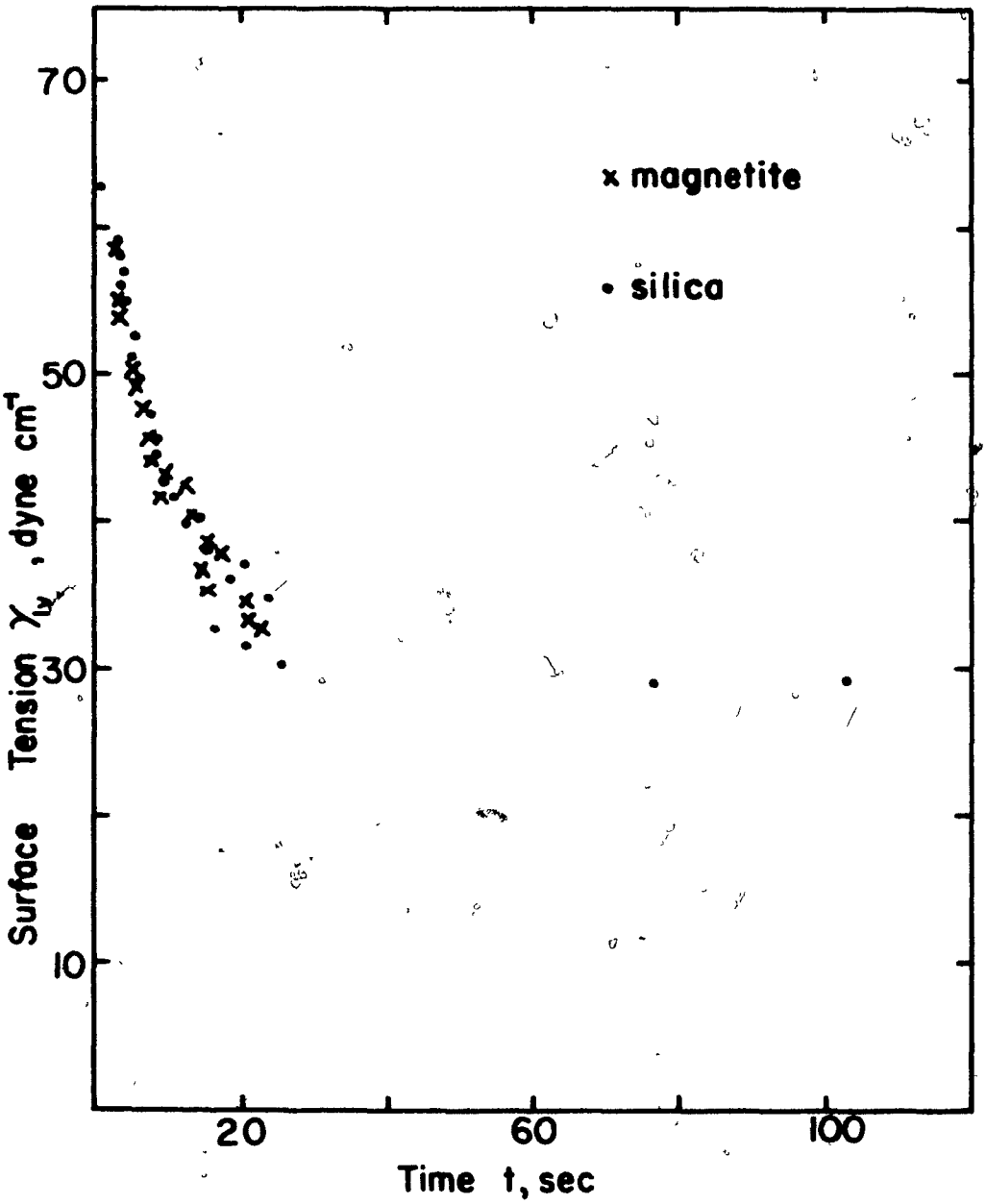
70
50
30
10
Surface Tension γ_{lv}, dyne cm^{-1}
x magnetite
• silica
20
60
100
Time t, sec

Both single and double-distilled water were employed in the above tests. No difference was detectable. Similarly whether "fresh" or "old" solutions were employed seemed immaterial.

Discussion

The pH level most thoroughly tested was around pH 9.7. From Chapter Two, this pH level was known to be in the range giving the most pronounced dynamic surface tension. Therefore, this pH was the most useful in testing the wetting and transfer models of flotation, in the manner outlined in Chapter One. So that the dynamic surface tension would relate to the bubble pick-up tests, the dynamic surface tension data was determined after sample conditioning. Comparing with Figure 2.9, total amine concentrations of 2.04 to 8.16×10^{-5} M show a marked change in the dynamic surface tension. A loss of collector from solution through adsorption onto the solid is indicated. Little change followed conditioning in 4.08×10^{-4} M solutions. The conditioning time of 30 min, although not necessarily sufficient for "true" equilibrium to be attained was chosen because it was used in the original flotation work on magnetite (47). The ability to reproduce the bubble age results suggests that 30 min conditioning time is sufficient for the bulk of the changes at the solid surface to be completed.

It was deduced (in Chapter One) that a decrease in pick-up with a decrease in γ_{LV} would support the transfer model. Based on evidence contained in Figures 3.4 to 3.9, the wetting model alone is supported.

The correlation between a decrease in pick-up and a decrease in γ_{LV} shown in Figures 3.4 to 3.9 is excellent and is supported by the contact angle data. In a sense, bubble armouring, has been measured. Figure 3.8A shows that a rapid decrease in γ_{LV} is accompanied by an equally rapid decrease in pick-up; Figure 3.6 and 3.7 identify slower rates of decrease in γ_{LV} with slower rates of decrease in pick-up. Eventually, with the dynamic surface tension all but lost (Figure 3.5), little decrease in pick-up occurs. The shape of the ϕ vs bubble age curves at various total amine concentrations (Figure 3.4) is similar to the γ_t vs t curves at the same pH (Figure 2.7). Figure 3.9 shows that the correlation between pick-up and γ_{LV} is maintained even through the dynamic γ_{LV} is obtained by desorbing collector from the magnetite. In comparison Figure 3.8B shows the same procedure as used in Figure 3.9 but with distilled water at natural pH. No decrease in γ_{LV} or pick-up was observed. That desorption had occurred is proved in Figure 3.10 where the desorbing solution has been adjusted to pH 9.7. It seems, in fact, that more collector was desorbed at natural pH than at pH 9.7.

Whenever the pick-up was constant, γ_{LV} was determined as constant. This was regardless of whether the situation was achieved by: 1) using very dilute solutions (Figure 3.5); 2) replacing the conditioning solution by distilled water at natural pH (Figure 3.8B); or 3) using solutions at pH $<$ 7 or $>$ 12 (Figures 3.11 and 3.12). In the case of solutions at pH $>$ 12 no pick-up at all was observed (Figure 3.11).

Figures 3.5 and 3.6 should be particularly sensitive to the transfer model since the change in γ_{LV} (and by inference $\bar{}_{LV}$) is more controlled. The rapid decrease in γ_{LV} shown in Figure 3.8A, it might be argued, could obscure any tendency for pick-up to increase at short time intervals. This argument is not applicable at 2.04 and 4.08 x 10^{-5} M solutions. However, only a tendency for the pick-up to decrease, correlating with a decrease in γ_{LV} is observed. In the case of quartz, although no direct evidence is forthcoming to support the wetting model (no decrease in pick-up was observed, see Figure 3.13) neither is there any in favour of the transfer model. Under no conditions was a systematic or reproducible increase in pick-up with bubble age observed. It is concluded, therefore, that in the system under investigation the transfer model is of little significance in comparison with the wetting model. This denial of the transfer model strongly supports the conclusion reached by Pope and Sutton (40). Hence attempting to ascertain the transfer mechanism may prove fruitless.

Establishing that γ_{LV} decreases with bubble age and that this can be detrimental to bubble-particle adhesion has broad ramifications. For instance, in the laboratory such tests of floatability as contact angle and bubble pick-up can be misleading if the possible influence of bubble age is not understood. Figure 3.15 gives ϕ as a function of total amine concentration. Curve a is at t = 0 and b at t = 300 sec. The former corresponds to the flotation recovery of magnetite detailed in Figure 2.14 whilst the latter coincides with the contact angle data. This supports the previous conclusion that the flotation of magnetite at pH 9.5 and total amine concentrations greater than 10^{-4} M is as much dependent on the generation of fresh bubbles as to "modification" of the surface chemistry of the solid.

Flotation, in general, would appear to benefit from the continuous creation of fresh bubbles, which is fundamental to the operation of a flotation machine. Due to the design of the Hallimond tube (used in establishing the flotation response of magnetite (47)),bubble-particle collision is effected almost immediately upon bubble generation. This emphasises the fresh bubble properties, and these favour attachment. In the industrial cell, however, bubble-particle collisions occur with bubbles both fresh and "aged". If only the collisions with fresh bubbles are productive (in the sense of yielding attachment), it is feasible that the Hallimond tube result will

FIGURE 3.15

a) Flotation Recovery of Magnetite Using Dodecylamine at pH 9.5 and Pick-Up at t = 0 sec, pH 9.7 ± 0.1

b) Contact Angle Using Dodecylamine at pH 9.5 and Pick-Up at t = 300 sec, pH 9.7 ± 0.1

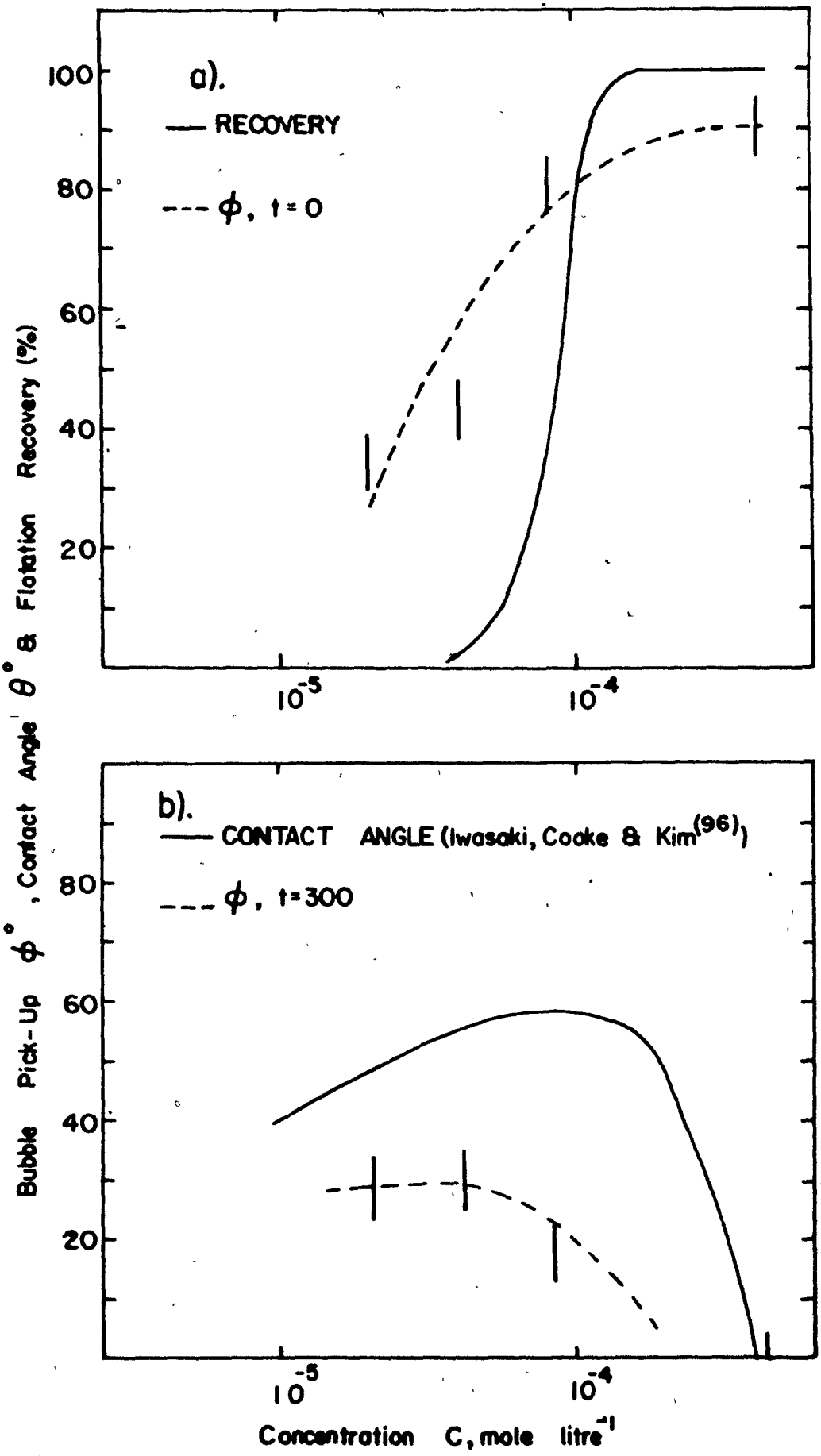
a).
RECOVERY
ϕ, t = 0
100
80
60
40
20
10^{-5}
10^{-4}
b).
CONTACT ANGLE (Iwasaki, Cooke & Kim[96])
ϕ, t = 300
80
60
40
20
10^{-5}
10^{-4}
Concentration C, mole litre^{-1}
Bubble Pick-Up ϕ°, Contact Angle θ° & Flotation Recovery (%)

not be achievable in an industrial cell. The same result may well be obtained at a lower concentration, or different pH, where the bubble does not age sufficiently to prevent adhesion. In this case, the result will be in response to a series of moderately productive collisions as opposed to the one highly productive collision involved in the Hallimond tube. The observed state of any bubbles in the vial after conditioning appears to testify to this possibility. At less than 8.16×10^{-5} M, the loaded bubble reflects a series of moderately productive collisions (Figures 3.5, 3.6 and 3.7 show even 300 sec "old" bubbles capable of some pick-up). The barren bubble in 4.08×10^{-4} M solutions emphasizes the poor pick-up power of bubbles which are anything other than fresh in such solutions.

In many cases the flotation result in the laboratory will reflect accurately the flotation result in industry because such aging problems do not exist. One area in which bubble aging may be an important consideration is the modern generation of flotation cells (e.g. column cells, and the large, Maxwell-type cells (98)). Especially in the former cell, the bubble will probably age more than in conventional cells. The decline in γ_{LV} as a function of bubble age in a flotation cell is complicated by the relative fluid motion tending to increase the rate of attainment of equilibrium (28) and the expansion of the rising bubble tending to delay equilibrium. Nevertheless,

that the exerted γ_{LV} can vary with bubble age remains true. The present work has demonstrated that the variation can have important consequences.

Further discussion of the implications of dynamic surface tension on flotation cell design would be too speculative. The data, however, demands that the wetting model be more fully described. Clearly, the different results for quartz and magnetite need explanation. Rogers et al. (15) noted that although the L-V interface was common in tests using different mineral substrates, no common cut-off in bubble-particle attachment was observed. Differences in mineral surface chemistry, modified by collector adsorption, were considered the reason. The observations correspond to the present case. As an illustration of the importance of the solid to the attachment, consider Figure 3.15a which shows ϕ increasing with total amine concentration (as expected). Since γ_{LV} is the same in all cases ($t = 0$, $\gamma_{LV} = 72$ dyne cm^{-1}) the increase in ϕ must be the result of changes in the solid surface chemistry. The Zisman model appears to be quite useful in describing the effect of the solid on bubble-particle attachment. In the case of Figure 3.15a, the increase in ϕ could be ascribed to a decreasing value of γ_C as the total amine concentration is increased. Such a decrease is to be expected (at least until γ_C has been reduced to a minimum).

By noting the value of γ_{LV} at which pick-up ceases, a measure of γ_c for the particular conditions can be made. For magnetite conditioned for 30 min in 4.08×10^{-4} M amine at pH 9.7, from Figure 3.8A, $\gamma_c^{Fe_3O_4}$ is approximately 45 dyne cm^{-1}. For quartz under identical conditions, on the other hand, the conclusion must be from Figures 3.13 and 3.14 that $\gamma_c^{SiO_2}$ is less than 30 dyne cm^{-1}.

Thus we have:

$$\gamma_c^{Fe_3O_4} \sim 45 \text{ dyne cm}^{-1}$$

$$\gamma_c^{SiO_2} < 30 \text{ dyne cm}^{-1}$$

The difference in γ_c reflects the difference in mineral surface chemistry.

It must be emphasized that these results are for the specified conditions only and no suggestion of a measure of γ_c for magnetite and quartz as "pure" samples is implied. All things being equal, it may be speculated that γ_c for pure quartz is lower than for magnetite. The value of γ_c determined here must reflect not only the solid in question but also the extent and nature of the adsorbed species. Consequently, γ_c is expected to be a function of collector concentration, pH and conditioning time (if short). The property of γ_c, of course, remains unaltered, the value simply changes to reflect the conditions.

The described technique of estimating γ_c using dynamic γ_{LV} data appears to meet the main requirement of such determinations, namely that there be no interaction between the liquid and solid phases (31). In the present case, the solid is pre-conditioned so that interaction is permitted to approach equilibrium and γ_{LV} is subsequently varied by controlling the bubble age, not by altering either of the phases. The particular advantage from the flotation viewpoint is that it enables some estimate of the surface energy of the solid to be obtained under the exact conditions which render the solid amenable to flotation.

Figure 3.16 is included in an attempt to clarify the role of γ_c in describing the observed results. If the conditioned sample could be isolated from the conditioning solution and the solid surface examined by determining the variation in contact angle, θ, with the surface tension of various test liquids (liquids having no reaction with either the solid or adsorbed collector) the result may be as in Figure 3.16. This figure is a Zisman plot, except that the liberty has been taken of assuming a linear relationship between θ and γ_{LV} instead of the more general relationship between cos θ and γ_{LV} (31). The value of γ_c is determined as the value of γ_{LV} at $\theta = 0$. For magnetite this intercept would occur at $\sim$ 45 dyne cm^{-1}, and for quartz, say, at $\sim$ 30 dyne cm^{-1}. Determinations of γ_c in the presence of adsorbed collectors have been made (31,109).

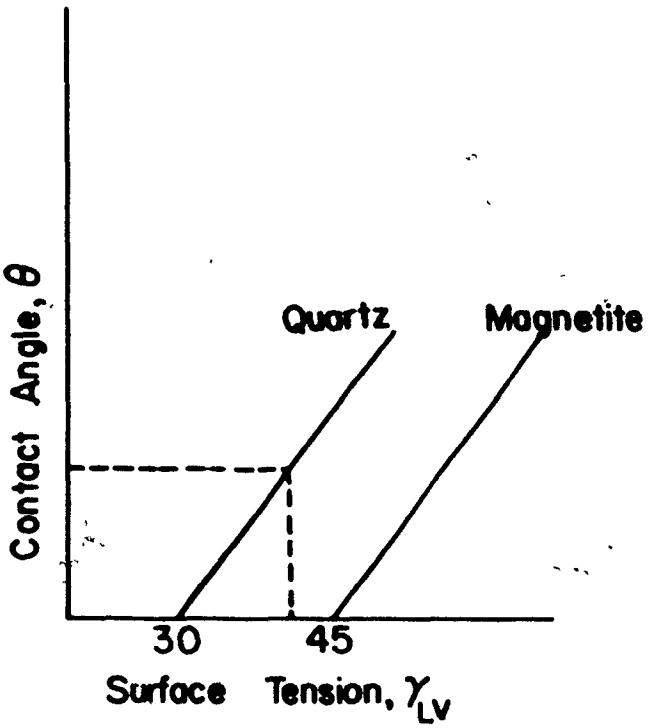

Figure 3.16 Diagrammatic Representation of Contact Angle as a Function of Surface Tension for Magnetite and Quartz conditioned for 30 min at 4.08×10^{-4} M Amine, pH 9.7

Figure 3.16 shows that if a liquid exerts a surface tension between $\gamma_c^{Fe_3O_4}$ and $\gamma_c^{SiO_2}$, a finite contact angle would develop on quartz whilst magnetite would remain wetted. (see dashed line on Figure 3.16). This same liquid, therefore, should yield a differential float, quartz reporting to the

floats and magnetite remaining as sinks. The implication is that, after conditioning a mixed sample of quartz and magnetite in 4.08×10^{-4} M amine at pH 9.7 for 30 min., then decanting the excess solution, a differential float of quartz can be effected if flotation is subsequently performed in a liquid exerting a surface tension between 30 and 45 dyne cm^{-1}. This possibility is worth investigating.

Figure 3.17 shows the result of such a procedure for a 35:65 w/w quartz:magnetite sample, the float being performed in methanol/water mixtures. These mixtures facilitated change of γ_{LV} and were completely miscible with the small quantity of conditioning solution unavoidably remaining after decantation. Up to 15% methanol, 100% recovery of both quartz and magnetite was obtained. Between 15% and 40% the magnetite recovery declined to zero with little apparent depression of the quartz; at $\sim$ 40%, nearly perfect separation was achieved. The γ_{LV} at 40% methanol is $\sim$ 40 dyne cm^{-1} (110), a value in the predicted range. At methanol concentrations greater than 65%, complete depression of both quartz and magnetite occurred.

It is more than probable that the presence of methanol not only caused a reduction in γ_{LV} but also increased γ_C by desorbing some of the adsorbed amine, methanol being an excellent solvent for molecular amine. For instance, flotation could not be regenerated after the test involving pure methanol by

FIGURE 3.17

Flotation Recovery of a 35/65 w/w Quartz/ Magnetite Mixture as a Function of Methanol Concentration after Conditioning at 4.08×10^{-4} M Amine, pH 9.7

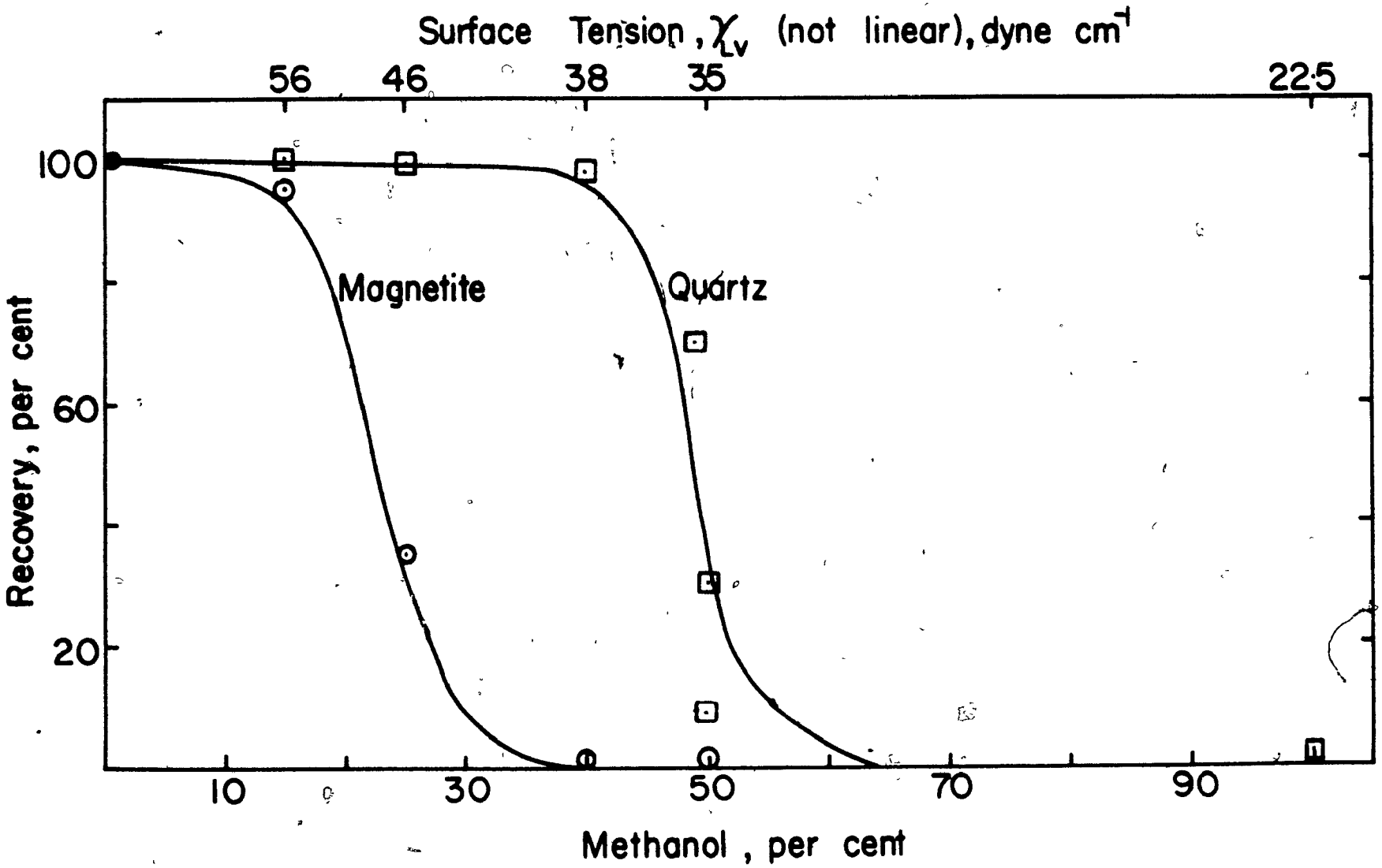
Surface Tension, γ_{Lv} (not linear), dyne cm^{-1}
56
46
38
35
22·5
100
60
20
Recovery, per cent
Magnetite
Quartz
10
30
50
70
90
Methanol, per cent

replacing by water as should be the case if γ_C remained unaltered.

An alternative procedure attempted was based on the ability to increase γ_C by desorbing some of the adsorbed collector. Figures 3.8 and 3.9 testify that desorption has an effect. If the desorption could be sufficiently well controlled such that $\gamma_C^{Fe_3O_4} > \gamma_{LV} > \gamma_C^{SiO_2}$ occurred then again, a differential float of quartz might be possible. Distilled water at pH 9.7 and 6.1 (natural pH) were employed as the desorbing medium. Table 3.1 gives the results.

TABLE 3.1

Controlled Desorption Using Distilled Water
Sample Conditioning: 4.08×10^{-4} M Amine, pH 9.7, 30 min

	Desorption	% Recovery in Floats	
		Silica	Magnetite
A	30 min, pH 9.7	100	80-90
B	30 min, pH 6.1, 1st cycle	100	60-70
C	30 min, pH 6.1, 2nd cycle	0	0

Somewhere between one and two desorption cycles employing "natural" distilled water a separation may be achieved. This procedure is similar, in principle, to the controlled adsorption advocated, for instance, by Marchandise (111). In practical terms, controlled desorption is probably more logical than employing alcohol/water mixtures as a medium for flotation.

The wetting model, especially the Zisman model has been shown to offer an explanation of the bubble aging phenomenon. However, two apparent contradictions remain. Firstly, the quartz sample, -65 + 100 mesh, gave results contrary to those reported by Smith and Lai (17) on a polished quartz specimen, and different too from those observed here for the glass* specimen. Since "smooth" surfaces are often prepared in order to investigate flotability such differences may be relevant. Secondly, the stability once contact had been achieved, although obviously vital to successful flotation is not immediately explicable and is again contrary to the observations of Smith and Lai (17). The following are tentatively proffered as explanations.

When a particle is contacted by a bubble, the bubble deforms. Deformation will also occur upon contacting a bubble with a flat specimen, but in the case of the particles, the deformation will probably be more pronounced. Upon deformation, the surface concentration of surfactant is locally decreased i.e. the surface tension is locally increased. An increase in γ_{LV} is favourable to de-wetting. As a consequence, particulate material may be easier to de-wet than flat specimens. This surface tension gradient will exist longer in solutions exhibiting slow adsorption characteristics because the local depletion is only slowly "repaired" by adsorption from the bulk

*frequently considered an approximation to quartz (e.g. ref. 4).

solution. The present system is, therefore, ideally suited. This property of a deformed bubble figures prominently in explaining the stability of froths, a subject which will be dealt with briefly in Chapter Five. The contradiction may well, therefore, be one of the physical contours of the surface. Buckenham and Rogers (112) in an earlier study of the quartz/alkaline dodecylamine system also noticed a discrepancy between contact angle and bubble pick-up data. The explanation was based on the irregular particles being able to reduce the induction time.

The explanation offered to account for the metastability of the bubble-particle adhesion once effected, also centers around the physical condition of the surface. A rough, irregular surface offers considerable resistance to the movement of the L-V interface across it, which is what is required if the adhesion is to fail with time. Thus although the wetting model may demand movement, the energy barrier associated with such movement may be sufficient to induce metastability. In the measurement of dynamic contact angles by Smith and Lai (17) it is notable that a well-polished specimen was employed and resistance due to roughness may be expected to lessen as a result. Buckenham and Rogers (112) noted no such "dynamics", indeed no other workers have in the much-studied dodecylamine system. The dynamic contact angles reported by Schulman and Leja (113) were in an entirely different system (polyoxyethylene

frothers). It is not unusual in contact angle work to attribute varying results for ostensibly equivalent systems to virtually unavoidable differences in surface preparation (114). The above discussion falls into that category.

Critical Surface Tension of Wetting and Flotation

Both the Harkins and Zisman wetting models predict the observed decrease in bubble pick-up with decreasing γ_{LV}. The Zisman model, however, proved simpler to use since only two energy terms, γ_{LV} and γ_C were involved. In the author's opinion, the Zisman model offers a number of advantages over the Harkins model.

Flotation, in the Zisman model, reduces to collision between a bubble exerting a certain surface tension, γ_{LV} and a solid whose critical surface tension of wetting is γ_C. If condition 1.5a is met flotation is possible, if condition 1.5b is met then flotation is impossible. The Zisman model emphasizes the relative surface energy of the bubble and solid prior to collision as opposed to the Harkins model which requires knowledge of the S-V interface, an interface which exists only after successful attachment has been achieved.

Another conceptual difficulty involved with the Harkins model surrounds the γ_{SL} term. Adsorption of surfactant at the S-L interface will tend to reduce γ_{SL}. Inspection of

Eqs. 1.2 and 1.3 show that a lowering of γ_{SL} is detrimental to flotation. Some workers (2-7) have circumvented the problem by assigning added adsorption at the S-V interface, thus lowering γ_{SV} to counterbalance the unfavourable decrease in γ_{SL} (and γ_{LV}, too). This argument has been advanced in other systems as well (8-10) and was considered in Chapter One. The bubble transfer model has been employed as a possible explanation of this added adsorption at the S-V interface. Not only does the present work fail to support the transfer model, but also the implication that adsorption at the S-L interface is undesirable is not tenable. Consider, for instance, the frequent need to condition the solid prior to flotation; conditioning involves the S-L interface almost exclusively. In the Zisman model adsorption would lower γ_c, and this is favourable to flotation.

The non-adhesion of bubbles exerting sufficiently low γ_{LV} values is explained using the Zisman model by stating that the γ_{LV} is below the critical value. In the Harkins model non-adhesion is predicted if γ_{LV} is less than $(\gamma_{SV} - \gamma_{SL})$. Taking $(\gamma_{SV} - \gamma_{SL})$ as a constant for the system, the Young equation gives a required reduction in γ_{LV} from 72 dyne cm^{-1} to 12 dyne cm^{-1} to accommodate the decline in θ from 80° to zero observed by Smith and Lai (17). The value of 12 dyne cm^{-1} is below that attainable in dodecylamine solutions. This observation led Smith and Lai (17) to argue that the dynamic contact

angle was partly caused by an increase in γ_{SV} (surfactant being "stripped off" by the retreating L-V interface). This would be detrimental to bubble-particle adhesion (see Eq. 1.2). Leja (21) in discussing the observations of Smith and Lai (17) considered the retreating bubble to be depositing a reversely oriented surfactant layer, thus increasing the "hydrophyllicity" of the solid surface. Both explanation however, depend on the bubble already being in retreat; any changes at the S-V and/or S-L interface must be the result of the bubbles' retreat, not its cause. This leaves a decreasing γ_{LV} to account for the dynamic θ values observed. This involved argument, invoking changes in the S-V and S-L interfaces, is a direct consequence of employing the Harkins model. The Zisman model offers a great simplification.

The critical surface tension of wetting can be measured. The present investigation has outlined a technique for determing γ_c under actual flotation conditions. This is a decided advantage over the Harkins model where γ_{SL} and γ_{SV} are recognized as indeterminate. In this respect, the Zisman model is less abstract than the Harkins model.

A working definition of the terms "hydrophobic" and "hydrophyllic", as they are employed in flotation, appears possible from introduction of the critical surface tension of wetting concept. Eq. 1.5a represents a hydrophobic condition, Eq. 1.5b a hydrophyllic one. This is felt to be important for, in flotation, reference is often made to rendering

a solid hydrophobic, meaning floatable, as if it were a property of the solid exclusively. However, a solid may well be water-repellent (the strict meaning of "hydrophobic") but not solution-repellent as required in flotation. In flotation, the term, it is claimed, refers to a relative property of the bubble (γ_{LV}) and solid (γ_C) such that γ_{LV} is greater than γ_C. Attempting to explain the transition from pick-up to non pick-up, described here, is impossible based on a concept of solid hydrophobicity. The successful flotation of magnetite using fresh bubbles at 4.08×10^{-4} M, pH 9.7 may be attributed to the fact that the fresh bubbles possess properties not too dissimilar from bubbles generated in surfactant-free water. In this sense, the solid surface will, therefore, appear hydrophobic. The bulk of flotation can be described in terms of solid hydrophobicity, but recognizing it as a relative property offers certain advantages. Control of γ_{LV} as well as γ_C to achieve the desired float is introduced; the differential float in the methanol/water mixture was a direct consequence.

Measurement of γ_C may prove useful in evaluating flotation reagents and in predicting possible flotation schemes. Changes in γ_C can be expected to reflect collector adsorption and any relevant chemical changes. The presence of amine-ion molecule complexes at pH 10 was considered a possible cause of the improved floatability of oxides at this pH; the extended

hydrocarbon chain of the complex would reasonably seem able to depress γ_c more than the simple amine ion. The concept (of γ_c) has expanded from the naturally low energy surfaces considered by Zisman to high energy surfaces through the work of Rhee (35,115,116) and others (117,118). Flotation dealing, mainly, with high surface energy solids converted to low energy surfaces by adsorption of surfactant suggests a closer analogy to the original work of Zisman. The concept has not been introduced into the flotation literature. Ginn (48) makes a passing reference to it and a recent paper by Parekh and Aplan (109) appears to deal with the topic but no details are available.

Few values of γ_c for solids treated by flotation are available. The γ_c for sulphur is quoted between 30 and 32 dyne cm^{-1} (119) depending on crystal structure. The γ_c of glass (frequently considered a reasonable approximation to quartz e.g. ref. 4) has been determined at 73 dyne cm^{-1} (118) although if the surface moisture was removed a value near 260 dyne cm^{-1} was obtained (118). The natural floatability of sulphur is supported by this data. Other naturally floatable substances could be tested e.g. talc, molybdenite, graphite, coal, etc. The higher surface energy solids ($\gamma_c > 72$ dyne cm^{-1}) present difficulties because liquids of γ_{LV} greater than the γ_c to be measured are required. The value of 73 dyne cm^{-1} for glass was determined using salt solutions. This increased the

surface tension of water sufficiently to yield finite contact angles. Incidentally, the improved flotation of coal in salt solutions (120,121) (so-called "salt flotation") may, in part, be due to the increase in γ_{LV} of such solutions. The higher γ_C for glass was determined using mercury and gallium as the liquid phases. The technique presented here utilizing dynamic surface tension data may have applications in other systems.

An assumption being made here is that γ_C measured by using dynamic γ_{LV} values is equivalent to the γ_C measured in a more conventional manner. Figure 3.16 makes this assumption. Confirmation of this assumption should be possible. Without alternate evidence, utilizing the critical surface tension of wetting concept of Zisman appears justified. Rance (122) has recently made a similar assumption in explaining the transition from a wetting to a non-wetting condition for ethanol on human hair at high relative humidity (50%). Initially, γ_{LV} of ethanol is less than the γ_C of human hair ($\sim$ 26 dyne cm^{-1} (122)) but, with time, absorption of atmospheric moisture occurs until γ_{LV} is raised above 26 dyne cm^{-1} and a finite contact angle is obtained. In general, the assumption that dynamic surface tension values exert the same properties (in this case wetting properties) as the equivalent equilibrium values is made, although this may not be recognized (55). Hansen and Wallace (55) seem to be the first to have raised the point. The validity of the assumption is still not known.

Induction Time and Interaction of Double Layer

Although the wetting models have proved very informative, the data would be well complemented by taking into account such factors as induction time and the interaction of the electrical double layers (that of the bubble and solid).

Induction time (or period) is the time required for the liquid film intervening between the bubble and solid to thin and rupture. Some workers have placed great importance on its role in flotation (22,121). It is possible that the induction time is sufficient to preclude bubble-particle attachment under actual flotation conditions even though the relative surface energies were favourable because of the limited bubble-particle contact time in a flotation cell. In the present case, the induction time was held more or less constant at a value (2-3 secs) well in excess of the probable available contact time so that the role played by the induction period is not known.

The interaction between the bubble and solid electrical double layers is considered to be a major factor in determining the flotation of fine particles (123). Much work has been directed towards understanding the double layer properties of the solid. However, comparatively little is known of the equivalent properties of the bubble. Even less is known of how the properties change with bubble age.

Recently, renewed interest in the bubble has prompted just such investigations (77,124). A technique for determining dynamic surface potentials is available (29).

In the present case, postulating that a build-up of surface charge on the bubble which is detrimental to bubble-particle attachment would offer, it seems, little improvement over the described wetting model. However, a surface charge model which predicted continued bubble-particle attachment even at low γ_{LV} might provide an alternative explanation to the continued pick-up of quartz with "aged" bubbles.

CHAPTER FOUR

ADSORPTION KINETICS

The dynamic surface tension data presented in Chapter Two must be the result either of a rate controlling diffusion process or of an energy barrier at the interface (25). In this Chapter, a diffusion model, based on the work of Fowkes (58) and Hansen (125,126) is developed to test the data.

Theory

Ward and Tordai (127) have developed the full solution to Ficks laws for adsorption into an interface with attendent "back-diffusion". The equation can be written:

$$\Gamma_t = 2\left(\frac{D}{\pi}\right)^{1/2} \left[C_o t^{1/2} - \int_0^{t^{1/2}} C_z \, d(t - z)^{1/2}\right] \quad \ldots 4.1$$

where Γ_t = surface concentration of solute (mole cm^{-2}) at time t

D = diffusion coefficient ($cm^2 sec^{-1}$), assumed constant

C_o = bulk concentration (mole cm^{-3})

C_z = concentration "just below" the surface at time "z" (sometimes called the sub-surface concentration (127), where z is a variable (127)).

The derivation of Eq. 4.1 (the "Ward and Tordai" equation) is well documented in the literature (13, 125, 127, 128). From the experimental dynamic surface tension curves and knowledge of the equilibrium surface tension/concentration relationship, an average value of the diffusion coefficient over a time interval t can be determined. If the calculated diffusion coefficient is not a function of time or bulk concentration and is in the classical range of 10^{-5} to 10^{-6} cm^2 sec^{-1} diffusion control is deemed proved (127). The details of the necessary calculations are given in the literature (24, 47, 55, 56, 127). Since, in the present case, the equilibrium surface tension/concentration relationship is not known, this procedure of testing for diffusion-control cannot be used. In addition, Hansen (126) and later Tsonopoulos et al (13), note that calculation of an average diffusion coefficient maybe misleading A more powerful test is to predict the dynamic surface tension data for given conditions and compare with the measured values.

a) Short-Time Solution

Assuming that the subsurface concentration approaches zero then Eq. 4.1 reduces to the Langmuir-Shaefer (129) equation.

$$\Gamma_t = 2C_o \left(\frac{Dt}{\pi}\right)^{1/2} \quad \text{.....4.2}$$

The stated assumption is approached only when the surface is "fresh", hence "short-time solution".

To use Eq. 4.2 an adsorption isotherm is required. Two have been employed, the Langmuir-Syskowski isotherm (130) and one derived thermodynamically by Fowkes (131). The basic assumption is that any adsorption isotherm valid for the equilibrium condition will also be valid under dynamic conditions, the bulk concentration term being replaced by the sub-surface concentration.

i) Langmuir-Syskowski Isotherm

The Langmuir equation can be written

$$\Gamma_t = \frac{a\,\Gamma_m\,C_t}{1 + aC_t} \qquad \text{.....4.3}$$

where Γ_m = monolayer surface concentration (mole cm^{-2})

a = Langmuir constant (cm^3 $mole^{-1}$)

Assuming $C_t \rightarrow 0$, Eq. 4.3 becomes:

$$\Gamma_t = a\,\Gamma_m\,C_t \qquad \text{.....4.3a}$$

sometimes called the "linear adsorption isotherm".

The Syskowski equation relates the surface tension to the solute concentration. Modifying for the dynamic case:

$$\gamma_o - \gamma_t = \Gamma_m RT \ln (1 + aC_t) \qquad \text{.....4.4}$$

where γ_o = solvent surface tension (dyne cm^{-1})

R = gas constant (8.31×10^7 erg $mole^{-1} {}^oK^{-1}$)

T = absolute temperature (298 ^oK)

When $C_t \rightarrow 0$, the logarithm expansion can be truncated to:

$$\gamma_o - \gamma_t = a \Gamma_m RT C_t \quad \text{.....4.4a}$$

Combining Eqs. 4.3a and 4.4a and substituting into Eq. 4.2 gives:

$$\gamma_o - \gamma_t = 2RT C_o \left(\frac{Dt}{\pi}\right)^{1/2} \quad \text{.....4.5}$$

A linear relationship between γ_t and $t^{1/2}$ is predicted, which is subject to experimental verification. From the slope, knowing C_o, D can be calculated. Showing that D is independent of C_o and has a value between 10^{-5} to 10^{-6} cm^2 sec^{-1} would support a diffusion control model. In the present case, neither C_o nor D are known. At best a value of $C_o(D)^{1/2}$ can be calculated.

An important limitation on the use of Eq. 4.5 is the requirement that the Langmuir-Syskowski relationship be satisfied. Non-ionic surfactants tend to meet the requirement (25, 130, 132). Dodecylamine acetate at natural pH has also been shown to obey the Syskowski equation (133). Also, the assumption that the sub-surface concentration must approximate zero is shown in Appendix III.1 to be valid only for $(\gamma_o - \gamma_t) < 3$ dyne cm^{-1}. Despite this limitation, Eq. 4.5 has been employed

for surface tension depression up to 20 dyne cm^{-1} (59,65). In the present case the bulk of the data refers to $(\gamma_o - \gamma_t) > 3$ dyne cm^{-1}.

ii) Fowkes Isotherm

In a surface layer of component 1 adsorbed from solvent 2 (in this case water), the mole fraction of solvent, x_2, in the surface is related to the decrease in surface tension by (131) (modified for dynamic case (58)):

$$\gamma_o - \gamma_t = -\frac{RT}{N\sigma_2} \ln x_2 \quad \ldots\ldots\ldots\ldots 4.6$$

where σ_2 = average partial molecular area of the solvent over the range of surface tension, γ_o to γ_t (cm^2). For water σ_2 = 9.7 - 10.0 $\AA^2$ (58).

N = Avogadro's number (6.025×10^{23})

By definition

$$\Gamma_t = \frac{1}{N A_1} \times 10^{16} \quad \ldots\ldots\ldots\ldots 4.7$$

where A_1 = area per adsorbed molecule ($\AA^2$)

A_1 is given by:

$$A_1 = \sigma_1 + \left(\frac{x_2}{1 - x_2}\right) \sigma_2 \quad \ldots\ldots\ldots\ldots 4.8$$

where σ_1 = the area occupied by a solute molecule or ion in the surface ($\AA^2$)

Combining Eqs. 4.7 and 4.2 gives

$$C_o(Dt)^{1/2} = \frac{\pi^{1/2}}{2NA_1} \times 10^{16} \qquad \text{.....4.9}$$

Knowing σ_1 and solving Eqs. 4.6, 4.8 and 4.9 for various values of x_2, the relationship between γ_t and A_1 and $C_o(D)^{1/2}$ can be computed. The graphs of γ_t vs A_1 and γ_t vs $C_o(Dt)^{1/2}$ are given in the Appendix. By comparing the numerically obtained γ_t vs $C_o(Dt)^{1/2}$ curve with the experimental γ_t vs $t^{1/2}$ curve, a value of $C_o(D)^{1/2}$ at any t can be estimated. If $C_o(D)^{1/2}$ is not a function of t then diffusion-control is indicated. In the only previous such use of the Fowkes isotherm (58), a good fit with the model was obtained for values of $(\gamma_o - \gamma_t)$ up to 20 dyne cm^{-1}. This is a considerable extension of the range permitted by the Langmuir-Syskowski relationship.

b) Long-Time Solution

This solution is due to Hansen (126). Assuming that $\Gamma_t \rightarrow \Gamma_e$, where Γ_e is the equilibrium surface concentration, the Ward and Tordai equation yields:

$$\frac{C_t}{C_o} = 1 - \frac{\Gamma_e}{C_o(\pi Dt)^{1/2}} \qquad \text{.....4.10}$$

Eq. 4.10 is sometimes referred to as the "Hansen assymptotic solution". Γ_t approaches Γ_e only if the surface is aged, hence the "long-time solution".

Modifying the Gibbs adsorption isotherm to the dynamic case, the following treatment is possible.

$$\Gamma_t = - \frac{C_t}{RT} \frac{\partial \gamma_t}{\partial C_t} \qquad \text{.....4.11}$$

Thus

$$\int_{\gamma_\infty}^{\gamma_t} d\gamma_t = - RT \int_{C_o}^{C_t} \Gamma_t \frac{dC_t}{C_t} \qquad \text{.....4.11a}$$

Assuming $\Gamma_t \longrightarrow \Gamma_e$ (a constant), and integrating

$$\gamma_t - \gamma_\infty = - \Gamma_e RT \ln \left(\frac{C_t}{C_o}\right) \qquad \text{.....4.11b}$$

Substituting Eq. 4.10 into 4.11b gives:

$$\gamma_t - \gamma_\infty = - \Gamma_e RT \ln \left[1 - \frac{\Gamma_e}{C_o(\pi Dt)^{1/2}}\right] \qquad \text{.....4.12}$$

For large values of t, the expansion can be simplified to the first term:

$$\gamma_t - \gamma_\infty = \frac{\Gamma_e^2 RT}{C_o(\pi Dt)^{1/2}} \qquad \text{.....4.13}$$

Hansen notes that Eq. 4.13 is valid only for values of $(\gamma_t - \gamma_\infty)$ less than 3 dyne cm^{-1}. The reasoning behind this limitation is given in Appendix III.2.

Equation 4.13 is not dependent on the applicability of a particular adsorption isotherm, being derived from the Ward and Tordai and Gibbs equations both of which make no assumptions concerning the adsorption isotherm operating. Consequently the determination of the stated limitation on the use of Eq. 4.13 which involves the Langmuir-Syskowski expression maybe a little misleading.

The linearity indicated by Eq. 4.13 is subject to experimental verification. From the slope, knowing Γ_e, $C_o(D)^{1/2}$ can be calculated. In the present case, Γ_e is not known under all conditions. However, Γ_m, the monolayer surface concentration can be calculated from the value of σ_1 introduced previously. Equation 4.13 can be modified by introducing the approximation $\Gamma_e \rightarrow \Gamma_m$ valid for $(\gamma_o - \gamma_\infty) > 35$ dyne cm^{-1} (as shown in Appendix III.3).

Values of $C_o(Dt)^{1/2}$ can, therefore, be calculated using the short-time and the long-time solutions. The values should be the same. From the estimated $C_o(D)^{1/2}$ value a numerical plot of γ_t vs $t^{1/2}$ can be constructed and tested against the experimental data.

Results and Discussion

The time-dependent surface tension of dodecylamine acetate solutions exhibited at pH 9.85 $\pm$ 0.05 (see Figure 2.7) will be examined. The data covers a wide range of amine

concentration and includes data where $(\gamma_o - \gamma_t)$ is greater than 35 dyne cm^{-1}, enabling the modified long-time solution to be used.

Since the bulk of the data refers to $(\gamma_o - \gamma_t) > 3$ dyne cm^{-1}, the short-time solution using the Fowkes isotherm was employed. Figure 4.1 gives the experimental plot of γ_t vs $t^{1/2}$. The suggested shape is similar to that shown by Fowkes (58).

In order to perform the necessary calculations to determine the constant, $C_o(D)^{1/2}$, σ_1 must be known. A value of 26.5 $\mathring{A}^2$ has been given for dodecylamine (133), a value supported by previous work in this laboratory (47). Fowkes (58) reports the same value for another 12-carbon surfactant, sodium dodecyl sulphate. The work of Finch (47) and Ruch and Bartell (134) indicates that σ_1 for amines is independent of pH. Hence, $\sigma_1 = 26.5$ $\mathring{A}^2$ is taken as valid at pH 9.85. Clearly, the result of using this estimate can only be as reliable as the estimate itself.

Substituting the known values, the following was obtained:

from Eq. 4.6

$$\gamma_t = 41.7 \ln x_2 + 72.0 \quad \text{.....4.6a}$$

from Eq. 4.8

$$A_1 = 26.5 + \left(\frac{x_2}{1 - x_2}\right) 9.8 \quad \text{.....4.8a}$$

FIGURE 4.1

Comparison of Numerical and Experimental Plot of γ_t vs $t^{1/2}$ for Dodecylamine Solutions at pH 9.85 at Various Concentrations

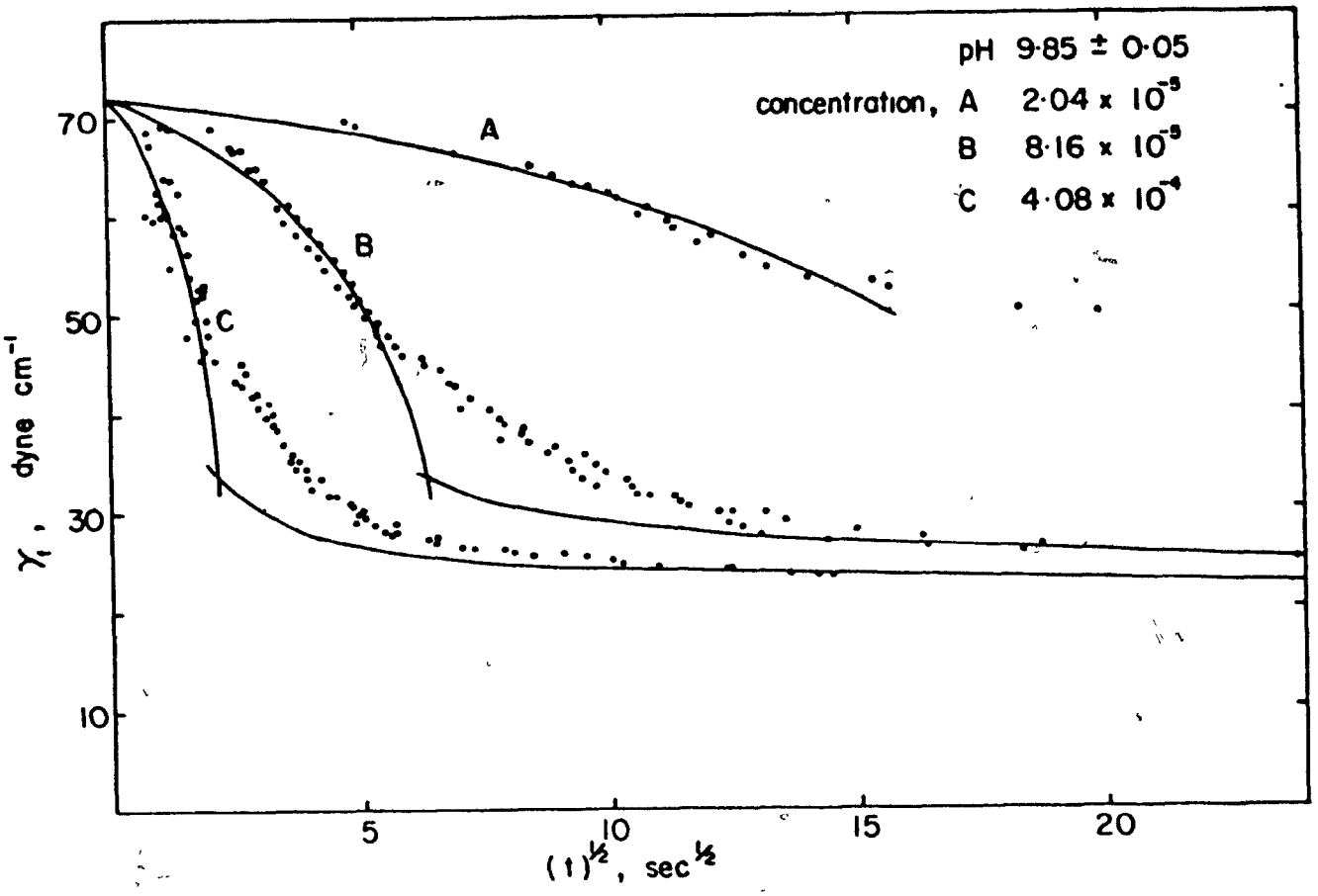
pH 9·85 ± 0·05
concentration, A 2·04 x 10⁻⁵
B 8·16 x 10⁻⁵
C 4·08 x 10⁻⁴
A
B
C
70
50
30
10
γt , dyne cm⁻¹
5
10
15
20
(t)½ , sec½

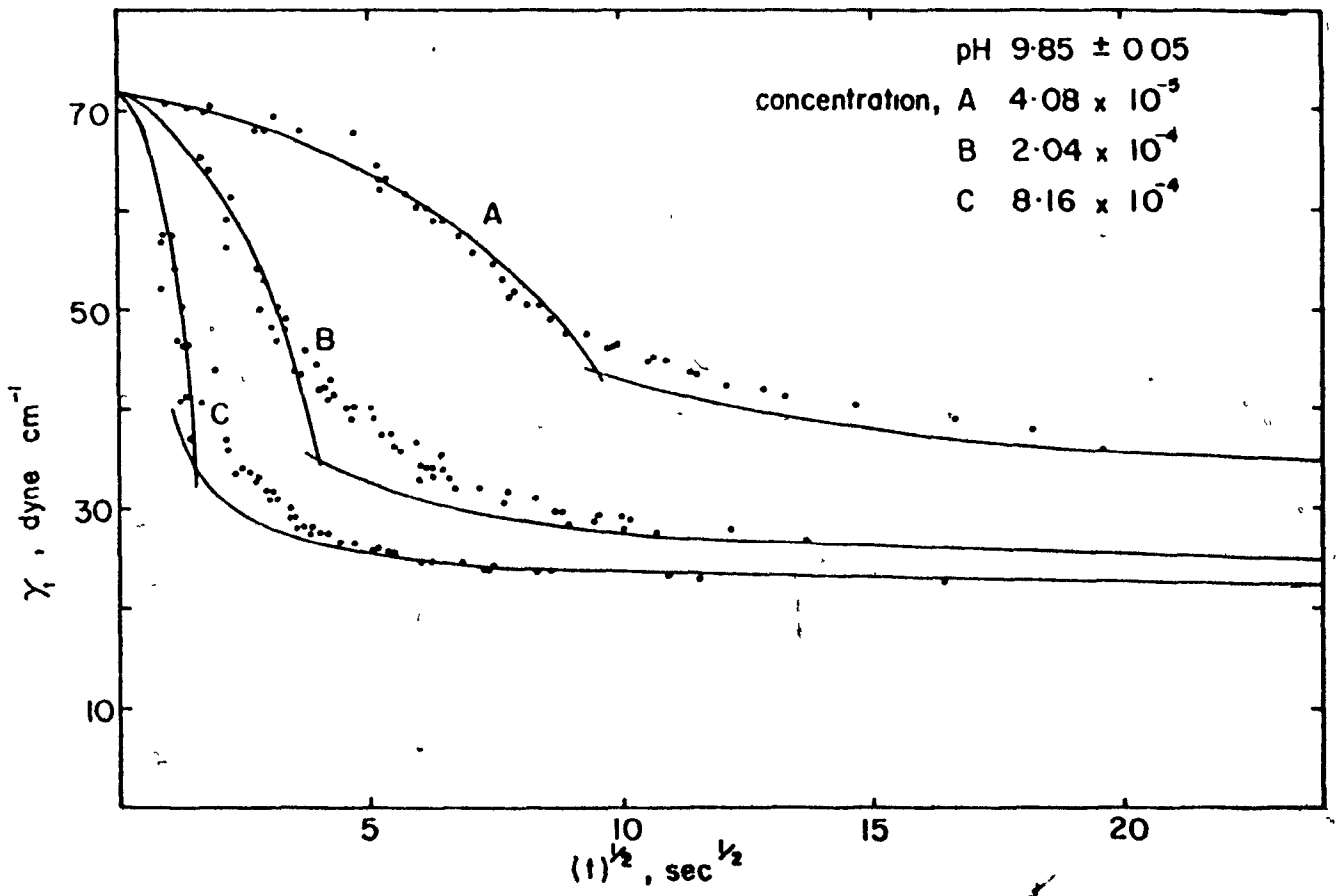
pH 9·85 ± 0·05
concentration, A 4·08 x 10⁻⁵
B 2·04 x 10⁻⁴
C 8·16 x 10⁻⁴
A
B
C
70
50
30
10
γt , dyne cm⁻¹
5
10
15
20
(t)½ , sec½

from Eq. 4.9

$$C_o(Dt)^{1/2} = \left(\frac{147}{A_1}\right) \times 10^{-10} \quad \text{.....4.9a}$$

The numerical solutions to these equations, including graphical relations, are given in Appendix III.4. From the comparison of the numerical solution with the experimental curves, values of $C_o(D)^{1/2}$ were calculated (see Appendix III.5). Up to $(\gamma_o - \gamma_t) = 20$ dyne cm^{-1}, $C_o(D)^{1/2}$ was constant within $\pm$ 10%. The "average" $C_o(D)^{1/2}$ value is given in Table 4.1.

Since σ_1 is 26.5 $\mathring{A}^2$, Γ_m is 6.3×10^{-10} mole cm^{-2}. Consequently, Eq. 4.13 becomes:

$$\gamma_t = \frac{55.5 \times 10^{-10}}{C_o(Dt)^{1/2}} + \gamma_\infty \quad \text{.....4.13a}$$

The slope ($55.5 \times 10^{-10}/C_o(D)^{1/2}$) and γ_∞ were determined by a linear regression analysis performed on the data within the range $(\gamma_t - \gamma_\infty) < 6$ dyne cm^{-1} (see Appendix III.6). The results are given in Table 4.1. This limitation was too severe in the case of 4.08×10^{-5} M amine solutions (although the result is included). No result is given for 2.04×10^{-5} M solutions because the restriction that $(\gamma_o - \gamma_\infty)$ be greater than 35 dyne cm^{-1} (in order for $\Gamma_e \rightarrow \Gamma_m$) did not hold.

TABLE 4.1

Calculated Values of $C_o(D)^{1/2}$

Concentration $C \times 10^5$ M	$C_o(D)^{1/2} \times 10^{10}$ mole cm^{-2} $sec^{-1/2}$ (±10%)			
	t-short		t-long	"Best" Value*
	Langmuir/ Syskowski	Fowkes		
2.04	0.24	0.22	--	0.22
4.08	0.43	0.42	0.30	0.42
8.16	0.71	0.69	0.65	0.69
20.4	1.25	1.25	0.96	1.15
40.8	1.85	2.32	1.31	2.05
81.6	3.04	3.11	2.05	2.75

*value used to calculate numerical γ_t vs $t^{1/2}$ relationship - see Figure 4.1

As Table 4.1 illustrates, the calculated values of $C_o(D)^{1/2}$ from the t-short and t-long cases agree reasonably well. This agreement, plus the constancy of $C_o(D)^{1/2}$ in the t-short case suggests a diffusion-controlled process. The tendency for the t-long solution to yield lower $C_o(D)^{1/2}$ values than the t-short solution may be related to the requirement that γ_t be close to γ_∞ to utilize Eq. 4.13. Taking too large a range of $(\gamma_t - \gamma_\infty)$ tends to increase the slope, hence decrease the calculated $C_o(D)^{1/2}$. Bendure (65), using the

same t-long solution, noted that the calculated values of D for a series of non-ionic surfactants were low in comparison with the "classical" range. In that work, no limitation on the applicability of Eq. 4.13 was included. The need to be aware of the limitations must be stressed.

The "best" values given in Table 4.1 are the values used in producing the numerical γ_t vs $t^{1/2}$ curves, shown as solid lines in Figure 4.1. For the t-short solution, the appropriate value of $C_o(D)^{1/2}$ was substituted into Eq. 4.9a, A_1 calculated as a function of $t^{1/2}$ and γ_t estimated from the γ_t vs A_1 curve. In the case of the t-long solution, the appropriate $C_o(D)^{1/2}$ and γ_∞ values were substituted into Eq. 4.13a and γ_t as a function of $t^{1/2}$ calculated directly (see Appendix III.7).

Figure 4.1 demonstrates a good fit between the numerical solution and the experimental data. Figure 4.1 also illustrates the agreement between the t-short and t-long solutions since the same value of $C_o(D)^{1/2}$ was used in both sets of calculations. Only at intermediate times do the experimental data deviate significantly from the theoretical curves. This is expected because of the restrictions placed on the t-short and t-long solutions.

The numerical fit to the data enables the γ_t vs $t^{1/2}$ relationship to be extrapolated to $t^{1/2} = 0$, i.e. $\gamma_t = \gamma_o = 72$ dyne cm^{-1}. By taking the limiting slope, it should be possible

to estimate $C_o(D)^{1/2}$ from Eq. 4.5 i.e. the t-short solution using the Langmuir-Syskowski isotherm. The estimate of the slope is given in Appendix III.8. The value of $C_o(D)^{1/2}$ is included in Table 4.1. The value closely agrees with those given by the other two techniques.

The indication is that the time-dependent surface tension exhibited by dodecylamine salt solutions at pH 9.85 is the result of a diffusion controlled adsorption process. This supports the qualitative reasoning given in Chapter Two concerning the extended "diffusion" path of non-ionic surfactants in comparison with ionic surfactants. However, without an independent measurement of C_o or D to check against the estimated $C_o(D)^{1/2}$ value, the diffusion-control model cannot be considered proved. The analysis probably represents the nearest one can come to such proof in a system about which so little is known. An attempt was made to measure D using a Zeiss diffusion apparatus with Schlieren optics. However, the solution proved too dilute ($C < 10^{-4}$ M to avoid precipitation) for the necessary difference in refractive index to be identified. Also, the D for the surface active species alone is required, the proposed technique could only give an average value reflecting all the various species present.

As stated, in order to use the Fowkes isotherm, σ_1 must be known. However, the analysis appears relatively insensitive to this quantity. For $\sigma_1 > 26.5$ $\mathring{A}^2$, the γ_t vs

$C_o(D)^{1/2}$ curve shifts to the left, resulting in lower estimates of $C_o(D)^{1/2}$. In addition, Γ_m becomes less than 6.3×10^{-10} mole cm^{-2} so that the estimate of $C_o(D)^{1/2}$ using Eq. 4.13a also decreases. Within $\pm$ 10%, variation in τ_1 probably would not alter the agreement with the diffusion model.

With knowledge of D, C_o could be calculated. Comparing this value of C_o with the known total amine concentration, C, the percent of C actually responsible for the observed surface activity could be estimated. This would help in elucidating the nature of the surface active species (free amine or complexes). This is an extension of the work of Fowkes who estimated the molecular weight of the surface active species from a determination of the dynamic surface tension. Figure 4.2 shows a plot of $C_o(D)^{1/2}$ vs C. The curve approaches linearity as C approaches 0. The limiting slope (at $C < 6 \times 10^{-5}$ M) is $K'(D)^{1/2}$ where K' is C_o/C, a measure of the percent amine present as the surface species. At such low concentrations, K' has meaning because at pH 9.85, the solution is free of precipitated amine. From the literature, assuming a similar diffusivity for dodecylamine and dodecyltrimethylamine in aqueous solution, then the diffusion coefficient (at natural pH) lies in the range 2 to 8×10^{-6} cm^2 sec^{-1} (135).

FIGURE 4.2

$C_o(D)^{1/2}$ as a Function of C

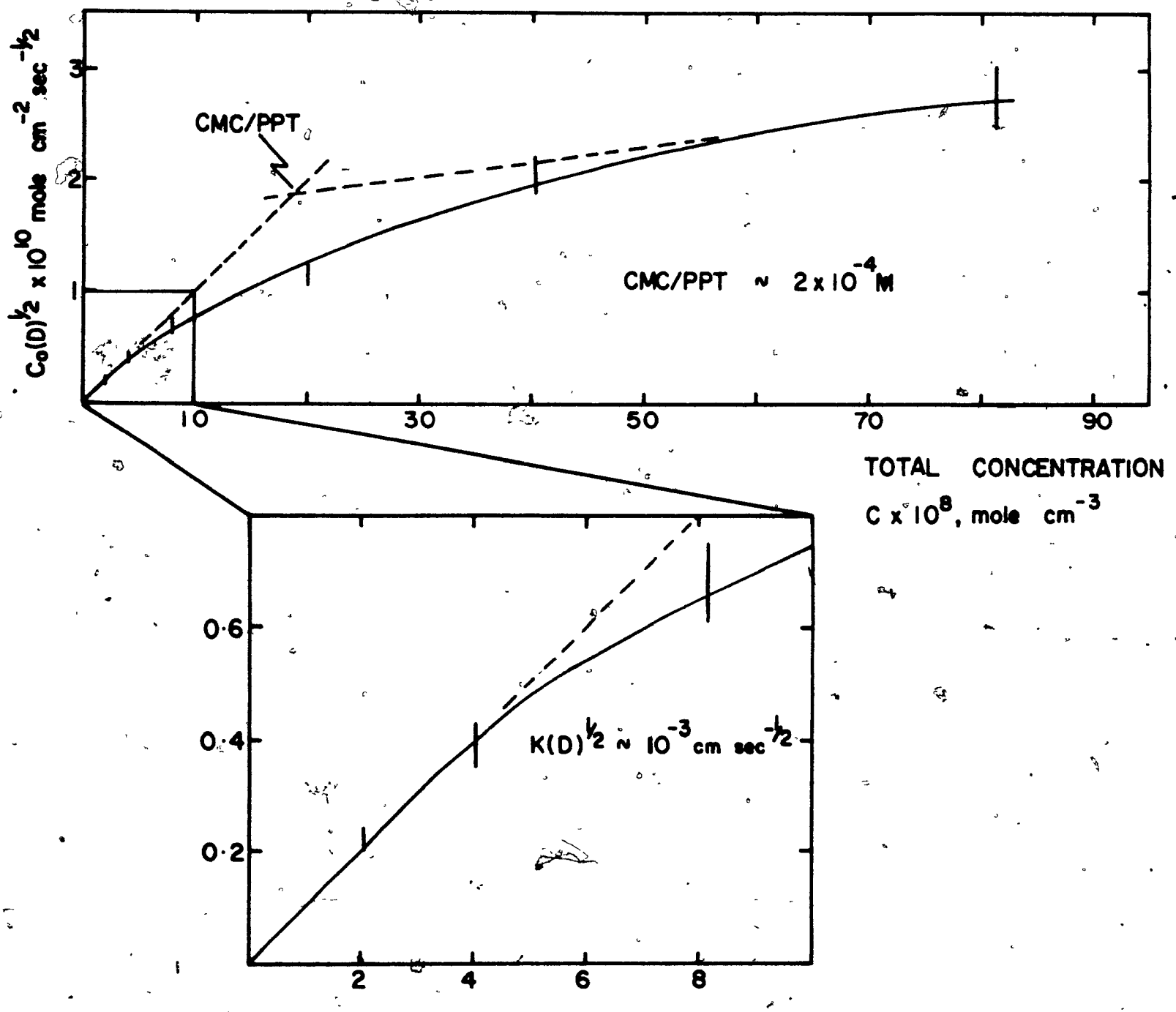
$C_0(D)^{1/2} \times 10^{10}$ mole cm^{-2} sec$^{-1/2}$
CMC/PPT
CMC/PPT ~ 2×10^{-4} M
1
2
4
10
30
50
70
90
TOTAL CONCENTRATION
C x 10^8, mole cm^{-3}
0·6
0·4
0·2
$K(D)^{1/2} \sim 10^{-3}$ cm sec$^{-1/2}$
2
4
6
8

The higher value indicates free ions, the lower, micelles. This range seems applicable in the present case, the nature of the surface active species at pH 9.85 being anything from free amine upto a proposed complex of six ions and molecules. The estimated $K'(D)^{1/2}$ is $\sim 10^{-3}$ cm $sec^{-1/2}$. Taking the quoted range of D, K' lies in the range ~35% to ~70%. At pH 9.85, the amine is present as 15% free amine and 85% amine ion, according to Figure 2.11. Assuming all the free amine is complexed and that this does not invalidate the calculation, then the range of K' corresponds to an x/y (RNH_3^+/RNH_2) ratio in the complex of from 1:1 to 3:1. This is similar to that determined from a measure of the "optimum" pH.

Included in Figure 4.2 is the intercept between the two limiting slopes. This intercept may have meaning as either the critical micelle concentration (cmc) or the precipitation concentration (ppt). The intercept is at approximately 2×10^{-4} M. The difficulty in distinguishing the cmc from the ppt in alkaline dodecylamine solutions has already been discussed (47). The cmc/ppt value is close to the calculated ppt; taking the results of Manser (94), the value is also close to the cmc.

The data shows an encouraging internal consistancy. Clearly a value of the diffusion coefficient would be most useful. A measure of the diffusion coefficient plus deter-

mination of the dynamic surface tension (so long as the rate of adsorption is diffusion-controlled) may provide a valuable tool in assessing the solution chemistry of flotation systems.

CHAPTER FIVE

OTHER SYSTEMS

This Chapter outlines briefly some other systems in which dynamic surface properties may play a role.

In any liquid, introduction of a fresh interface (another liquid or vapour) will produce a dynamic effect. This reflects the time required for readjustment of the interfacial molecules to the new equilibrium conditions. As well as surfactant solutions, dynamic effects have been noted in inorganic electrolyte solutions (77) and in pure water (136-138). The dynamic surface tension reported for pure water (136-138) has recently been questioned (13,74). Tsonopoulos et al (13) have calculated t_∞ for pure water is less than 10^{-9} sec, beyond the capabilities of present measuring techniques.

Flotation

Of major importance to the flotation industry are xanthate collectors. These substances demonstrate little surface tension depression over the concentration range of practical importance (139-142) (upto 100 mg. litre^{-1}). The indication (139-141) is that equilibrium is attained rapidly, although time effects have been noted in the interfacial tension of pine oil-water in the present of xanthate (139). The effect

of dixanthogen, an oxidation product of xanthate ion, on the solution surface tension may be worth studying in view of the controversy over the role of dixanthogen in flotation (143-145). Leja and Schulman (43) reported an increase in surface pressure of a xanthate film, which was attributed to oxidation to dixanthogen. Similar considerations may apply to dithiophosphates (146).

Other frequently used collectors are fatty acids and their salts. Powney (76) and recently Cante et al (147) have shown a similar pH dependence of the surface tension of laurate solutions to that shown here for dodecylamine. The minimum surface tension occurred around pH 7.8-8.0. Figure 5.1a gives the dynamic surface tension of 3.5×10^{-3} M (0.1%) sodium laurate solutions at pH 7.6 and 9.5, determined by the procedure outlined in Chapter Two. The increase in γ_∞ with pH is clearly shown. Upon adding acid to the natural solution a dense precipitate of lauric acid formed; the dynamic surface tension became erratic.

In studying flotation, frequently the collector alone is considered. However, the presence of modifying agents and frothers can control flotation. The presence of neutral molecules has been observed to promote flotation in certain systems (17,78,112,148), sometimes with accompanying dynamic effects (17,148). Somasundaran and Moudgil (148) have reported an improvement in the flotation of alumina using sodium dodecyl sulphate in the presence of dissolved hydrocarbons (methane and

FIGURE 5.1

a) Dynamic Surface Tension of 0.1% Sodium Laurate Solution at pH 7.6 and 9.5

b) Dynamic Surface Tension of Pine Oil-Amine Mixtures at Natural pH

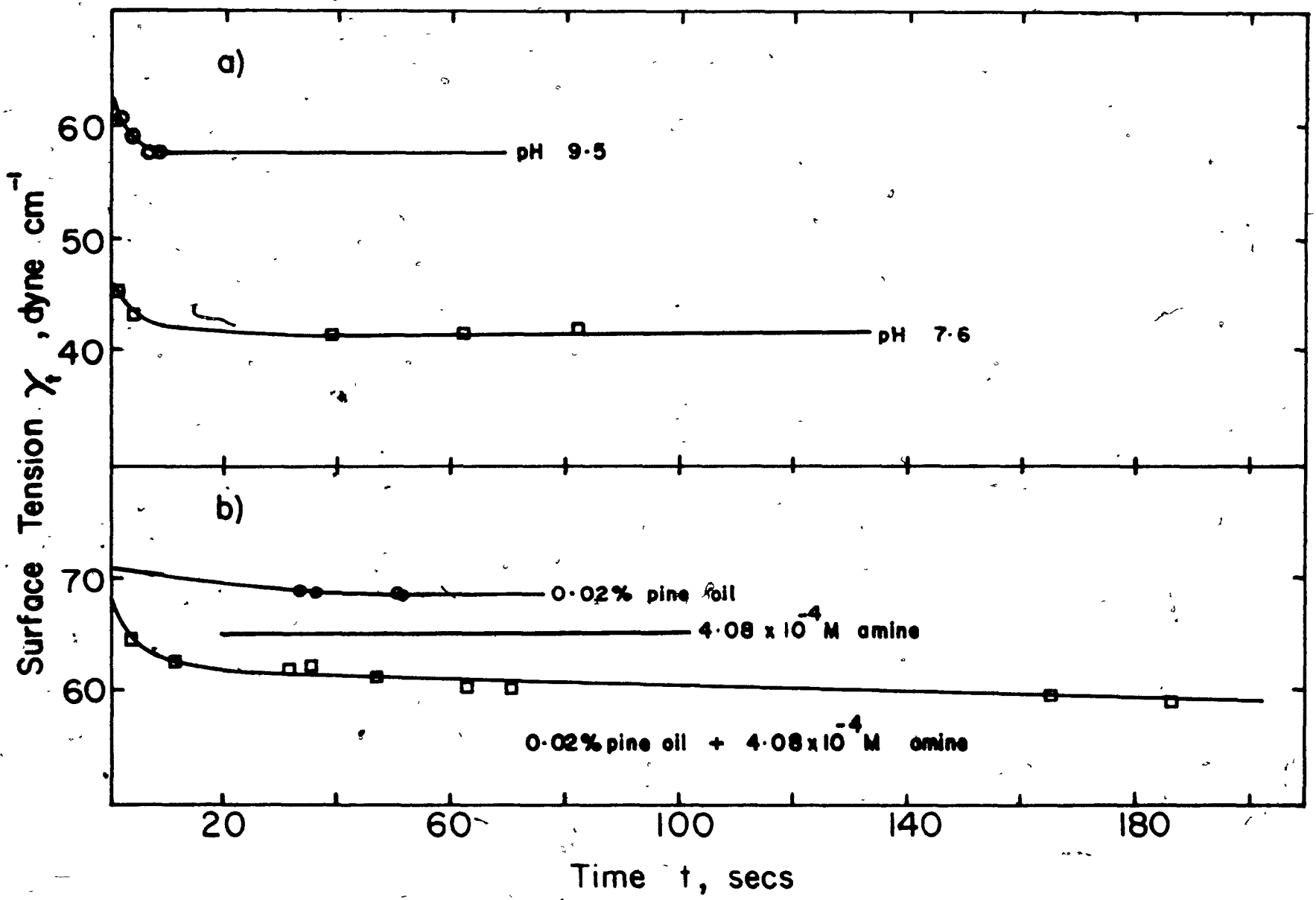
a)
b)
pH 9·5
pH 7·6
0·02% pine oil
4·08 x 10⁻⁴ M amine
0·02% pine oil + 4·08 x 10⁻⁴ M amine
Surface Tension χt, dyne cm⁻¹
Time t, secs
60
50
40
70
60
20
60
100
140
180

butane); a pronounced dynamic surface tension was also reported. Smith and Lai (17) observed dynamic contact angles in dodecylamine solutions at pH less than 9 in the presence of dodecyl alcohol. Buckenham and Rogers (112) demonstrated improved floatability of quartz using a dodecylamine collector in the presence of pine oil as frother at pH 4.1. Figure 5.1b shows the effect of adding pine oil to natural solutions of dodecylamine acetate. A depression of γ_∞ and an increase in t_∞ is observed in comparison with the pine oil or amine alone. Inorganic ions are also known to affect flotation recovery and an effect on the adsorption kinetics is to be expected (73).

Foams and Detergents

In order for a froth to resist deforming forces* a force opposing the deformation must be established. Gibbs (149) proposed that a surface tension gradient could supply this force, a proposition which has been frequently endorsed (26,27,73,150-154). Upon deformation, a local increase in length of the surface occurs with a consequent local decrease in the surface concentration of surfactant. This results in a surface tension gradient away from the point of maximum deformation i.e. a force opposing the deformation is generated.

*resulting from thermal or mechanic shock or film-drainage.

The faster the surface tension gradient is destroyed by adsorption of surfactant from the bulk solution, the less effect this restoring force will have. One measure of the rate of adsorption is the dynamic surface tension. Bickerman (151) and Burcik (73) have shown a correlation between increased froth stability and a slow rate of surface tension depression. Many workers consider the slower the rate the better (151-154), although Burcik (73) favours a "moderate" rate. The fast rate in pure liquids supports the poor foam stability observed.

Dervichian (153) and Donnan (154) have shown that maximum foam stability was attained at a concentration of surfactant such that $[\gamma_{t\to o}/\gamma_{\infty}]$ was a maximum. Clearly, the lower γ_{∞} the greater the surface tension gradient produced. However, that a low γ_{∞} alone can characterize frothing has been discredited on many occasions. Consider the change in γ_{∞} and froth stability upon ethanol additions to water. Bickerman (151) notes that foam exhibiting the longest collapse-time gave γ_{∞} values in the range 54-70 dyne cm^{-1}. In flotation, good frothing is achieved with pine oil additions causing only slight surface tension depression (140) (see Figure 5.1b).

In addition to his contribution to the theory of foaming, Burcik (73) also demonstrated a correlation between dynamic surface tension and detergency. As the rate of surface tension depression increased so too did the detergency, i.e. the ability to remove "soil" from cloth. This remained the

case whether the change in surface tension depression was effected by temperature or pH change, or the addition of inorganic salts.

Summary

Any process which involves the creation of fresh interfaces warrants investigation of the adsorption kinetics. This is especially so when surface active substances are present. In many instances, the desirable property of the system is provided by the adsorption kinetics displayed.

CHAPTER SIX

CONCLUSIONS; CLAIMS TO ORIGINAL RESEARCH; SUGGESTIONS FOR FUTURE WORK

Conclusions

Chapter One

The wetting and transfer models of flotation can be tested from a knowledge of the dynamic surface tension.

Chapter Two

1. The technique of Kuffner provides a simple method for determining dynamic surface tension.

2. The dynamic surface tension of dodecylamine acetate solutions is strongly pH-dependent between pH 7 and 13; up to pH 10, t_∞ increases; γ_∞ decreases, at pH > 10, t_∞ decreases and γ_∞ increases. A maximum surface activity is displayed between pH 9.5 and 10.5.

3. The dynamic surface tension is relatively insensitive to the presence of ions other than hydroxyl ions.

4. The pH-dependence is explained by assuming that an RNH_3^+-RNH_2 complex is the dominant surface active species present in solution. The free amine, RNH_2, is either poorly surface active or is present mainly in the hydrated form, RH_2NHOH at pH > 10.5.

5. The RNH_3^+/RNH_2 ratio in the complex is estimated between 1:1 and 5:1. This estimate assumes no surface pH effects, hydration reactions or that the simple hydrolysis model is affected by generation of this complex (not necessarily valid).

6. The similarity between the "optimum" pH and the natural pH of free, saturated dodecylamine solutions is considered to be the result of complex formation.

7. The dynamic contact angle observed by Smith and Lai (17) in the dodecylamine/quartz system at pH > 9 and concentrations greater than 10^{-4} M has been explained.

8. The 100% flotation recovery of magnetite at pH 9.5 and concentrations greater than $\sim 1.2 \times 10^{-4}$ M and the zero contact angle measured in the same system have been reconciled.

9. The excellent flotation recovery of oxides between pH 8 and 11 coincides with the maximum surface activity of amine solutions. The highly surface active species (considered to be complexes) can greatly modify the solid surface chemistry. This, coupled with the strong de-wetting power of fresh bubbles, give good flotation conditions.

Chapter Three

1. The decrease in bubble pick-up of magnetite with bubble age is closely correlated to the decrease in surface tension. This is in agreement with the wetting model and raises doubts concerning the veracity of the transfer model.

2. Similar evidence was accrued from captive bubble experiments on glass and freshly-cleaved hematite. For quartz, pick-up was independent of the exerted surface tension.

3. Attachment, once established, did not exhibit any "dynamic" properties. Surface roughness was considered to be a contributing factor to this "metastability".

4. The Zisman wetting model, introducing a critical surface tension of wetting, γ_c, proved useful in explaining the observed difference between magnetite and quartz pick-up. The γ_c for magnetite and quartz was estimated after 30 min. conditioning at pH 9.7 $\pm$ 0.1 and amine concentration of 4.08×10^{-4} M as;

$$\gamma_c^{Fe_3O_4} \sim 45 \text{ dyne cm}^{-1}$$

$$\gamma_c^{SiO_2} < 30 \text{ dyne cm}^{-1}$$

This difference was exploited in a differential float employing a water/methanol flotation medium. Good separation was

achieved at a surface tension of ~ 40 dyne cm^{-1} (in the predicted range).

5. The Zisman model was shown to offer a number of advantages over the Harkins model.

i) γ_c can be measured, whereas γ_{SL} and γ_{SV} are indeterminate.

ii) the requirement that $\Gamma_{SV} > \Gamma_{SL}$, which has introduced many conceptual difficulties, is not necessary in the Zisman model.

iii) the Zisman model emphasises the solid and bubble properties prior to collision.

6. A working definition of the terms "hydrophobic" and "hydrophyllic", as they are employed in flotation, is possible using the γ_c concept. The possibility of effecting differential flotation by control of γ_{LV} is thus introduced.

Chapter Four

1. The t-short solution to the Ward and Tordai diffusion equation coupled with the Fowkes surface model and the t-long solution of Hansen, modified for monolayer coverage, were used to test for diffusion control.

2. The agreement between the "theoretical" curves and experimental data indicates a diffusion-controlled process. Calculation of $C_o(D)^{1/2}$ using the Langmuir-Syskowski isotherm agrees with that given by the Fowkes isotherm.

3. From a plot of $C_o(D)^{1/2}$ vs C, and assuming "reasonable" values for D (2 to 8 x 10^{-6} $cm^2 sec^{-1}$), C_o/C was determined at 35% to 70%. Taking the calculated per cent amine present as RNH_2 at pH 9.85 (~15%), this range (of C_o/C) fits an RNH_3^+-RNH_2 complex with an RNH_3^+:RNH_2 ratio of 1:1 to 3:1. This ratio is consistent with that found from optimum pH measurements.

Claims to Original Research

1. The relative adsorption density at the S-L and S-V interface in typical oxide/amine flotation systems has been determined by utilizing the approach of Smolders (8).

2. Dynamic surface tension of dodecylamine as a function of pH (pH 7-13) and total amine concentration (2.04 x 10^{-5} M to 8.16 x 10^{-4} M) has been measured. The influence of alien ions was also tested.

3. A decrease in surface activity above pH 10 is shown.

4. Evidence is presented of RNH_3^+-RNH_2 complex formation.

5. The dynamic contact angle phenomenon of Smith and Lai (17) is explained.

6. The 100% recovery of magnetite and zero contact angle in amine solutions greater than 10^{-4} and pH > 9 have been reconciled.

7. The variation in surface activity with pH has been shown to correspond to the flotation response of oxides.

8. The wetting and transfer models of flotation have been tested using dynamic surface tension data.

9. A decrease in pick-up of magnetite has been correlated with a decrease in solution surface tension.

10. The critical surface tension of wetting concept has been introduced. Dynamic surface tension data has been used to estimate critical surface tensions of wetting of magnetite and quartz.

11. A differential float of quartz from magnetite has been achieved using water/methanol solutions as flotation medium.

12. The t-short and t-long solutions to the Ward and Tordai equation using the Fowkes isotherm and the Hansen assymptotic solution modified for monolayer coverage has been employed to test diffusion control.

Suggestions for Future Work

1. Dynamic surface tension work on other surfactant systems known to exhibit a bubble aging phenomenon would indicate if a correlation between γ_{LV} and de-wetting power was general.

2. Knowledge of the dynamics of such systems which show a decrease in induction time with bubble age would be informative.

3. Dynamic surface tension determination on mixed systems (collector/frother, collector/modifier) may help ellucidate the surface active species generated by such mixtures.

4. The possibility of measuring the γ_c of collector coated minerals should be investigated, with a view to effecting a differential float by exploiting any pronounced differences in γ_c.

5. The technique of measuring γ_c outlined in this work (using dynamic surface tension data) should be examined. It should be possible to show if the γ_c so measured is the same as the γ_c measured conventionally.

6. The influence of surface condition should be considered. A smooth surface and a crushed sample of the same material should yield the same γ_c. This is subject to experimental verification.

APPENDIX I

CHAPTER TWO

CALIBRATION AND RESULTS

Contents

CALIBRATION

$$\gamma_t = K\Delta h$$

K determined against water assuming surface tension of 72.0 dyne cm^{-1}.

Measurement of Δh(cm)

Glass tip (r_1)

1	2	3
16.30	16.18	16.26

Metal tip (r_2)

1	2
11.18	11.18

Glass tip (r_1):

$\Delta h = 16.25 \pm 0.04$

$\gamma_t = 4.43\ \Delta h$

Metal tip (r_2):

$\Delta h = 11.18$

$\gamma_t = 6.44\ \Delta h$

Estimate of Errors:

Error in "Δh": a) reading, $\pm$ 0.05 cm

b) hydrostatic, $\pm$ 0.05 cm

error in $\Delta h \pm 0.1$ cm

Error in "K":

r_1: a) Δh, $\pm$ 0.1 cm in 16 cm

error $\pm$ 0.6%

b) temp., $\pm$ 0.3 dyne cm^{-1} in 72 dyne cm^{-1}

error $\pm$ 0.5%

error in K_{r_1} $\pm$ 1.1%

r_2: a) Δh, $\pm$ 0.1 cm in 11 cm

error $\pm$ 1%

b) temp., as above

error in K_{r_2} $\pm$ 1.5%

Error in "γ_t":

Lowest γ_t recorded ~ 25 dyne cm^{-1}

r_1: Δh 5 cm

error $\pm$ 2%

error in γ_t: $\pm$ 3%

r_2: Δh 3 cm

error $\pm$ 3%

error in γ_t: $\pm$ 4.5%

This represents the worst conditions i.e. max^m error

Calibration equations:

r_1: $\gamma_t = 4.43\ \Delta h \pm 0.8$ dyne cm^{-1}

r_2: $\gamma_t = 6.44\ \Delta h \pm 1.2$ dyne cm^{-1}

Error in "t":

Stop-watch read to $\pm$ 0.1 sec.

$t > 1$ sec

error $< \pm$ 10%

$t > 10$ sec

error $< \pm$ 1%

Bulk of data for $t > 10$ sec, nearly all data for $t > 1$ sec.

TABLE I.1

Dynamic Surface Tension of Dodecylamine Acetate Solutions: Comparison of Bubbling Tips

8.16×10^{-5} M, pH 9.85 ± 0.05

r_1			r_2		
t (secs)	Δh (cm)	γ_t (dyne cm^{-1})	t (secs)	Δh (cm)	γ_t (dyne cm^{-1})
13.6	13.84	61.3	6.5	10.40	67.0
14.6	13.60	60.2	8.1	10.10	65.1
16.5	13.28	58.8	9.5	9.84	63.4
18.0	12.94	57.3	11.2	9.58	61.7
20.7	12.60	55.8	13.1	9.36	60.3
22.3	12.36	54.7	14.7	9.08	58.5
24.1	12.04	53.3	17.3	8.82	56.8
25.8	11.78	52.2	19.3	8.60	55.4
27.9	11.46	50.7	21.6	8.38	54.0
29.6	11.16	49.4	24.0	8.18	52.7
31.7	10.88	48.2	27.1	7.98	51.3
34.0	10.60	46.9	29.9	7.78	50.1
39.6	10.36	45.9	34.5	7.58	48.8
44.0	10.06	44.5	37.9	7.38	47.5
47.1	9.80	43.4	42.4	7.18	46.2
58.8	9.14	40.5	48.4	7.00	45.1
63.2	8.84	39.1	52.0	6.70	43.2
69.1	8.60	38.1	62.5	6.52	41.9

TABLE 1.2

Dynamic Surface Tension: Comparison of Dodecylamine Acetate and Hydrochloride

a) 4.08×10^{-4} M, pH 9.85 ± 0.05

DODECYLAMINE ACETATE

t (secs)	Δh (cm)	γ_t (dyne cm^{-1})	t (secs)	Δh (cm)	γ_t (dyne cm^{-1})	t (secs)	Δh (cm)	γ_t (dyne cm^{-1})
2.0	14.16	62.7	1.4	13.60	60.2	3.1	12.98	57.5
1.5	12.46	55.2	2.6	12.22	54.1	2.0	11.66	51.6
6.2	11.22	49.7	3.8	11.20	49.6	5.8	10.76	47.6
0.8	1.344	59.5	9.3	10.02	44.4	8.4	9.84	43.6
4.1	12.16	53.8	8.1	9.60	42.5	8.8	9.58	42.4
5.7	11.24	49.8	12.7	9.34	41.4	10.2	9.36	41.4
6.8	10.98	48.6	11.7	9.04	40.0	9.3	9.06	40.1
9.3	10.12	44.8	13.1	8.80	39.0	12.1	8.82	39.1
9.7	9.84	43.6	11.7	8.60	38.1	13.3	8.60	38.1
8.1	9.58	42.4	9.9	8.36	37.0	15.9	8.36	37.0
9.3	8.80	39.0	15.3	8.10	35.9	15.9	8.10	35.9
11.1	8.62	38.2	14.1	7.82	34.6	16.9	7.94	35.2
13.9	8.36	37.0	18.7	7.60	32.7	17.9	7.72	34.2
13.9	8.14	36.0	19.6	7.40	32.8	22.9	7.54	33.4
15.3	7.96	35.2	24.2	7.18	31.8	24.2	7.24	32.1
15.4	7.68	34.0	20.3	7.00	31.0	25.6	7.00	31.0
20.3	7.54	33.4	27.2	6.80	30.1	33.7	6.80	30.1
24.7	7.30	32.3	29.8	6.60	29.2	41.8	6.60	29.2
28.2	7.06	31.3	38.1	6.40	28.3	55.4	6.42	28.4
34.8	6.84	30.3	54.7	6.20	27.5	73.1	6.26	27.7
42.3	6.68	29.6	77.0	6.06	26.8	120.8	6.08	26.9
55.3	6.50	28.8	112.0	5.92	26.2	145.0	5.94	26.3
69.5	6.30	27.9	148.4	5.76	25.5	1.3	9.56	61.6*
101.0	6.14	27.2				0.6	10.66	68.7*
194.6	5.96	26.4				*metal tip		
260.0	5.80	25.7						

TABLE 1.2 (cont'd)

DODECYLAMINE HYDROCHLORIDE

t (secs)	Δh (cm)	γ_t (dyne cm^{-1})	t (secs)	Δh (cm)	γ_t (dyne cm^{-1})	t (secs)	Δh (cm)	γ_t (dyne cm^{-1})
2.2	13.36	59.2	1.4	13.64	60.4	0.6	13.60	60.2
3.7	12.02	53.2	3.6	11.94	52.9	3.8	11.74	52.0
3.1	11.18	49.5	4.1	10.80	47.8	2.4	10.88	48.2
3.4	10.28	45.5	7.0	9.74	43.1	7.6	10.00	44.3
8.8	9.54	42.2	8.2	9.48	42.0	8.7	9.56	42.3
10.2	9.36	41.4	8.7	9.20	40.7	11.1	8.84	39.1
10.7	9.06	40.1	9.7	8.98	39.8	12.8	8.60	38.1
10.4	8.82	39.1	11.1	8.74	38.7	13.0	8.40	37.2
11.3	8.62	38.2	12.1	8.50	37.6	13.6	8.20	36.3
12.1	8.40	37.2	13.1	8.28	36.7	14.0	8.00	35.4
13.7	8.20	36.3	13.3	8.00	35.4	16.7	7.76	34.4
14.7	7.89	35.3	15.9	7.80	34.5	16.7	7.76	34.4
13.9	7.80	34.5	18.2	7.60	33.7	19.0	7.54	33.4
15.8	7.60	33.7	18.0	7.40	32.8	20.3	7.32	32.4
16.4	7.36	32.6	20.4	7.20	31.9	23.3	7.02	31.1
19.4	7.18	31.8	23.3	6.98	30.9	25.3	6.84	30.3
23.0	7.00	31.0	25.0	6.78	30.0	26.0	6.68	29.6
26.0	6.80	30.1	33.0	6.60	29.2	28.2	6.50	28.8
24.1	6.60	29.2	32.9	6.40	28.3	30.5	6.38	28.3
32.5	6.48	28.7	43.0	6.22	27.5	40.1	6.20	27.5
32.2	6.34	28.1	53.8	6.00	26.6	49.6	6.00	26.6
42.4	6.14	27.2	72.0	5.86	25.9	64.5	5.90	26.1
62.7	6.00	26.6	101.5	5.76	25.5	90.3	5.80	25.7
82.4	5.88	26.0	155.6	5.56	24.6	120.0	5.62	24.9
105.6	5.68	25.2				210.0	5.26	23.3
152.4	5.54	24.5						
186.3	5.32	23.6						
> 7 min	5.18	22.9						

TABLE 1.2 (cont'd)

b) 8.16×10^{-4} M, pH 9.85 ± 0.05

DODECYLAMINE ACETATE

t (secs)	Δh (cm)	γ_t (dyne cm^{-1})	t (secs)	Δh (cm)	γ_t (dyne cm^{-1})	t (secs)	Δh (cm)	γ_t (dyne cm^{-1})
1.1	13.00	57.6	0.7	12.80	56.7	0.8	12.96	57.4
1.7	10.48	46.4	2.0	10.46	46.3	1.4	10.54	46.7
3.8	9.96	44.1	1.8	9.30	41.2	1.5	9.18	40.6
4.8	8.20	36.3	4.6	8.36	37.0	2.2	8.36	37.0
7.4	7.40	32.8	6.8	7.64	33.8	5.4	7.62	33.7
8.7	7.20	31.9	7.5	7.40	32.8	8.8	7.20	31.9
12.3	6.60	29.2	9.5	7.20	31.9	9.7	6.98	30.9
12.7	6.40	28.3	9.1	7.00	31.0	11.1	6.78	30.0
16.3	6.22	27.5	12.1	6.80	30.1	12.1	6.58	29.1
22.0	6.04	26.7	12.1	6.60	29.2	15.2	6.38	28.3
25.9	5.88	26.0	13.8	6.40	28.3	17.3	6.22	27.5
29.7	5.76	25.5	15.0	6.22	27.5	20.2	6.04	26.7
36.4	5.56	24.6	19.9	6.06	26.8	26.6	5.88	26.0
53.2	5.42	24.0	26.8	5.94	26.3	29.9	5.78	25.6
69.7	5.38	23.6	30.0	5.76	25.5	38.9	5.60	24.8
			47.0	5.60	24.8	54.4	5.42	24.0
			55.6	5.48	24.3	119.6	5.34	23.6
			73.0	5.38	23.8	270.0	5.12	22.7
			134.2	5.18	22.9			

TABLE 1.2 (b) (cont'd)

DODECYLAMINE HYDROCHLORIDE

t (secs)	Δh (cm)	γ_t (dyne cm^{-1})	t (secs)	Δh (cm)	γ_t (dyne cm^{-1})	t (secs)	Δh (cm)	γ_t (dyne cm^{-1})
0.7	11.76	52.1	1.3	12.22	54.1	1.7	11.38	50.4
4.3	9.42	41.7	2.8	9.14	40.5	4.4	9.50	42.1
4.8	8.78	38.9	6.6	8.02	35.5	6.6	8.68	38.4
9.1	7.76	34.4	9.5	7.84	34.7	7.7	8.22	36.4
7.8	7.50	33.2	9.7	7.60	33.7	7.8	8.06	35.7
9.5	7.30	32.3	11.3	7.40	32.8	8.7	7.82	34.6
11.1	7.06	31.3	12.5	7.16	31.7	11.5	7.68	34.0
12.3	6.80	30.1	15.3	6.96	30.8	11.7	7.46	33.0
14.5	6.58	29.1	16.7	6.76	29.9	11.8	7.32	32.4
15.3	6.38	28.3	18.3	6.56	29.0	12.6	6.98	30.9
17.0	6.20	27.5	21.0	6.36	28.2	12.8	6.70	29.7
19.5	6.00	26.6	22.8	6.16	27.3	15.2	6.50	28.8
23.9	5.82	25.8	22.6	6.04	26.7	17.6	6.32	28.0
29.2	5.66	25.1	28.5	5.86	25.9	20.1	6.10	27.0
28.2	5.46	24.2	35.3	5.64	25.0	22.9	5.92	26.2
39.9	5.36	23.7	41.0	5.54	24.5	27.4	5.76	25.5
41.9	5.14	22.8	29.9	5.34	23.6	34.7	5.60	24.8
54.1	5.00	22.1	50.4	5.20	23.0	35.4	5.40	23.9
81.1	4.94	21.9	86.3	5.10	22.6	54.4	5.24	23.2
109.4	4.78	21.2	133.9	4.96	22.0	59.5	5.04	22.3
> 5 min	4.60	20.8	199.2	4.78	21.2	131.9	4.94	21.9
			> 5 min	4.66	20.9	256.9	4.80	21.3

TABLE I.3

Dynamic Surface Tension of Dodecylamine Acetate Solution; Effect of Buffering

a) 4.08×10^{-5} M, pH 9.85 ± 0.05

Buffered			Non-Buffered			Non-Buffered (after 30 min)		
Initial pH 9.9			Initial pH 9.9			Initial pH 9.8		
Final pH 9.8			Final pH 9.8			Final pH 9.4		
t (secs)	Δh (cm)	γ_t (dyne cm^{-1})	t (secs)	Δh (cm)	γ_t (dyne cm^{-1})	t (secs)	Δh (cm)	γ_t (dyne cm^{-1})
29.2	14.52	64.3	30.9	14.48	64.1	30.2	14.84	65.7
33.2	14.20	62.9	35.5	14.18	62.8	34.8	14.48	64.1
36.9	13.86	61.4	37.7	13.82	61.6	37.6	14.10	62.5
39.8	13.58	60.1	42.7	13.56	60.1	4.34	13.86	60.8
42.7	13.24	58.6	44.8	13.20	58.5	49.7	13.30	58.9
49.0	12.56	55.6	53.9	12.58	55.7	57.3	12.88	57.1
53.2	12.28	54.4	57.4	12.20	54.0	74.6	12.46	55.2
60.5	11.96	53.0	68.2	11.96	53.0	78.5	12.16	53.9
62.0	11.63	51.5	68.8	11.68	51.7	96.1	11.78	52.2
72.0	11.38	50.4	76.0	11.38	50.4			
83.1	11.10	49.2	72.9	11.10	49.2			
55.2	9.94	44.0	58.5	9.50	42.1			
62.2	9.36	41.5	63.1	9.32	41.3			
67.2	9.20	40.8	75.0	9.00	39.9			
68.2	9.00	39.9	76.9	8.78	38.9			
76.1	8.80	39.0						

TABLE 1.3 (cont'd)

b) 8.16×10^{-5} M, pH 9.5

Buffered			Non-Buffered			Non-Buffered (after 30 min)		
Initial pH 9.6 Final pH 9.5			Initial pH 9.6 Final pH 9.5			Initial pH 9.5 Final pH 8.5		
t (secs)	Δh (cm)	γ_t (dyne cm^{-1})	t (secs)	Δh (cm)	γ_t (dyne cm^{-1})	t (secs)	Δh (cm)	γ_t (dyne cm^{-1})
9.0	15.04	66.6	11.3	14.80	65.6	21.8	13.56	60.1
13.7	14.40	63.8	15.3	14.20	62.9	24.8	12.92	57.2
15.8	14.04	62.2	20.0	13.30	58.9	28.0	12.60	55.8
20.0	13.20	58.5	21.7	12.96	57.4	29.2	12.36	54.8
22.7	12.84	56.9	23.4	12.60	55.8	33.3	12.04	53.3
25.0	12.60	55.8	24.5	12.36	54.8	46.5	11.80	52.3
25.6	12.26	54.3	27.2	12.00	53.2	49.8	11.50	50.9
27.2	11.98	53.1	27.5	11.76	52.1	75.4	11.22	49.7
29.0	11.70	51.8	28.8	11.50	50.9			
30.4	11.44	50.7	31.0	11.32	50.1			
32.3	11.16	49.4	33.0	10.96	48.6			
35.0	10.96	48.6	40.3	10.52	46.6			
37.4	10.64	47.1	43.8	10.40	46.1			
45.4	10.40	46.1	48.3	10.20	45.2			
48.7	10.16	45.0	52.0	9.92	43.9			
50.1	9.94	44.0	54.6	9.76	43.2			

TABLE 1.3 (cont'd)

c) 4.08×10^{-4} M, DAA, pH 9.85

Buffered

t (secs)	Δh (cm)	γ_t (dyne cm^{-1})	t (secs)	Δh (cm)	γ_t (dyne cm^{-1})	t (secs)	Δh (cm)	γ_t (dyne cm^{-1})
3.6	13.48	59.7	2.7	13.74	60.8	2.1	13.88	61.5
5.4	12.30	54.5	5.0	13.50	59.8	5.0	12.50	55.4
5.9	10.90	48.3	4.1	12.50	55.4	7.3	11.38	50.4
9.0	9.90	43.8	6.7	11.62	51.5	8.6	10.40	46.1
14.0	9.00	39.9	7.9	10.90	48.3	10.4	9.44	41.8
17.4	8.46	37.5	9.8	10.20	45.2	11.7	9.14	40.5
20.9	7.94	35.2	11.5	9.60	42.5	22.8	8.06	35.7
22.5	7.70	34.1	13.4	9.10	40.3	25.6	7.78	34.4
25.1	7.40	32.8	18.7	8.22	36.4	27.0	7.50	33.2
28.6	7.20	31.9	21.0	8.02	35.5	30.2	7.26	32.1
50.5	6.70	29.7	23.0	7.70	34.1	38.8	6.93	30.7
64.8	6.50	28.8	25.4	7.48	33.1	18.4	6.71	29.7
128.2	6.26	27.7	43.3	6.70	29.7	75.0	6.48	28.7
214.6	6.04	26.7	54.0	6.48	28.7	100.8	6.26	27.7
			79.6	6.30	27.9			
			145.4	6.10	27.0			
			236.8	5.90	26.1			

Non-Buffered - see Table 1.2

TABLE I.4

Dynamic Surface Tension of Dodecylamine Acetate Solutions at $C = 4.08 \times 10^{-5}$ M: Effect of pH

t (secs)	Δh (cm)	γ_t (dyne cm^{-1})	t (secs)	Δh (cm)	γ_t (dyne cm^{-1})	t (secs)	Δh (cm)	γ_t (dyne cm^{-1})
			pH 6.90 ± 0.05					
			no effect $\gamma_\infty = 70.0$					
			pH 7.85 ± 0.05					
			no effect $\gamma_\infty = 69.0$					
			pH 8.85 ± 0.05					
44.6	14.44	63.9	45.8	14.26	63.1	48.7	14.20	62.9
52.6	14.06	62.3	57.6	13.90	61.5	62.0	13.86	61.4
71.8	13.66	60.5	69.6	13.54	59.9	78.7	13.50	59.8
161.9	13.26	58.7	120.2	13.20	58.4	132.2	13.14	58.2
50.2	14.26	63.1						
68.3	13.88	61.5						
84.9	13.54	60.0						
114.2	13.18	58.4						

TABLE I.4 (cont'd)

t (secs)	Δh (cm)	γ_t (dyne cm^{-1})	t (secs)	Δh (cm)	γ_t (dyne cm^{-1})	t (secs)	Δh (cm)	γ_t (dyne cm^{-1})
			pH 9.6 ± 0.1					
24.1	14.56	64.5	26.2	14.40	63.8	24.4	14.36	63.4
24.8	14.18	62.8	25.8	13.98	61.9	25.3	13.88	61.5
30.1	13.80	61.1	30.9	13.62	60.3	31.9	13.56	60.0
33.0	13.44	59.5	37.0	13.26	58.7	36.4	13.16	58.3
37.8	13.08	57.9	44.2	12.86	56.9	42.4	12.76	56.5
45.1	12.72	56.3	50.0	12.50	55.4	51.6	12.42	55.0
54.0	12.36	54.7	58.8	12.16	53.8	64.6	12.00	53.1
59.2	11.96	53.0	69.4	11.80	52.3	67.5	11.68	51.7
84.5	11.62	51.5	95.1	11.44	50.7	79.7	11.42	50.6
107.5	11.30	50.0	224.6	11.14	49.3	100.0	11.02	48.8
> 5 min	10.94	48.3	> 5 min	10.76	47.7	164.6	10.80	47.8
						> 5 min	10.70	47.2
			pH 9.85 ± 0.05					
22.9	14.52	64.3	29.0	14.68	65.0	24.7	14.78	65.4
33.2	14.20	62.9	32.3	14.36	63.6	27.4	14.40	63.8
36.9	13.86	61.4	35.0	14.02	62.1	32.2	14.12	62.5
39.8	13.58	60.0	38.9	13.68	60.6	35.7	13.76	60.9
42.7	13.24	58.6	40.1	13.38	59.2	39.3	13.44	59.5
47.6	12.88	57.0	44.7	13.02	57.7	42.2	13.08	57.9
49.0	12.56	55.6	48.6	12.68	56.1	45.1	12.76	56.5
53.2	12.28	54.4	53.0	12.40	54.9	47.7	12.42	55.0
60.5	11.96	53.0	56.7	12.08	53.5	59.2	12.20	54.0
62.0	11.63	51.5	61.5	11.80	52.3	57.4	11.94	52.9
72.2	11.38	50.4	66.9	11.50	50.9	60.3	11.60	51.4
83.1	11.10	49.2	75.1	11.20	49.6	67.5	11.38	50.4
			76.4	10.94	48.4			
			88.0	10.76	47.6			

TABLE I.4 (cont'd)

t (secs)	Δh (cm)	γ_t (dyne cm^{-1})	t (secs)	Δh (cm)	γ_t (dyne cm^{-1})	t (secs)	Δh (cm)	γ_t (dyne cm^{-1})
			pH 9.85 ± 0.05 (cont'd)					
28.9	14.30	63.3	28.3	14.36	63.6	26.5	14.60	64.6
32.9	13.96	61.8	27.3	14.00	62.0	35.7	13.64	60.4
38.3	13.62	60.3	34.5	13.72	60.8	39.8	13.30	58.9
41.1	13.28	58.8	38.0	13.38	59.2	44.4	12.96	57.4
45.6	12.94	57.3	43.9	13.00	57.6	47.3	12.62	55.9
49.7	12.60	55.8	48.2	12.64	56.0	52.5	12.28	54.4
55.0	12.30	54.5	52.8	12.32	54.6	58.6	11.98	53.0
59.7	12.00	53.1	55.5	12.00	53.1	62.7	11.70	51.8
61.8	11.62	51.5	64.0	11.66	51.5	70.4	11.36	50.3
66.5	11.38	50.4	68.3	11.38	50.4	77.2	11.00	48.7
73.4	11.00	48.7	73.4	11.00	48.7	86.7	10.76	47.6
79.0	10.76	47.6	81.8	10.78	47.7	97.8	10.48	46.4
95.2	10.46	46.3	96.2	10.50	46.5	118.7	10.16	45.0
112.2	10.12	44.8	115.2	10.18	45.1	132.0	9.84	43.6
141.2	9.86	43.7	130.6	9.88	43.7	164.4	9.54	42.2
171.9	9.52	42.2	147.0	9.60	42.5	2.0	10.94	70.5*
207.0	9.24	40.9	175.8	9.36	41.4	1.0	10.98	70.7*
233.4	8.96	39.7	215.4	9.14	40.5	13.6	10.80	69.6*
301.6	8.62	38.2	279.6	8.84	39.1	21.5	10.54	67.9*
386.2	8.36	37.0	330.0	8.54	38.0	28.5	10.26	66.1*

* metal tip

TABLE 1.4 (cont'd)

t (secs)	Δh (cm)	γ_t (dyne cm^{-1})	t (secs)	Δh (cm)	γ_t (dyne cm^{-1})	t (secs)	Δh (cm)	γ_t (dyne cm^{-1})
			pH 10.1 ± 0.1					
6.5	15.56	68.9	3.5	14.50	68.2			
20.8	14.92	66.1	30.1	14.26	63.2			
27.3	14.56	64.5	35.0	13.92	61.7			
34.5	14.20	62.9	38.7	13.60	60.2			
42.1	13.84	61.3	40.2	13.28	58.8			
45.6	13.54	60.0	42.5	12.96	57.4			
52.4	13.20	58.5	48.4	12.60	55.8			
55.1	12.88	57.1	52.7	12.34	54.7			
53.6	12.56	55.6	56.0	12.00	53.2			
60.7	12.30	54.5	63.6	11.76	52.1			
70.1	12.00	53.2	67.0	11.42	50.6			
71.6	11.68	51.7	72.4	11.12	49.3			
78.2	11.40	50.5	70.8	10.86	48.1			
85.9	11.14	49.4	93.3	10.00	44.3			
92.5	10.86	48.1	116.2	9.72	43.1			
97.0	10.58	46.9	101.1	9.42	41.7			
96.0	10.32	45.7						
92.0	10.00	44.3						
128.3	9.74	43.1						
140.5	9.50	42.1						
			pH 10.2 ± 0.1					
7.0	15.42	68.3	7.0	15.60	69.1			
33.2	14.00	62.0	25.0	14.80	65.6			
37.0	13.74	60.9	28.5	14.44	64.0			
40.1	13.40	59.4	33.4	14.10	62.5			
45.1	13.02	57.7	36.7	13.78	61.0			

TABLE 1.4 (cont'd)

t (secs)	Δh (cm)	γ_t (dyne cm^{-1})	t (secs)	Δh (cm)	γ_t (dyne cm^{-1})	t (secs)	Δh (cm)	γ_t (dyne cm^{-1})
			pH 10.2 ± 0.1 (cont'd)					
45.7	12.72	56.3	39.6	13.40	59.4			
51.8	12.38	54.8	44.6	13.02	57.7			
54.3	12.02	53.2	45.7	12.72	56.3			
59.6	11.78	52.2	51.2	12.38	54.8			
55.3	11.43	50.6	57.3	12.02	53.3			
71.0	11.16	49.4	57.1	11.76	52.1			
70.0	10.82	47.9	77.0	11.18	49.5			
74.8	10.60	47.0	84.9	10.86	48.1			
101.0	10.38	46.0	73.7	10.56	46.8			
101.9	10.02	44.4	82.6	10.24	45.4			
88.8	9.78	43.3	96.2	9.96	44.1			
122.7	9.50	42.1	120.1	9.64	42.7			
			117.2	9.40	41.6			
			pH 10.4 ± 0.1					
5.0	15.60	69.0	7.0	15.48	68.6			
16.4	14.98	66.4	29.8	14.60	64.7			
29.0	14.60	64.7	35.0	14.22	63.0			
33.7	14.20	62.9	40.4	13.82	61.2			
38.5	13.82	61.2	46.4	13.48	59.7			
39.3	13.50	59.8	48.8	13.12	58.1			
43.3	12.74	56.4	54.8	12.78	56.6			
44.3	12.74	56.4	54.6	12.40	54.9			
49.6	12.40	54.9	64.7	12.08	53.5			

TABLE 1.4 (cont'd)

t (secs)	Δh (cm)	γ_t (dyne cm^{-1})	t (secs)	Δh (cm)	γ_t (dyne cm^{-1})	t (secs)	Δh (cm)	γ_t (dyne cm^{-1})
			pH 10.4 ± 0.1 (cont'd					
61.2	12.06	53.4	57.4	11.78	52.2			
66.4	11.78	52.2	75.7	11.44	50.7			
74.9	11.48	50.9	83.1	11.16	49.4			
68.3	11.16	49.4	73.9	10.80	47.8			
67.7	10.84	48.0	83.0	10.56	46.8			
100.6	10.58	46.9	83.5	10.24	45.4			
98.3	10.20	45.2	100.7	9.92	43.9			
105.8	9.90	43.9	138.0	9.60	42.5			
			111.3	9.36	41.5			
			pH 10.8 ± 0.1					
31.7	15.00	66.4	45.2	14.36	63.6	27.5	15.40	68.2
44.0	14.36	63.6	47.1	14.18	62.8	42.4	14.76	65.4
48.5	14.16	62.7	38.1	13.90	61.5	46.5	14.40	63.8
48.6	13.80	61.1	50.4	13.56	60.0	52.6	14.06	62.3
56.2	13.46	59.6	56.5	13.16	58.3	52.6	13.68	60.6
52.1	13.12	58.1	82.7	12.52	55.4	58.8	13.36	59.2
61.6	12.76	56.5	85.2	12.08	53.5	65.4	13.00	57.6
			85.8	11.76	52.1	77.0	12.56	55.6
			170.5	10.54	46.7			
						82.6	12.16	53.8
						85.9	11.84	52.4
						127.4	11.26	50.0
						121.8	10.94	48.4
						132.4	10.66	47.2

TABLE 1.4 (cont'd)

t (secs)	Δh (cm)	γ_t (dyne cm^{-1})	t (secs)	Δh (cm)	γ_t (dyne cm^{-1})	t (secs)	Δh (cm)	γ_t (dyne cm^{-1})
			pH 10.8 ± 0.1 (cont'd)					
						154.1	10.36	45.9
						173.7	10.06	44.5
						239.3	9.76	43.2
						272.6	9.44	41.8
						323.0	9.14	40.5
						431.3	8.82	39.1
			pH 10.8 ± 0.1					
44.1	13.94	61.7	19.9	15.00	66.4	28.5	14.34	63.5
50.5	13.60	60.2	23.9	14.72	65.2	35.2	13.98	61.9
62.1	13.16	58.3	30.2	14.36	63.6	41.5	13.68	60.6
69.9	12.78	56.6	36.8	14.00	62.0	51.8	13.32	49.0
80.4	12.40	54.9	46.4	13.60	60.2	60.9	12.96	57.4
93.3	12.08	53.5	47.3	13.24	58.6	69.0	12.58	55.7
106.2	11.76	52.1	57.5	12.94	57.3	77.8	12.20	54.0
114.8	11.40	50.5	69.3	12.58	55.7	95.6	11.80	52.3
48.0	11.12	49.2	85.6	12.08	53.5	101.6	11.46	50.7
25.7	10.78	47.7	108.4	11.44	50.7	112.6	11.16	49.4
163.6	10.48	46.4	116.8	11.16	49.4	130.2	10.94	48.4
198.6	9.94	44.0	108.5	10.60	46.9	127.5	10.60	46.9
325.4	9.32	41.3	172.0	10.34	45.8	202.2	10.32	45.7
			210.2	9.94	44.0	221.9	9.94	44.0
			44.5	9.36	41.4	490.1	9.54	43.2
			422.2	9.16	40.6	734.2	9.20	40.7
			394.8	8.90	39.4			

TABLE 1.4 (cont'd)

t (secs)	Δh (cm)	γ_t (dyne cm^{-1})	t (secs)	Δh (cm)	γ_t (dyne cm^{-1})	t (secs)	Δh (cm)	γ_t (dyne cm^{-1})
			pH 11.7 ± 0.01					
38.9	16.00	70.9	179.7	15.56	68.9	4.7	16.00	70.8
233.5	15.72	69.6	137.7	15.30	67.7	25.0	16.00	70.8
232.9	15.12	67.0	169.3	15.00	66.4	77.0	15.98	70.8
650.2	14.74	65.3	319.8	14.72	65.2	169.6	15.22	67.4
			> 10 min	14.60	64.1			

TABLE 1.5

Dynamic Surface Tension of Dodecylamine Acetate Solutions at $C = 8.16 \times 10^{-5}$ M; Effect of pH

t (secs)	Δh (cm)	γ_t (dyne cm^{-1})	t (secs)	Δh (cm)	γ_t (dyne cm^{-1})	t (secs)	Δh (cm)	γ_t (dyne cm^{-1})
			pH 9.4 ± 0.1					
8.1	14.00	62.0	7.8	13.96	61.8	7.3	14.00	62.0
11.4	13.36	59.2	11.0	13.20	58.4	9.7	13.98	61.9
15.8	12.60	55.8	16.2	12.60	55.8	13.0	13.24	58.6
22.6	12.00	53.1	19.8	11.98	53.0	18.2	12.60	55.8
32.8	11.50	50.9	27.6	11.42	50.6	29.2	1.200	53.1
41.0	10.90	48.3	38.8	10.80	47.8	32.7	11.44	50.7
64.0	10.39	46.0	70.8	10.30	45.6	41.2	10.80	47.8
			pH 9.85 ± 0.05					
13.6	13.84	61.3	14.4	13.76	60.9	11.7	13.72	60.8
14.6	13.84	61.3	16.2	13.44	59.5	12.7	13.44	59.5
14.5	13.28	58.8	18.0	13.20	58.4	14.5	13.20	58.4
18.0	12.94	57.3	19.2	12.88	57.0	16.2	12.84	56.9
20.7	12.60	55.8	20.4	12.58	55.7	18.0	12.60	55.8
22.3	12.36	54.7	22.0	12.30	54.5	19.0	12.30	54.5
24.1	12.04	53.3	24.2	12.00	53.1	21.2	11.96	53.0
25.8	11.78	52.2	25.0	11.76	52.1	23.9	11.75	52.1
27.9	11.46	50.7	26.9	11.44	60.7	24.5	11.50	50.9
29.6	11.16	49.4	28.0	11.16	49.4	26.3	11.22	49.7
31.7	10.88	48.2	30.9	10.88	48.2	28.2	10.96	48.5
34.0	10.60	46.9	33.7	10.60	46.9	30.2	10.70	47.4
39.6	10.36	45.9	40.0	10.36	45.9	34.9	10.40	46.1
44.0	10.06	44.5	45.2	10.12	44.8	40.2	10.18	45.1
47.1	9.80	43.4	49.3	9.80	43.4	43.7	9.92	43.9
72.5	9.50	42.1	55.1	9.58	42.4	48.2	9.72	43.0
58.8	9.14	40.5	55.4	9.30	41.2	53.1	9.44	41.8
63.2	8.84	39.1	61.7	9.12	40.4	50.5	9.20	40.7
69.1	8.60	38.1	61.6	8.80	39.0	61.8	8.98	39.8

TABLE 1.5 (cont'd)

t (secs)	Δh (cm)	γ_t (dyne cm^{-1})	t (secs)	Δh (cm)	γ_t (dyne cm^{-1})	t (secs)	Δh (cm)	γ_t (dyne cm^{-1})
			pH 9.85 ± 0.05 (cont'd)					
71.8	8.40	37.2	75.0	8.60	38.1	69.3	8.76	38.8
77.1	8.18	36.2	77.3	8.36	37.0	61.8	8.50	37.6
84.3	7.96	35.2	87.0	8.16	36.1	79.6	8.32	36.8
86.0	7.76	34.4	95.1	7.92	35.1	91.5	8.14	36.0
90.0	7.56	33.5	98.8	7.70	34.1	94.6	7.88	34.9
95.4	7.40	32.9	108.0	7.52	33.3	128.1	7.24	32.1
111.4	7.20	31.9	109.7	7.40	32.8	140.4	7.00	31.0
131.6	7.00	31.0	118.0	7.18	31.8	155.2	6.94	30.7
148.9	6.80	30.1	127.9	7.00	31.0	173.1	6.76	29.9
155.8	6.61	29.3	134,7	6.92	30.6	186.6	6.58	29.1
153.6	6.52	28.9	156.7	6.78	30.0	244.5	6.40	28.3
160.3	6.40	28.3	185.4	6.60	29.2	332.5	6.22	27.5
171.3	6.28	27.8	226.0	6.40	28.3	> 14 min	6.08	27.1
207.4	6.16	27.3	266.5	6.22	27.5	6.5	10.40	67.0*
269.4	6.00	26.6	350.4	6.02	26.7	8.1	10.10	65.1*
233.4	5.80	25.7	> 18 min	5.90	26.1	9.5	9.84	63.4*
567.8	5.64	25.0						

* metal tip

			pH 10.2 ± 0.2					
7.9	15.16	67.1	12.7	14.08	62.3	8.5	14.64	64.8
14.4	13.96	61.8	15.1	13.76	60.9	12.2	13.94	61.7
17.0	13.62	60.3	17.3	13.38	59.2	14.3	13.58	60.1
18.8	13.20	58.4	12.7	13.00	57.6	16.6	13.16	58.3
29.0	12.52	55.4	21.5	12.66	56.1	18.3	12.80	56.7
25.7	12.14	53.8	23.8	12.38	54.8	21.0	12.52	55.4

TABLE 1.5 (cont'd)

pH 10.2 ± 0.2 (cont'd)

t (secs)	Δh (cm)	γ_t (dyne cm^{-1})	t (secs)	Δh (cm)	γ_t (dyne cm^{-1})	t (secs)	Δh (cm)	γ_t (dyne cm^{-1})
27.0	11.80	52.3	25.5	12.00	53.1	23.0	12.18	53.9
29.6	11.48	50.8	28.0	11.72	51.9	25.2	11.82	52.3
30.6	11.12	49.2	28.0	11.38	50.4	38.4	11.22	49.7
44.6	10.20	45.2	34.9	10.76	47.6	34.4	10.86	48.1
45.1	9.84	43.6	44.1	10.42	46.1	46.2	9.84	43.6
46.5	9.52	42.2	43.5	10.04	44.5	50.1	9.58	42.4
50.4	9.24	40.9	43.0	9.72	43.0	36.2	9.28	41.1
53.8	9.00	39.9	46.5	9.42	41.7	58.4	9.00	39.9
60.1	8.70	38.5	48.8	9.18	40.6	65.3	8.66	38.3
63.4	8.40	37.2	54.0	8.90	39.4	70.2	8.40	37.2
70.0	8.20	36.3	58.1	8.62	38.2	76.3	8.16	36.1
76.4	7.98	35.3	65.0	8.36	37.0	76.6	7.88	34.9
86.8	7.66	33.9	70.1	8.12	36.0	91.9	7.66	33.9
95.4	7.42	32.9	75.1	7.90	35.0	100.6	7.40	32.8
88.6	7.20	31.9	79.5	7.62	33.7	97.0	7.20	31.9
105.4	7.06	31.3	90.4	7.40	32.8	124.2	7.00	31.0
109.9	6.80	30.1	96.0	7.20	31.9	137.0	6.66	29.5
256.0	6.68	29.6	92.2	7.00	31.0	139.8	6.46	28.6
147.8	6.32	28.0	116.8	6.82	30.2	150.7	6.40	28.3
> 5 min			122.5	6.62	29.3	355.1	5.90	26.1
			121.0	6.52	28.9	> 10 min	5.74	25.2
			135.6	6.42	28.4			
			156.1	6.28	27.8			
			192.1	6.12	27.1			
			> 5 min	5.90	26.1			

TABLE 1.5 (cont'd)

t (secs)	Δh (cm)	γ_t (dyne cm^{-1})	t (secs)	Δh (cm)	γ_t (dyne cm^{-1})	t (secs)	Δh (cm)	γ_t (dyne cm^{-1})
			pH 10.85 ± 0.05					
12.8	14.28	63.3	11.6	15.00	66.4	13.8	15.04	66.6
9.8	14.00	62.0	15.4	14.62	64.7	18.2	14.60	64.6
11.8	13.50	59.8	17.3	14.28	63.2	10.2	14.20	62.9
20.7	13.16	58.3	23.3	13.92	61.6	22.7	13.92	61.6
30.7	12.80	56.7	23.6	13.58	60.1	30.2	13.56	60.0
31.1	12.56	55.6	28.5	13.20	58.4	32.8	13.16	58.3
39.4	12.28	54.4	34.7	12.92	57.2	36.8	12.78	56.6
43.0	11.96	53.0	39.0	12.60	55.8	41.8	12.50	55.4
53.1	11.70	51.8	43.8	12.26	54.3	36.2	12.20	54.0
67.8	11.40	50.5	46.2	11.98	53.0	50.2	11.90	52.7
59.3	11.14	49.4	52.8	11.68	51.7	57.0	11.62	51.5
84.4	10.86	48.1	54.2	11.36	50.3	18.0	11.16	49.4
79.0	10.60	47.0	59.7	11.02	48.8	70.2	11.02	48.8
78.4	10.30	45.6	55.1	10.74	47.6	78.4	10.80	47.8
81.4	9.98	44.2	74.8	10.46	46.3	94.2	10.58	46.8
120.8	9.76	43.2	81.8	10.16	45.0	100.3	10.30	45.6
127.0	9.52	42.2	99.8	9.84	43.6	113.2	10.00	44.3
109.0	9.24	40.9	116.7	9.58	42.4	107.8	9.76	43.2
129.4	9.00	39.9	131.8	9.32	41.3	147.2	9.56	42.3
106.6	8.76	38.8	133.8	9.08	40.2	170.0	9.32	41.3
121.1	8.52	37.7	102.6	8.80	39.0	169.8	9.06	40.1
125.7	8.28	36.7	191.7	8.58	38.0	200.3	8.80	39.0
163.6	8.10	35.9	202.3	8.28	36.7	232.2	8.60	38.1
196.3	7.86	34.8	232.8	8.06	35.7	253.1	8.48	37.5
317.9	7.66	33.9	431.8	7.72	34.2	281.6	8.20	36.3
						330.0	8.00	35.4

TABLE TABLE 1.6

Dynamic Surface Tension of Dodecylamine Acetate Solutions at C = 4.08×10^{-4}M: Effect of pH

t (secs)	Δh (cm)	γ_t (dyne cm^{-1})	t (secs)	Δh (cm)	γ_t (dyne cm^{-1})	t (secs)	Δh (cm)	γ_t (dyne cm^{-1})
			pH 6.9 ± 0.05					
			no effect					
			γ_∞ = 65.0					
			pH 7.85 ± 0.05					
6.3	11.36	50.3	4.5	11.56	51.2	2.2	11.84	52.4
28.3	10.60	46.9	47.7	10.60	46.9	11.4	10.96	48.5
83.5	10.36	45.9	195.0	10.36	45.9	36.2	10.68	47.3
271.7	10.12	44.8				95.0	10.36	45.9
						816.6	10.0*	44.6
1.1	12.20	54.0	1.6	11.96	53.0			
15.3	11.00	48.7	11.3	11.18	49.5			
36.8	10.76	47.6	22.6	10.86	48.1			
143.6	10.40	46.1	66.2	10.58	46.8			
1074.3	10.10	44.7	614.5	10.24	45.3			
			pH 8.85 ± 0.05					
2.3	13.28	58.8	2.3	13.50	59.8	2.3	13.10	58.0
4.1	12.04	53.3	3.6	12.28	54.4	4.3	11.84	52.4
5.4	11.18	49.5	6.4	11.08	49.1	6.1	11.02	48.8
8.1	10.30	45.6	8.9	10.26	45.4	8.8	10.12	44.8
10.7	9.82	43.5	11.1	9.72	43.0	10.4	9.66	42.8
16.0	9.28	41.1	16.4	9.24	40.9	15.9	9.16	40.6

TABLE 1.6 (cont'd)

t (secs)	Δh (cm)	γ_t (dyne cm^{-1})	t (secs)	Δh (cm)	γ_t (dyne cm^{-1})	t (secs)	Δh (cm)	γ_t (dyne cm^{-1})
			pH 8.85 ± 0.05 (cont'd)					
19.0	9.06	40.1	18.6	9.00	39.9	19.2	8.90	39.4
23.7	8.84	39.1	19.6	8.72	38.6	22.4	8.68	38.4
27.7	8.60	38.1	25.8	8.52	37.7	24.8	8.46	37.5
25.3	8.34	36.9	29.5	8.28	36.7	25.9	8.22	36.4
41.8	8.10	35.9	33.6	8.08	35.8	33.6	8.02	35.5
47.5	7.90	35.0	41.5	7.88	34.9	45.8	7.56	33.5
60.5	7.70	34.1	50.3	7.66	33.9	56.1	7.36	32.6
75.3	7.50	33.2	54.8	7.48	33.1	73.8	7.16	31.7
101.6	7.36	32.6	85.6	7.26	32.1	109.6	6.94	30.7
			74.2	7.06	31.3	183.2	6.80	30.1
			pH 9.85 ± 0.05					
			see TABLE 1.2					
			pH 10.85 ± 0.05					
2.3	12.16	53.8	4.5	12.40	54.9	5.2	12.70	56.2
7.9	10.48	46.4	7.3	10.92	48.4	5.5	11.70	51.8
4.5	9.66	42.8	6.0	10.34	45.8	6.0	11.00	48.7
8.3	8.88	39.3	4.9	9.40	41.6	15.2	10.74	47.6
27.8	8.14	36.0	9.3	8.78	38.9	13.7	10.42	46.1
15.0	7.88	34.9	45.0	8.32	36.8	22.0	10.00	44.3
9.2	7.60	33.7	37.6	8.04	35.6	21.0	9.70	41.6
82.3	7.24	32.1	58.2	7.80	34.5	21.0	9.26	41.0
22.2	7.18	31.8				17.0	8.98	39.7
53.6	6.64	29.4				10.2	8.76	38.8

TABLE 1.6 (cont'd)

t (secs)	Δh (cm)	γ_t (dyne cm^{-1})	t (secs)	Δh (cm)	γ_t (dyne cm^{-1})	t (secs)	Δh (cm)	γ_t (dyne cm^{-1})
			pH 10.85 ± 0.05					
199.1	6.28	27.8				38.1	8.42	37.3
136.0	5.96	26.4				25.1	7.84	34.7
						78.3	7.44	32.9
						53.7	7.30	32.3
						44.6	7.14	31.6
						55.1	6.90	30.6
						220.0	6.54	29.0
						230.2	6.36	28.2
5.0	12.40	54.9	4.9	12.64	56.0			
11.1	11.56	51.2	7.1	12.14	43.8			
13.5	10.70	47.4	11.1	11.52	51.0			
16.7	10.40	46.1	11.0	11.16	49.4			
18.1	10.06	44.5	19.9	9.82	43.5			
18.3	9.80	43.4	22.3	9.56	42.3			
19.5	9.58	42.4	19.3	9.26	41.0			
28.3	9.32	41.3	23.7	8.98	39.8			
27.0	8.92	39.5	23.0	8.76	38.8			
27.0	8.60	38.1	17.8	8.52	37.7			
49.7	8.24	36.5	44.8	8.20	36.3			
53.6	8.04	35.6	63.8	7.92	35.1			
64.3	7.80	34.5	87.3	7.62	33.7			
108.7	7.44	32.9	90.1	7.32	32.4			
63.5	7.20	31.9	90.7	7.02	31.1			
48.9	6.98	30.9	26.4	6.78	30.0			
74.6	6.68	29.6	153.0	6.60	29.2			

TABLE 1.6 (cont'd)

t (secs)	Δh (cm)	γ_t (dyne cm^{-1})	t (secs)	Δh (cm)	γ_t (dyne cm^{-1})	t (secs)	Δh (cm)	γ_t (dyne cm^{-1})
			pH 11.60 ± 0.05					
8.7	15.30	67.7	1.8	15.96	70.7	2.2	15.80	70.0
17.7	14.84	65.7	7.6	15.38	68.1	3.3	15.80	70.0
30.8	14.42	63.9	19.3	15.02	66.5	29.5	14.82	65.6
72.4	14.14	62.6						
1.8	15.70	69.5	5.2	15.76	69.8	12.3	15.20	67.3
30.4	14.76	65.4	18.2	15.30	67.7	25.2	14.82	65.6
58.8	14.30	63.3	20.7	14.78	65.4	47.5	14.44	63.9
			50.3	14.38	63.7	64.3	14.08	62.3
			84.0	13.98	61.9	426.3	13.46	59.6
			467.2	13.08	57.9			
			pH 12.25 ± 0.05					
5.1	15.30	67.8	66.5	15.18	67.3			
14.5	15.30	67.8	> 5 min	14.80	65.6			
> 2 min	14.68	65.0						
			pH 12.5 ± 0.05					
9.3	15.48	68.5	5.1	14.80	70.0	1.7	15.84	70.1
8.3	15.50	68.6	187.1	15.40	68.2	9.7	15.56	68.9
> 5 min	15.10	66.9	> 6 min	15.04	66.4	> 8 min	15.20	67.4

TABLE 1.7

Dynamic Surface Tension of Dodecylamine Acetate Solutions in the Presence of 10^{-2} M Sodium Acetate

t (secs)	Δh (cm)	γ_t (dyne cm^{-1})	t (secs)	Δh (cm)	γ_t (dyne cm^{-1})	t (secs)	Δh (cm)	γ_t (dyne cm^{-1})
2.1	13.36	59.2	1.4	15.80	70.0	1.6	13.54	60.0
3.6	11.88	52.6	1.5	15.50	68.7	3.4	11.82	52.4
6.2	10.42	46.2	2.1	13.84	61.3	4.1	11.05	49.0
7.4	10.18	45.1	2.1	13.76	61.0	8.1	9.80	43.4
7.8	10.00	44.3	4.1	11.56	51.2	8.9	9.64	42.7
6.3	9.14	40.5	6.0	11.00	48.7	9.7	9.44	41.8
13.7	8.34	36.9	6.3	10.36	45.9	11.8	8.82	39.1
14.3	8.14	36.1	6.1	9.62	42.6	10.3	8.64	38.3
15.0	8.00	35.4	9.9	9.40	41.6	12.7	8.44	37.4
14.6	7.80	34.6	11.1	9.20	40.8	10.5	8.26	36.6
14.9	7.62	33.8	12.1	9.00	39.9	14.4	8.06	35.7
16.2	7.44	33.0	10.7	8.78	38.9	12.1	7.90	35.0
16.5	7.26	32.2	14.5	8.60	38.1	15.5	7.72	34.2
17.3	7.10	31.5				19.5	7.52	33.3
20.1	6.96	30.8				16.3	7.40	32.8
20.5	6.72	29.8				16.4	7.20	31.9
21.3	6.54	29.0				19.3	7.04	31.2
22.1	6.40	28.4				22.6	6.84	30.3
27.9	6.30	27.9				30.2	6.68	29.6
29.3	6.18	27.4				38.1	6.56	29.1
30.9	6.06	26.8				36.1	6.40	28.4
38.2	5.88	26.0				46.1	6.24	27.6
46.2	5.78	25.6				63.6	6.06	26.8
57.3	5.70	25.3						
67.1	5.54	24.5				79.0	5.92	26.2
						107.4	5.82	25.8
						143.6	5.64	25.0
						> 5 min	5.50	24.4

TABLE 1.8

Dynamic Surface Tension of Dodecylamine Acetate Solutions at pH 9.85 ± 0.05, Effect of Total Amine Concentration

t (secs)	Δh (cm)	γ_t (dyne cm^{-1})	t (secs)	Δh (cm)	γ_t (dyne cm^{-1})	t (secs)	Δh (cm)	γ_t (dyne cm^{-1})
			2.04×10^{-5} M					
45.4	15.70	69.6	25.4	15.64	69.3	49.0	14.98	66.3
122.0	14.38	63.7	80.2	14.48	64.1	72.2	14.70	65.1
119.4	14.12	62.6	93.5	14.20	62.9	87.3	14.36	63.6
123.0	13.80	61.1	104.2	13.94	61.7	102.1	14.04	62.2
134.8	13.54	60.0	11.38	13.56	60.0	118.5	13.68	60.6
147.6	13.18	58.4	128.4	13.24	58.6	127.0	13.34	59.1
161.3	12.86	57.0	140.0	12.94	57.3	146.2	13.02	57.7
178.3	12.58	55.7	163.7	12.60	55.8	235.1	12.02	53.2
190.9	12.28	54.4	176.3	12.34	54.6			
217.7	12.04	53.3	227.6	12.08	53.5			
244.7	11.84	52.6	> 5 min	11.82	52.4			
333.2	11.56	51.3						
394.8	11.24	49.8						
23.0	15.76	69.8						
31.9	15.16	67.1						
63.6	14.82	65.6						
76.0	14.46	64.0						
89.2	14.16	62.7						
			4.08×10^{-5} M					
			see TABLE 1.4					
			8.16×10^{-5} M					
			see TABLE 1.5					

TABLE 1.8 (cont'd)

t (secs)	-Δh (cm)	γ_t (dyne cm^{-1})	t (secs)	Δh (cm)	γ_t (dyne cm^{-1})	t (secs)	Δh (cm)	γ_t (dyne cm^{-1})
			2.04×10^{-4}M					
5.1	13.88	61.5	3.3	14.46	64.0	2.8	14.74	65.3
4.5	12.74	56.4	4.6	13.34	59.1	5.6	13.30	58.9
8.4	12.08	53.5	5.2	12.18	53.9	7.5	12.20	54.0
10.0	11.36	50.3	7.9	11.20	50.0	11.0	10.86	48.1
11.2	11.06	49.0	9.1	10.90	48.3	13.3	9.84	43.6
11.4	10.70	47.4	10.1	10.54	46.7	16.6	9.52	42.2
14.1	10.38	46.0	12.5	9.90	43.8	17.6	9.26	41.0
16.0	10.04	44.5	17.5	9.58	42.4	25.3	8.68	38.4
18.1	9.70	43.0	20.6	9.06	40.1	26.5	8.40	37.2
18.6	9.40	41.6	21.4	8.78	38.9	31.6	8.06	35.7
22.2	9.10	40.3	27.9	8.46	37.5	36.1	7.78	34.4
26.0	8.82	39.0	31.0	8.18	36.2	38.4	7.50	33.2
30.2	8.50	37.6	37.8	7.70	34.1	51.7	7.26	32.1
35.4	8.26	36.6	35.6	7.46	33.0	68.9	7.02	31.1
41.3	7.96	35.2	45.1	7.22	32.0	90.4	6.70	29.7
42.0	7.70	34.1	59.0	6.96	30.8	80.6	6.48	28.7
43.7	7.48	33.1	77.1	6.76	29.9	114.7	6.30	27.9
56.7	7.22	32.0	102.3	6.54	29.0	> 6 min	5.96	26.3
44.2	7.02	31.1	147.8	6.34	28.1			
74.8	6.74	29.8						
89.7	6.52	28.9						
101.0	6.32	28.0						
189.6	6.12	27.1						

4.08×10^{-4}M
see TABLE 1.2a)

8.16×10^{-4}M
see TABLE 1.2b)

TABLE 1.9

Dynamic Surface Tension of Free Dodecylamine Solutions at Saturation: Effect of Increasing pH

t (secs)	Δh (cm)	γ_t (dyne cm^{-1})	t (secs)	Δh (cm)	γ_t (dyne cm^{-1})	t (secs)	Δh (cm)	γ_t (dyne cm^{-1})
			20 Hours of Contact Natural pH					
3.5	7.50	33.2	0.8	8.18	36.2	3.4	7.60	33.7
2.3	6.80	30.1	2.2	7.78	34.4	4.8	6.96	30.8
7.5	6.10	27.0	2.5	7.06	31.3	3117	5.20	23.0
7.7	5.98	26.5	2.3	6.78	30.0	22.7	5.00	22.1
8.9	5.60	24.8	12.9	6.42	28.4	17.1	4.80	21.3
			12.9	5.82	25.8			
			20.3	5.54	24.5			
			91.2	5.14	22.8			
			34.9	4.92	21.8			
1.0	8.00	35.4	1.2	7.78	34.4			
9.9	6.54	29.0	5.6	6.70	29.7			
10.5	6.18	27.4	8.2	6.36	28.2			
21.9	5.84	25.9	8.7	5.96	26.4			
29.0	5.60	24.8	21.2	5.64	25.0			
28.9	5.02	22.2	19.7	5.36	23.7			
43.7	4.44	19.7	27.0	4.82	21.3			
			pH 11.65					
7.5	15.78	69.9	8.1	15.72	69.6	12.1	15.62	69.2
514.3	15.40	68.2	40.6	15.32	67.8	55.8	15.34	67.9
86.1	14.86	65.8	349.9	14.42	63.9	328.9	15.00	66.4

CALCULATION OF $[3RNH_3^{3+}.RNH_2]$ FOR FIGURE 2.12

Basic Equations

$$RNH_2 + H_2O \underset{}{\overset{K_1}{\rightleftharpoons}} RNH_3^+ + OH^-$$

$$K_1 = 4.3 \times 10^{-4} \quad (93)$$

$$H_2O \quad \overset{K_2}{\rightleftharpoons} \quad H^+ + OH^-$$
$$H_2O$$

$$K_2 = 10^{-14}$$

$$RNH_3^+ \overset{K_3}{\rightleftharpoons} RNH_2 + H^+$$

$$K_3 = 2.4 \times 10^{-11}$$

Assumptions

1) no precipitation (i.e. concentrations less than 2×10^{-5}M).
2) the complex is 3:1 ion:molecule.
3) the maximum possible complex formation is achieved (i.e. complex, RNH_3^+ and RNH_2 do not coexist in solution).
4) the ionization constant for dodecylamine (K_1) is valid for the calculations.

TABLE 1.10

Per Cent Amine Present as RNH_3^+, $3RNH_3^+.RNH_2$ and RNH_2 (or $RNH_2.H_2O$)

pH	RNH_2	RNH_3^+	$3RNH_3^+.RNH_2$
8	-	99.04	0.96
9	-	90.8	9.2
9.5	-	72.0	28.0
10.0	-	22.6	77.4
10.14	-	-	100.0
10.5	23.9	-	76.1
11.0	61.3	-	38.7
12.0	94.7	-	5.3

APPENDIX II

CHAPTER THREE

RESULTS

Contents

Bubble Pick-Up of Magnetite: ($\phi \pm 5^{o}$)

i) Distilled Water, $\phi = 0^{o}$

ii) 4.08×10^{-4}M, natural pH, see photographic record in text.

iii) 4.08×10^{-4}M, pH 12.2, see photographic record in text.

TABLE II.1

Bubble Pick-Up (ϕ) of -65 + 100 Mesh Magnetite at pH 9.7 ± 0.1

t (sec)	ϕ (^{o})	t (sec)	ϕ (^{o})	t (sec)	ϕ (^{o})
		C = 1.02×10^{-5}M (no flotation)			
< 1	30	< 1	35	< 1	35
7.5	15	9	15	12	20
17	20	18	20	18	< 10
27	15	30	35	57	30
57	25	57	15	59	20
117	45	117	30	117	20
		C = 2.04×10^{-5}M (no flotation)			
< 1	40	< 1	25	< 1	50
5	20	5	35	5	50
5	15	5	30	5	20
14	30	16	30	17	30
20	30	20	45	57	30
58	60	58	30	58	40
59	40	60	35	120	40
178	30	300	30		

TABLE II.1 (cont'd)

$C = 4.08 \times 10^{-5} M$

t (sec)	ϕ (°)	t (sec)	ϕ (°)	t (sec)	ϕ (°)
< 1	60	< 1	90	< 1	50
< 1	45	< 1	15	< 1	80
< 1	25	< 1	60	< 1	90
5	35	5	40	10	40
12	30	12	30	13	40
15	30	16	40	30	30
33	30	60	30	60	35
88	30	89	45	89	30
90	10				
< 1	50	< 1	40	< 1	50
< 1	50	< 1	40	< 1	40
2	40	5	20	5	40
9	40	9	30	9	50
9	50	10	30	10	25
15	30	24	30	30	40
117	40	120	25	177	30
297	35	298	30		

$C = 8.16 \times 10^{-5} M$ (~50% flotation)

< 1	85	< 1	90	< 1	75
9	70	10	55	11	60
11	50	15	50	15	45
25	45	30	35	30	30
59	25	60	30	65	20
120	20	300	15	300	15

TABLE II.1 (cont'd)

t (sec)	ϕ (°)	t (sec)	ϕ (°)	t (sec)	ϕ (°)
$C = 4.08 \times 10^{-4}$ M (100% flotation)					
< 1	90	< 1	90	< 1	90
< 1	90	< 1	90	< 1	90
13	20	13	10	15	0
15	15	20	0	59	0
61	0				
< 1	90	< 1	90	< 1	90
< 1	90	< 1	90	< 1	90
5	0	5	40	5	0
5	20	5	0	5	20
9	10	10	20	11	0
11	0	13	0	15	0
17	0	28	10	30	0
57	0	58	0	300	0

Bubble Pick-Up of Quartz ($\phi \pm 5^{o}$)

i) Distilled Water, $\phi \sim 25^{o}$

TABLE II.2

Bubble Pick-Up of -65 + 100 Mesh Quartz at pH 9.7 ± 0.1 (Acid Leached of "As Prepared")

$C = 4.08 \times 10^{-4}$M (100% flotation)

t (sec)	ϕ (^{o})	t (sec)	ϕ (^{o})	t (sec)	ϕ (^{o})
< 1	90	< 1	90	< 1	90
< 1	90	< 1	90	10	90
10	90	15	80	30	90
60*	90	300*	80	300*	90

* tendency to drop load on tapping holder - but inconclusive

TABLE II.3

Bubble Contact Experiments

pH 9.7 ± 0.1, C
$C = 4.08 \times 10^{-4}$M

t (sec)	Contact Glass/Hematite	t (sec)	Contact Glass/Hematite
< 1	Excellent	< 1	Excellent
> 5	Poor	> 5	Poor
> 30	Zero	> 30	Zero

TABLE 11.4

Flotation of a Mixed (35:65 w/w) Quartz: Magnetite Sample in Methanol/Water Mixtures After 30 min. Conditioning in 4.08×10^{-4}M Amine at pH 9.7 ± 0.1

Methanol (%)	Floats				Sinks			
	Quartz		Magnetite		Quartz		Magnetite	
	(gm)	(%)	(gm)	(%)	(gm)	(%)	(gm)	(%)
0	0.27	100	0.69	100	0	0	0.0	0
15	0.25	100	0.70	95	0	0	0.05	5
25	0.41	98	0.24	35	0.01	2	0.46	65
40	0.32	99	0.01	1	0.01	1	0.56	99
50	0.11	22	0	0	0.51	78	0.56	100
50	0.25	62	0	0	0.15	38	0.61	100
50	0.04	12	0	0	0.27	96	0.75	100
100*	0.01	3	0	0	0.24	97	0.80	100

* replacing 100% methanol with distilled water gave zero recovery of both quartz and magnetite.

TABLE 11.5

Flotation of a Mized (~35:65 w/w) Quartz: Magnetite Sample After 30 min Desorption in Distilled Water, Following Conditioning in 4.08×10^{-4}M Amine at pH 9.7 ± 0.1 for 30 Min.

		Floats				Sinks			
		Quartz		Magnetite		Quartz		Magnetite	
	Desorption	(gm)	(%)	(gm)	(%)	(gm)	(%)	(gm)	(%)
A.	pH 9.7	0.25	100	0.71	98	0	0	0.01	2
B.	pH 6.1 (I)	0.31	99	0.60	80	0.01	1	0.15	20
C.	pH 6.1 (II)*	0.02	9	0.07	5	0.16	91	0.96	95

* C 2nd desorption, after B

TABLE 11.6

Dynamic Surface Tension of Dodecylamine Acetate Solutions After Conditioning ~ One Gramme Magnetite Samples

t (secs)	Δh (cm)	γ_t (dyne cm^{-1})	t (secs)	Δh (cm)	γ_t (dyne cm^{-1})	t (secs)	Δh (cm)	γ_t (dyne cm^{-1})
			2.04×10^{-5}M, pH 9.7 ± 0.1					
			no effect, γ_∞ = 69.0 ± 1.0					
			4.08×10^{-5}M, pH 9.7 ± 0.1					
144.0	14.58	65.3	61.3	15.56	69.7	79.5	15.42	69.1
162.0	14.14	63.3	134.7	14.76	66.1	117.0	15.02	67.3
224.8	13.68	61.3	151.9	14.26	63.9	144.9	14.56	65.2
286.4	13.26	59.4	211.3	13.82	61.9	183.7	14.06	63.0
			8.16×10^{-5}M, pH 9.7 ± 0.1					
15.7	15.52	69.5	14.5	15.40	69.0	20.6	14.80	66.3
42.5	14.34	64.2	44.3	14.20	63.6	41.0	14.20	63.6
50.1	13.80	61.8	54.6	13.66	61.2	54.4	13.64	61.1
61.1	13.26	59.4	64.7	13.08	58.6	62.9	13.04	58.4
69.7	12.66	56.7	81.7	12.44	55.7	81.1	12.44	55.7
83.3	12.16	54.5	119.4	11.82	53.0	119.2	11.84	53.0
128.9	11.58	51.9	> 5 min			> 5 min		
> 5 min								
			4.08×10^{-4}M, pH 9.7 ± 0.1					
4.3	12.14	55.0	0.5	13.82	62.6	3.8	12.84	58.2
4.3	12.00	54.4	3.3	13.00	58.9	3.5	12.64	57.3
7.6	10.36	46.9	4.3	12.24	55.4	4.3	12.58	57.0
8.3	10.02	45.4	5.8	11.00	49.8	5.8	11.60	52.5
8.3	9.86	44.7	6.3	11.00	49.8	6.9	10.94	49.6
9.1	9.40	42.6	6.8	10.60	48.0	6.9	10.60	48.0
14.5	8.76	40.0	7.5	10.42	47.2	7.3	10.20	46.2

TABLE II.6 (cont'd)

t (secs)	Δh (cm)	γ_t (dyne cm^{-1})	t (secs)	Δh (cm)	γ_t (dyne cm^{-1})	t (secs)	Δh (cm)	γ_t (dyne cm^{-1})
			4.08×10^{-4}M, pH 9.7 ± 0.1 (cont'd)					
15.3	8.42	38.1	8.5	9.80	44.4	8.5	10.00	45.3
18.5	7.96	36.1	10.7	9.20	41.7	8.3	9.78	44.3
20.4	6.96	31.5	20.1	8.20	37.1	9.1	9.60	43.5
25.4	6.68	30.3	23.8	7.70	34.9	10.1	9.12	41.3
76.7	6.42	29.1	16.1	7.22	32.7	10.3	8.80	39.9
> 4 min						15.7	8.50	38.5
			3.8	12.42	56.3	19.4	7.94	36.0
			3.6	12.24	55.4	13.7	6.98	31.6
			5.3	11.32	51.3	45.0	6.70	30.4
			6.5	10.82	49.0	103.8	6.50	29.4
			7.7	10.40	47.1			
			7.8	9.94	45.0			
			8.9	9.60	43.5			
			9.5	9.24	41.9			

TABLE II-7

Dynamic Surface Tension Generated by 30 Min. Desorption into Distilled Water After Conditioning for 30 Min in 4.08×10^{-4} M at pH 9.7 ± 0.1

t (secs)	Δh (cm)	γ_t (dyne cm^{-1})	t (secs)	Δh (cm)	γ_t (dyne cm^{-1})	t (secs)	Δh (cm)	γ_t (dyne cm^{-1})
			Distilled Water, pH 9.7 ± 0.1					
17.5	15.18	68.0	13.9	15.22	68.2			
30.7	14.24	63.8	25.6	14.76	66.1			
35.7	13.84	62.0	33.7	14.32	64.2			
42.0	13.44	60.2	39.1	13.84	62.0			
48.2	13.06	58.5	46.1	13.42	60.1			
53.4	12.62	56.5	52.0	12.98	58.2			
59.7	12.22	54.7	59.8	12.54	56.2			
57.3	11.82	53.0	65.7	12.12	54.3			
75.6	11.46	51.3	74.6	11.70	52.4			
85.1	11.08	49.6	91.3	11.34	50.8			
105.5	10.76	48.2	109.3	10.98	49.2			
142.3	10.40	46.6	155.9	10.62	47.6			
> 5 min			> 5 min					
			Distilled Water, Natural pH					
2.7	15.56	69.9						
6.7	15.92	71.3						
11.3	15.62	70.0						
19.5	15.62	70.0						
49.7	15.62	70.0						
> 5 min								
			Distilled Water, Natural pH with Subsequent Adjustment to pH 9.7					
6.4	15.44	69.2	7.0	15.38	68.9	3.2	15.56	69.7
20.5	14.30	64.1	17.0	14.78	66.2	19.7	14.00	62.7
22.0	13.92	62.4				21.1	13.64	61.1
24.6	13.62	61.0				24.2	13.32	59.7
27.7	13.26	59.4				26.5	12.96	58.1
28.6	12.90	57.8				28.5	12.62	56.5
31.7	12.54	56.2				30.7	12.26	54.9
33.8	12.22	54.7				34.1	11.96	53.6

TABLE II.7 (cont'd)

t (secs)	Δh (cm)	γ_t (dyne cm^{-1})	t (secs)	Δh (cm)	γ_t (dyne cm^{-1})	t (secs)	Δh (cm)	γ_t (dyne cm^{-1})
Distilled Water, Natural pH with Subsequent Adjustment to pH 9.7 (cont'd)								
36.4	11.88	53.2				35.8	11.60	52.0
39.9	11.54	51.7						
43.8	11.24	50.4						
47.2	10.96	49.1						
53.3	10.64	47.7						
61.3	10.32	46.2						
75.7	10.04	45.0						
79.8	9.74	43.6						
92.9	9.46	42.4						
107.8	9.20	41.2						
122.5	8.92	40.0						
141.0	8.74	39.2						
167.6	8.48	38.0						

TABLE 11.8

Dynamic Surface Tension of Dodecylamine Acetate Solutions after Conditioning ~0.3 Gramme Quartz Sample

t (secs)	Δh (cm)	γ_t (dyne cm^{-1})	t (secs)	Δh (cm)	γ_t (dyne cm^{-1})	t (secs)	Δh (cm)	γ_t (dyne cm^{-1})
3.1	13.24	58.7	1.3	13.24	58.7			
3.3	12.16	53.9	3.9	12.42	55.0			
5.7	11.36	50.3	4.8	11.56	51.2			
5.9	11.10	49.2	7.0	10.58	46.9			
6.8	10.80	47.8	6.7	10.38	46.0			
7.3	10.58	46.9	8.3	10.04	44.5			
7.5	10.36	45.9	11.2	9.86	43.7			
9.5	10.10	44.7	10.5	9.62	42.6			
9.7	9.82	43.5	11.9	9.40	41.6			
12.1	9.60	42.5	13.7	9.14	40.5			
8.7	9.36	41.5	10.5	8.98	39.8			
13.1	9.14	40.5	11.5	8.78	38.9			
14.7	8.96	39.7	15.2	8.58	38.0			
15.1	8.74	38.7	17.5	8.38	37.1			
17.0	8.50	37.7	13.7	8.16	36.1			
14.1	8.28	26.7	18.7	7.96	35.3			
15.5	7.94	35.2						
20.7	7.76	34.4						
20.8	7.60	33.7						
22.7	7.40	32.8						

APPENDIX III

CALCULATION OF $C_o(D)^{1/2}$

Contents

III.1 Limitation on Application of Equation 4.5

The assumption:

$$C_t \rightarrow 0 \qquad (1)$$

The Syskowski equation:

$$\gamma_o - \gamma_t = \Gamma_m RT \ln [1 + aC_t] \qquad (2)$$

Expanding:

$$\gamma_o - \gamma_t = \Gamma_m RT [aC_t - \tfrac{1}{2}(aC_t)^2 + \tfrac{1}{3}(aC_t)^3 + \ldots] \qquad (3)$$

The zero order approximation:

$$\gamma_o - \gamma_t = \Gamma_m RT\, a\, C_t \quad (\text{cf Eq. 4.5}) \qquad (4)$$

The first order approximation:

$$\gamma_o - \gamma_t = \Gamma_m RT\, a\, C_t [1 - \tfrac{1}{2}(aC_t)] \qquad (5)$$

Substituting zero order approximation into first order approximation:

$$\gamma_o - \gamma_t = \Gamma_m RT\, a\, C_t [1 - \tfrac{1}{2}(\frac{\gamma_o - \gamma_t}{\Gamma_m RT})] \qquad (6)$$

For $\frac{1}{2}(\frac{\gamma_o - \gamma_t}{\Gamma_m RT}) < 0.1$, Eq. (6) is within 10% of Eq. (4). Hence:

$$\gamma_o - \gamma_t < 0.2\, \Gamma_m RT \qquad (7)$$

Taking $\Gamma_m = 6 \times 10^{-10}$ mole cm^{-1} (the value for simple alcohols, carboxylic acids (125,155) and amines (133)), $R = 8.3 \times 10^7$ erg $mole^{-1}$ $^oK^{-1}$ and $T = 300^oK$:

$$\Gamma_m RT = 15 \text{ dyne } cm^{-1} \qquad (8)$$

Hence:

$$\gamma_o - \gamma_t < 3 \text{ dyne } cm^{-1} \qquad (9)$$

III.2 Limitation on Application of Equation 4.13

Assuming the Langmuir/Syskowski relationship:

$$\gamma_o - \gamma_t = \Gamma_m RT \ln [1 + aC_t] \qquad (10)$$

and:

$$\gamma_o - \gamma_\infty = \Gamma_m RT \ln [1 + aC_o] \qquad (11)$$

hence:

$$\gamma_t - \gamma_\infty = - \Gamma_m RT \ln \left[\frac{1 + aC_t}{1 + aC_o}\right] \qquad (12)$$

by making the following substitution:

$$C_t = C_o - \Delta C_o$$

i.e. equilibrium is approached, Eq. (12) becomes:

$$\gamma_t - \gamma_\infty = - \Gamma_m Rt \ln \left[1 - \frac{a \Delta C_o}{1 + aC_o}\right] \qquad (13)$$

expanding:

$$\gamma_t - \gamma_\infty = \Gamma_m RT \left[\frac{a\Delta C_o}{1 + aC_o} - \frac{1}{2}\left(\frac{a\Delta C_o}{1 + aC_o}\right)^2 + \frac{1}{3}\left(\frac{a\Delta C_o}{1 + aC_o}\right)^3 - \cdots\cdot\right] \tag{14}$$

Substituting a re-arranged Langmuir equation:

$$\Gamma_m = \Gamma_e \left(\frac{1 + aC_o}{aC_o}\right) \tag{15}$$

gives:

$$\gamma_t - \gamma_\infty = \Gamma_e RT \frac{\Delta C_o}{C_o}\left[1 - \frac{1}{2}\left(\frac{a\Delta C_o}{1 + aC_o}\right) + \frac{1}{3}\left(\frac{a\Delta C_o}{1 + aC_o}\right)^2 - \cdots\cdot\right] \tag{16}$$

The Hansen assymptotic solution (Eq. 4.10) can be modified:

$$\frac{C_o - \Delta C_o}{C_o} = 1 - \frac{\Gamma_e}{C_o(\pi Dt)^{1/2}} \tag{17}$$

thus:

$$\frac{\Delta C_o}{C_o} = \frac{\Gamma_e}{C_o(\pi Dt)^{1/2}} \tag{18}$$

combining with Eq. (15) gives:

$$\frac{a\Delta C_o}{1 + aC_o} = \frac{\Gamma_e^2}{\Gamma_m C_o(\pi Dt)^{1/2}} \tag{19}$$

Thus Eq. (16) can be written:

$$\gamma_t - \gamma_\infty = \frac{\Gamma_e^2 RT}{C_o(\pi Dt)^{1/2}}\left[1 - \frac{1}{2}\frac{\Gamma_e^2}{C_o \Gamma_m (\pi Dt)^{1/2}} + \cdots\right] \tag{20}$$

The zero order approximation:

$$\gamma_t - \gamma_\infty = \frac{\Gamma_e^2 RT}{C_o(\pi Dt)^{1/2}} \quad \text{(cf Eq. 4.13)} \qquad (21)$$

The first order approximation

$$\gamma_t - \gamma_\infty \frac{\Gamma_e^2 RT}{C_o(\pi Dt)^{1/2}} \left[1 - \frac{1}{2}\frac{\Gamma_e^2}{C_o\Gamma_m(\pi Dt)^{1/2}}\right] \qquad (22)$$

Substituting the zero order approximation into the first order approximation

$$\gamma_t - \gamma_\infty = \frac{\Gamma_e^2 RT}{C_o(\pi Dt)^{1/2}} \left[1 - \frac{1}{2}\left(\frac{\gamma_t - \gamma_\infty}{\Gamma_m RT}\right)\right] \qquad (23)$$

For $\frac{1}{2}\left(\frac{\gamma_t - \gamma_\infty}{\Gamma_m RT}\right) < 0.1$, Eq. (23) is within 10% of Eq. (21).

Substituting the value of $\Gamma_m RT$ (Eq. (8)):

$$\gamma_t - \gamma_\infty < 3 \text{ dyne cm}^{-1} \qquad (24)$$

III.3 Restriction Placed on Equation 4.13 by Assuming $\Gamma_e = \Gamma_m$

Assuming the Langmuir/Syskowski relationship:

Syskowski equation:

$$\gamma_o - \gamma_\infty = \Gamma_m RT \ln [1 + aC_o] \qquad (25)$$

Langmuir isotherm:

$$\Gamma_e = \frac{\Gamma_m a C_o}{1 + a C_o} \qquad (26)$$

If $\Gamma_e \longrightarrow \Gamma_m$, then $1 + aC_o \longrightarrow aC_o$.

For $aC_o > 10$, error is $< 10\%$.

Hence:

$$\gamma_o - \gamma_\infty > \Gamma_m RT \ln 10 \qquad (27)$$

$$> 2.3 \times 15$$

$$\gamma_o - \gamma_\infty > 35 \text{ dyne cm}^{-1} \qquad (28)$$

III.4 Numerical Solution to Equations 4.6a, 4.8a and 4.9a

x_2	$A_{1_{o_2}}$ (A^2)	γ_t (dyne cm^{-1})	$C_o(Dt)^{1/2} \times 10^{10}$ (mole cm^{-2})
0.1	27.6	< 0	5.33
0.2	29.0	5.0	5.08
0.3	30.7	21.9	4.76
0.4	33.0	33.8	4.45
0.5	36.3	43.1	4.05
0.6	41.2	50.7	3.57
0.7	49.3	57.1	2.98
0.75	55.9	60.0	2.62
0.8	65.7	62.7	2.24
0.82	71.1	63.7	2.07
0.85	82.0	65.2	1.79
0.88	98.4	66.7	1.49
0.9	114.8	67.6	1.28

FIGURE III.1

Y_t as a Function of A_1

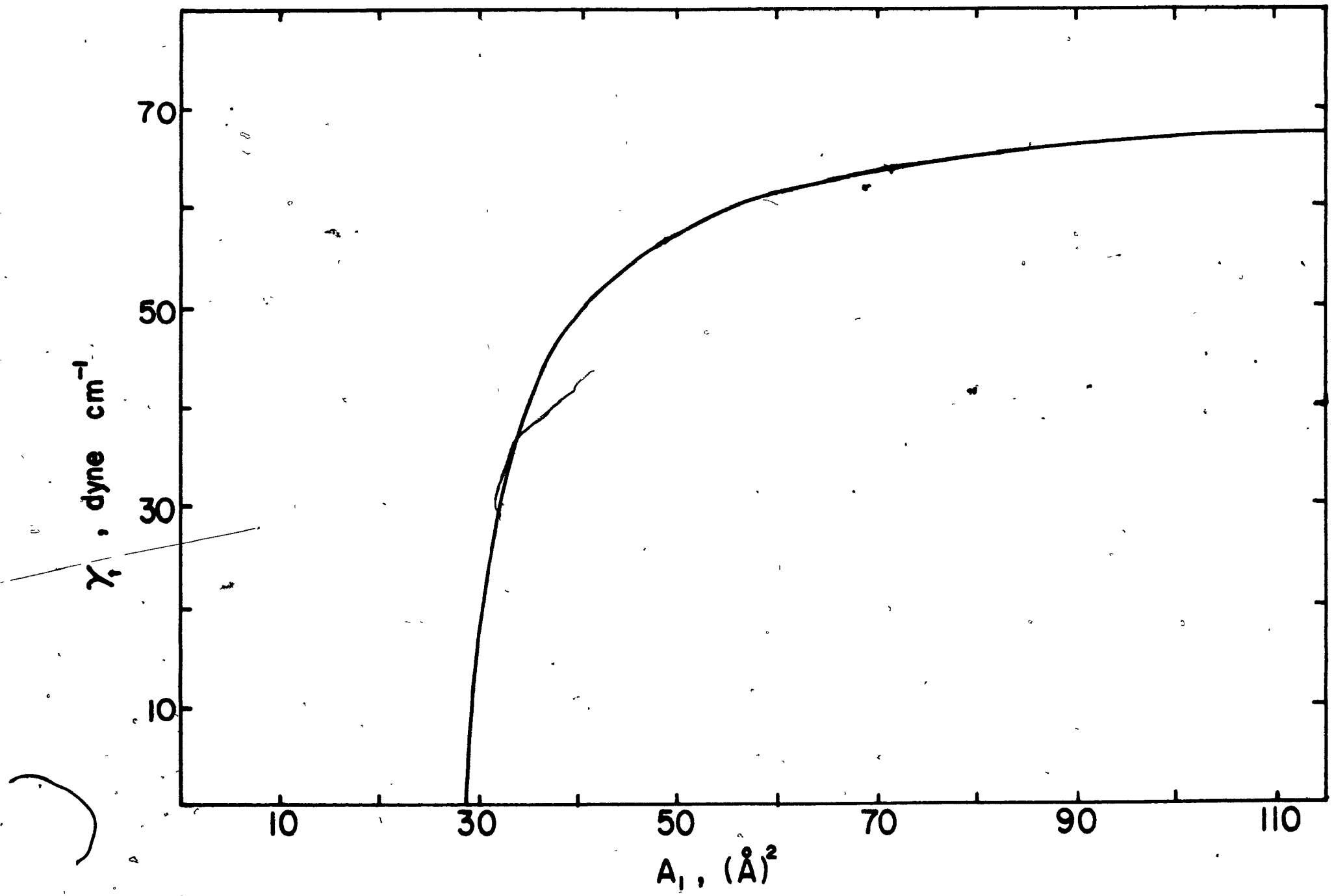
70
50
30
10
γ_s , dyne cm^{-1}
10
30
50
70
90
110
A_1 , (Å)^2

FIGURE III.2

γ_t as a Function of $C_o(Dt)^{1/2}$

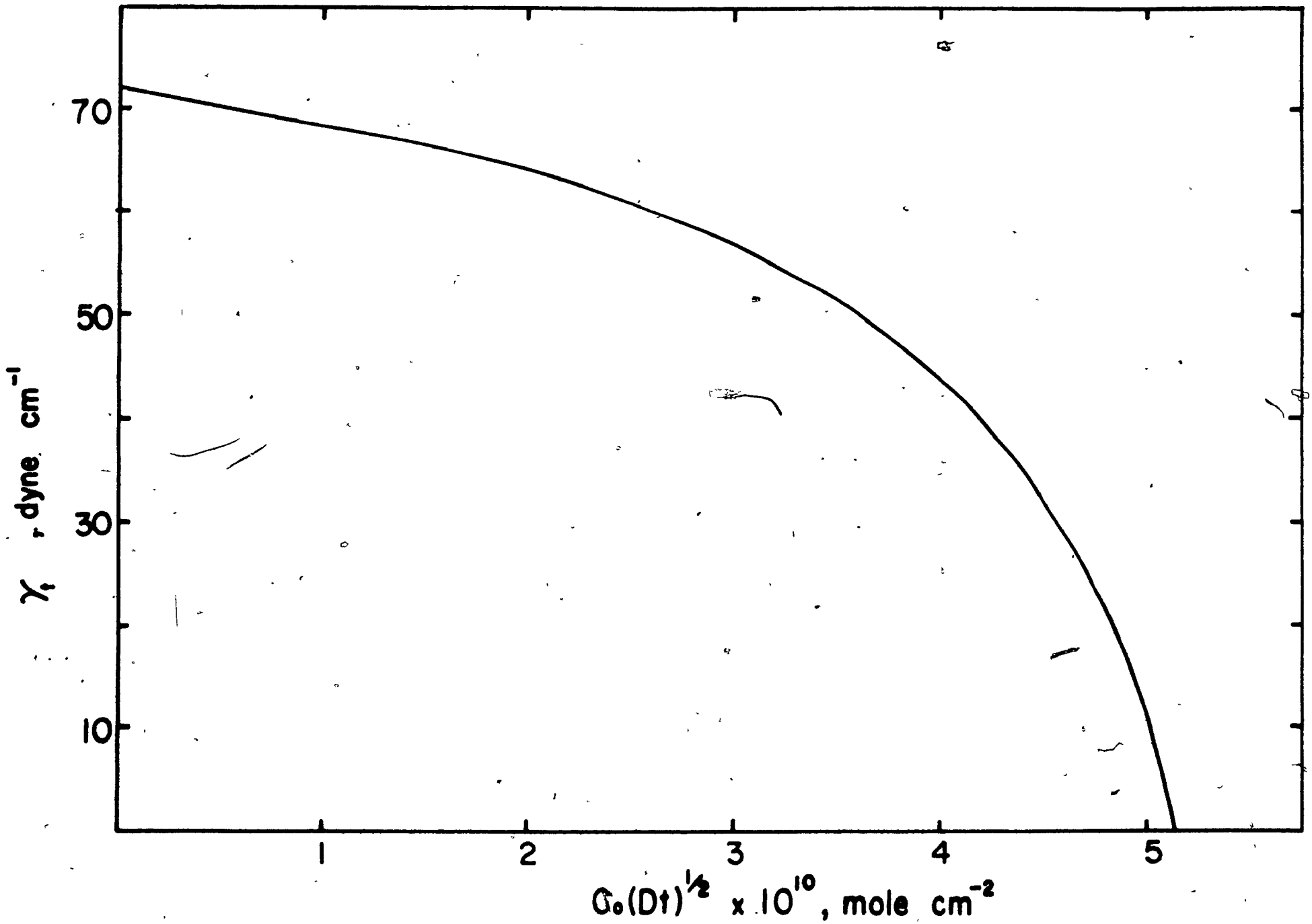
70
50
30
10
γ_t , dyne cm^{-1}
1
2
3
4
5
$G_o(Dt)^{1/2} \times 10^{10}$, mole cm^{-2}

III.5 Evaluation of $C_o(D)^{1/2}$ Using t-short Solution and the Fowkes Isotherm

Values of γ_t and $t^{1/2}$ are estimated from the experimental plot (see Figure 4.1). The corresponding value of $C_o(Dt)^{1/2}$ is estimated from the accompanying graph of γ_t vs $C_o(Dt)^{1/2}$. The value of $C_o(D)^{1/2}$ is then calculated ($C_o(Dt)^{1/2} / t^{1/2}$).

$t^{1/2}$ $(sec)^{1/2}$	γ_t dyne cm^{-1}	$C_o(Dt)^{1/2} \times 10^{10}$ mole cm^{-2}	$C_o(D)^{1/2} \times 10^{10}$ mole $cm^{-2} sec^{-1/2}$
	$C = 2.04 \times 10^{-8}$ mole cm^{-3}		
7.0	67.0	1.37	0.195
8.0	65.7	1.70	0.212
9.0	64.0	2.02	0.224
10.0	62.5	2.27	0.227
11.0	60.3	2.55	0.232
12.0	58.0	2.86	0.238
		"Average"	0.22 ± 0.02
	$c = 4.08 \times 10^{-8}$ mole cm^{-3}		
5.5	62.5	2.23	0.406
6.0	60.5	2.53	0.422
6.5	58.5	2.80	0.431
7.0	56.0	3.07	0.438
7.5	53.5	3.31	0.441
8.0	51.0	3.52	0.440

$t^{1/2}$ $(sec)^{1/2}$	γ_t dyne cm^{-1}	$C_o(Dt)^{1/2} \times 10^{10}$ mole cm^{-2}	$C_o(D)^{1/2} \times 10^{10}$ mole cm^{-2} $sec^{-1/2}$
	$C = 4.08 \times 10^{-8}$ mole cm^{-3} (cont'd)		
8.5	49.0	3.78	0.420
9.0	47.5	3.78	0.420
10.0	45.5	3.92	0.392
		"Average"	0.42±0.02
	$C = 8.16 \times 10^{-8}$ mole cm^{-3}		
3.3	62.5	2.27	0.687
3.5	61.5	2.40	0.685
3.7	60.3	2.57	0.695
4.0	58.7	2.77	0.692
4.3	56.8	3.00	0.695
4.5	55.2	3.15	0.700
4.7	53.9	3.27	0.696
5.0	51.2	3.51	0.701
5.2	50.0	3.61	0.693
5.5	48.2	3.73	0.677
		"Average"	0.69±0.01
	$C = 2.04 \times 10^{-7}$ mole cm^{-3}		
1	67.4	1.275	1.275
1.5	63.6	2.100	1.400
2.0	60.0	2.600	1.300

$t^{1/2}$ $(sec)^{1/2}$	γ_t dyne cm^{-1}	$C_o(Dt)^{1/2} \times 10^{10}$ mole cm^{-2}	$C_o(D)^{1/2} \times 10^{10}$ mole $cm^{-2} sec^{-1/2}$
	$C = 2.04 \times 10^{-7}$ mole cm^{-3} (cont'd)		
2.5	56.1	3.075	1.230
3.0	51.5	3.500	1.170
3.5	45.0	3.950	1.130
		"Average"	1.25±0.15
	$C = 4.08 \times 10^{-7}$ mole cm^{-3}		
0.6	66.5	1.50	2.50
0.7	65.5	1.72	2.46
0.8	64.2	1.98	2.48
0.9	63.0	2.20	2.44
1.0	62.0	2.35	2.35
1.1	60.5	2.55	2.32
1.3	58.0	2.86	2.20
1.5	54.8	3.18	2.12
1.8	49.5	3.65	2.03
2.0	45.0	3.95	1.97
		"Average"	2.32±0.15
	$C = 8.16 \times 10^{-7}$ mole cm^{-3}		
0.5	66.0	1.62	3.24
0.6	65.0	1.82	3.04
0.75	62.5	2.27	3.03
0.8	61.0	2.47	3.09

$t^{1/2}$ $(sec)^{1/2}$	γ_t dyne cm^{-1}	$C_o(Dt)^{1/2} \times 10^{10}$ mole cm^{-2}	$C_o(D)^{1/2} \times 10^{10}$ mole $cm^{-2} sec^{-1/2}$
	$C = 8.16 \times 10^{-7}$ mole cm^{-3} (cont'd)		
0.9	58.0	2.82	3.14
1.0	55.0	3.17	3.17
1.2	49.5	3.65	3.04
1.4	43.5	4.02	2.87
		"Average"	3.11±0.1

III.6 Determination of $C_o(D)^{1/2}$ from t-long Solution (Eq. 4.13a). Linear Regression Analysis

Concentration $(C)_5$ $M \times 10^5$	Intercept (γ_∞) dyne cm^{-1}	Slope dyne $sec^{1/2} cm^{-1}$	$C_o(D)^{1/2} \times 10^{10}$ mole $cm^{-2} sec^{-1}$	Correlation Coefficient
2.04*	--	--	--	--
4.08**	27.9	182.6	0.30	0.996
8.16	21.6	85.9	0.64	0.883
2.04	23.0	57.5	0.96	0.857
4.08	21.0	42.2	1.31	0.975
8.16	20.7	26.9	2.05	0.977

* Equation 4.13a not applicable: $\gamma_o - \gamma_\infty < 35$ dyne cm^{-1}

** Of doubtful value: $\gamma_t - \gamma_\infty > 6$ dyne cm^{-1}

III.7 Sample Calculation of Numerical Evaluation of γ_t vs $t^{1/2}$ Curves

Consider $C = 8.16 \times 10^{-4}$ M

t-short

$$A_1 = \frac{147 \times 10^{-10}}{2.75 \times 10^{-10}\ t^{1/2}}$$

$$A_1 = \frac{53.5}{t^{1/2}}$$

Solve numerically and determine γ_t from accompanying plot of γ_t vs A_1.

t-long

$$\gamma_t = \frac{55.5 \times 10^{-10}}{2.75 \times 10^{-10}\ t^{1/2}} + 20.7$$

$$\gamma_t = \frac{20.2}{t^{1/2}} + 20.7$$

Solve numerically and obtain γ_t direct.

VIII.8 Estimate of $C_o(D)^{1/2}$ from the Limiting Slope of the γ_t vs $t^{1/2}$ Curves as $t^{1/2} \to 0$ Employing Eq. 4.5

Rewriting Eq. 4.5 to apply to Figure 4.1:

$$\gamma_t = -2RT\ C_o \left(\frac{Dt}{\pi}\right)^{1/2} + \gamma_o$$

$$\text{Limiting slope} = -\frac{2RT}{\pi^{1/2}} C_o (D)^{1/2}$$

$$= -2.8 \times 10^{10} C_o (D)^{1/2}$$

Concentration (C) M x 10^5	Intercepts*	Limiting Slope dyne $cm^{-1} sec^{-1/2}$	$C_o(D)^{1/2} \times 10^{10}$ ± 10% mole $cm^{-2} sec^{-1/2}$
2.04	(9,66)	- 0.67	0.24
4.08	(7.63.5)	- 1.21	0.43
8.16	(4,64)	- 2.00	0.71
20.4	(3,62.5)	- 3.17	1.25
40.8	(3,56.5)	- 5.16	1.85
81.6	(2,55)	- 8.50	3.04

* Other intercept is (0,72)

APPENDIX IV

CHAPTER FIVE

RESULTS

Contents

TABLE IV.1

Dynamic Surface Tension of Sodium Laurate Solutions

t (secs)	Δh (cm)	γ_t (dyne cm^{-1})	t (secs)	Δh (cm)	γ_t (dyne cm^{-1})	t (secs)	Δh (cm)	γ_t (dyne cm^{-1})
			3.5×10^{-3}M, pH 7.6 (natural)					
1.0	10.22	45.3						
0.4	10.20	45.2						
4.3	9.76	43.2						
81.9	9.50	42.1						
62.0	9.44	41.8						
38.9	9.36	41.5						
			3.5×10^{-3}M, pH 9.5					
1.7	13.70	60.7						
3.6	13.30	58.9						
6.1	13.00	57.6						
8.5	13.00	57.6						
> 100	12.58	55.7						

TABLE IV.2

Dynamic Surface Tension of Pine Oil and Pine Oil + Amine Solutions

t (secs)	Δh (cm)	γ_t (dyne cm^{-1})	t (secs)	Δh (cm)	γ_t (dyne cm^{-1})	t (secs)	Δh (cm)	γ_t (dyne cm^{-1})
			PINE OIL 0.02%					
33.8	15.56	68.9	51.0	15.48	68.6	36.2	17.75	68.7
52.3	15.42	68.3	> 5 min	15.24	67.5			
> 3 min	15.26	67.6						
			0.02% PINE OIL + 4.08×10^{-4} M AMINE, NATURAL pH					
3.6	14.50	64.2	35.3	14.06	62.3	11.1	14.08	62.4
31.2	13.98	61.9	70.5	13.60	60.2	47.0	13.76	61.0
63.0	13.56	60.1	166.3	13.26	58.7	155.0	13.38	59.3

BIBLIOGRAPHY

1. Rao, S.R., "Xanthates and Related Compounds", Marcel Dekker, N.Y. 1971, Chap. 7.

2. Overbeek, J.Th.G., de Bruyn, P.L. and Schuhmann, R.Jr., Trans AIME 199, 519 (1954).

3. Aplan, F.F. and de Bruyn, P.L., Trans AIME 226, 235 (1963).

4. Somasundaran, P., ibid 241, 105 (1968).

5. Lin, I.J. and Metzer, A., J. Coll. Interface Sci. 40, 137 (1972).

6. Finch, J.A. and Smith, G.W., Can. Met. Quart. 11(4), 569 (1972).

7. Finch, J.A. and Smith, G.W., J. Coll. Interface Sci. to be published.

8. Smolders, C.A., In "Chem. Phys. and Appl. of Surf. Act. Substances", vol. II (Ed. J.Th.G. Overbeek) Gordon and Breach, Lon., N.Y., Paris 1964, pp.343-349.

9. Murphy, W.J., Roberts, M.W. and Ross, J.R.H., Trans Farad. Soc. (2) 1190 (1972).

10. Minto, R. and Davenport, W.G., Trans IMM 81 C36 (1972).

11. Sandvik, K.L. and Digrè, M., ibid 77 C61 (1968).

12. Taggart, A.F. and Hassialis, M.D., Trans AIME 169, 259 (1946).

13. Tsonopoulos, C., Newman, J. and Prausnitz, J.M., J. Chem. Eng. Sci. 26, 817 (1971).

14. Wark, I.W., J. Phys. Chem. 40, 662 (1936).

15. Rogers, J., Sutherland, K.L., Wark, E.E. and Wark, I.W., Trans AIME 169, 287 (1946).

16. Smith, R.W., ibid 226, 427 (1963).

17. Smith, R.W. and Lai, R.M.W., ibid 235, 413 (1966).

18. Rao, S.R., Private Communication, 1972.

19. Lee, A.F., J.S. Afr. Inst. Min and Metall. 70 94 (1969), Discussion, ibid 71, 77 (1970).

20. Klassen, V.I. and Mokrousov, V.A., "An Introduction to the Theory of Flotation", Butterworths, London, 1963 p. 261-6..

21. Leja, J., Discussion of ref. 17 and author's reply, Trans AIME 238, 189 (1967).

22. Eigeles, M.A. and Volkenkova, V.S., In "Mineral Processing" (Ed. A. Roberts) Pergamon Press, 1965 pp. 513-27.

23. Adam, N.K., "The Physics and Chemistry of Surfaces", Oxford Univ. Press, Oxford, 1941, Chap. III.

24. Moillet, J.L., Collie, B. and Black, W., Surface Activity 2nd Ed., D. Van Norstrand, Princeton, N.J. 1961 pp. 113-131.

25. Lange, H., J. Colloid Sci. 20, 50 (1965).

26. Dupré, A., Ann. Chim. Phys. (4). 7, 406 (1866); 9, 328 (1866).

27. Rayleigh, J.W.S., Proc. Roy. Soc. (London) 47, 281 (1890).

28. Okun, D. and Baers, J.K., ref. 8 pp. 1179-88.

29. Posner, A.M. and Alexander, A.M., J. Coll. Sci. 8, 585 (1953).

30. Harkins, W.D., "The Physical Chemistry of Surface Films", Chap. 2, Reinhold, New York, 1952.

31. Zisman, W.A., In "Contact Angle, Wettability and Adhesion", Chap. 1, Washington, D.C., Am. Chem. Soc. 1964 (Adv. in Chem. Ser. No. 43).

32. Young, T., Phil. Trans. Roy. Soc. p. 84 (1805).

33. Fowkes, F.M., In "Chemistry and Physics of Interfaces", Chap. 1, Am. Chem. Soc., Washington, D.C. 1965.

34. Dann, J.R., J. Coll. Interface Sci. 32, 302 (1970).

35. Rhee, S.K., J. Am. Ceram. Soc. 54, 376 (1971).

36. Smith, H.G., Written Contribution in Discussion of Ref. 112.

37. Gaudin, A.M. and Bloecher, F.W.Jr., Trans AIME 187, 499 (1952).

38. Wada, M., VIII Int. Miner. Process Congr. Leiningrad, 1965 Preprint D-8, p

39. Sandvik, K.L., Discussion of Ref. 4 and author's reply, Trans AIME 241, 341-2 (1968).

40. Pope, M.I. and Sutton, D.I., Powder Techn. 5, 101 (1972).

41. Ter-Minassian-Seraga, L., ref. 31, Chap. 8.

42. Fowkes, F.W., In "Treatise on Adhesion and Adhesives", (Ed. R.L. Patrick) Marcel Dekker, N.Y. 1967, vol. 1 (Theory) Chap. 9.

43. Leja, J. and Schulman, J.H., Trans AIME 199, 221 (1954).

44. Leja, J., Trans IMM 66, 425 (1956/7).

45. Meloy, T.P., In "Froth Flotation" 50th Anniv. Vol. (Ed. D.W. Fuerstenau) 1960, pp. 247-58.

46. Spedden, H.R. and Hannan, W.S.Jr., Trans AIME 183, 208 (1949).

47. Finch, J.A., M.Sc. Thesis, McGill University, 1971.

48. Ginn, M.E., In "Cationic Surfactants" (Ed. E. Jungermann) Marcel Dekker, N.Y. 1970 Chap. 10.

49. Major-Marothy, G., Bull. CIM 60, 1060 (1967).

50. Dean, S.R. and Ambrose, P.M., U.S. Bur. Mines Bull. 449, 1 (1944).

51. Burcik, E.J. and Vaughn, C.R., J. Coll. Sci. 6, 522 (1951).

52. Kloubek, J., Tenside 5, 317 (1968).

53. Partridge, A.C. and Smith, G.W., Trans IMM 80, C199 (1971).

54. Alexander, A.E., Trans. Faraday Soc. 37, 15 (1941).

55. Hansen, R.S. and Wallace, T.C., J. Phys. Chem. 63, 1085 (1959).

56. Hommelen, J.R. and Defay, R., J. Colloid Sci. 14, 401 (1959).

57. Kuffner, R.J., ibid 16, 497 (1960).

58. Fowkes, F.M., J. Phys. Chem. 67, 1094 (1963).

59. Baret, J.F., Armand, L., Bernard, M. and Danoy, G., Trans Faraday Soc. 2439 (1967).

60. Kippenham, C. and Tegeler, D., J. Am. Inst. Chem. Engrs. 16, 314 (1970).

61. Adam, N.K. and Shute, H.L., Trans Faraday Soc. 34, 758 (1938).

62. Brown, A.S., Robinson, R.A., Sirois, E.H., Thibault, H.G., McNeill, W. and Tofias, A., J. Phys. and Colloid Chem. 56, 701 (1952).

63. Kragh, A.M., Trans Faraday Soc. 60, 225 (1964).

64. Schwen, Tenside 3, 69 (1966).

65. Bendure, R.L., J. Coll. Interface Sci. 35, 238 (1971).

66. Austin, M., Bright, B.B. and Simpson, E.A., ibid 23, 108 (1967).

67. Simon, J., Ann. Chim. Phys. 32, 5 (1851).

68. Kloubek, J., J. Coll. Interface Sci. 41, 1(1972); 41, 7 (1972); 41, 17 (1972).

69. Chemical Engineers' Handbook (Ed. Perry, R.H., Chilton, C.H. and Kirkpatrick, S.D.) 4th Edition, Chap. 5.

70. Partridge, A.C., M.Sc. Thesis, McGill University, Montreal 1970.

71. Harwood, J.H. and Ralston, A.W., J. Org. Chem. 12, 740 (1947).

72. Gaudin, A.M., "Flotation" 2nd ed. McGraw-Hill, N.Y. Toronto, London, 1957 pp. 260-77.

73. Burcik, E.J., J. Coll. Sci. 8, 520 (1953).

74. Caskey, J.A. and Barlage, W.B., J. Coll. Interface Sci. 35, 46 (1971).

75. Shedlovsky, L., Annals New York Academy of Sciences, 46, 427 (1946).

76. Powney, J., Trans. Faraday Soc. 31, 1510 (1935).

77. Dibbs, H.P., Sirois, L.L. and Bredin, R., Dept. Energy, Mines and Resources, Mines Branch, Ottawa, Res. Rep. R248, 1972.

78. Fuerstenau, D.W. and Modi, H.J., Trans AIME 217, 381 (1960).

79. Li, H.C. and de Bruyn, P.L., Surface Science 5, 203 (1966).

80. MacKenzie, J.M.W., Minerals Sci. Engng. 3, 25 (1971).

81. Shafrin, E.G. and Zisman, W.A., In "Monomolecular Layers" (Ed. Sobotka, H.) Am. Assoc. Adv. Sci. Wash. D.C. 1954 pp. 129-160.

82. Joy, A.S., Watson, D. and Cropton, R.W.G., Trans IMM 73, 323 (1964).

83. Shergold, H.L. and Mellgren, O., Trans AIME 247, 149 (1970).

84. Hetzfeld, S.H., Corrin, M.L. and Harkins, W.D., J. Phys. and Colloid Chem. 54, 271 (1950).

85. Fuerstenau, D.W. and Yamada, B.J., Trans AIME 223, 50 (1962).

86. Partridge, A.C. and Smith, G.W., Can. Met. Quart. 10, 229 (1971).

87. Belajee, S.R. and Iwasaki, I., Trans AIME 244, 407 (1969).

88. Hendriks, D.W. and Smith, G.W., Can. Met. Quart. 11, 303 (1972).

89. Ghigi, G. and Botre, C., Trans. IMM 75 C240 (1966).

90. Ghigi, G. ibid 77, C212 (1968).

91. Sidgwick, N.V., "The Organic Chemistry of Nitrogen", Clarendon Press, Oxford, 1966 (Eds. Millar, T. and Springall, H.D.) p. 105.

92. Roman, R.J., Fuerstenau, M.C. and Seidel, D.C., Trans AIME 241, 56 (1968).

93. Hoerr, C.W., McCorkle, M.R. and Ralston, A.W., J. Am. Chem. Soc. 65, 328 (1943).

94. Manser, R.M., Rep. LR67 (MST) Warren Spring Lab. Herts. England 1967 24 p.

95. Finch, J.A. and Smith, G.W., Trans IMM 81, C213 (1972).

96. Iwasaki, I., Cooke, S.R.B. and Kim, Y.S., Trans AIME 217, 381 (1960).

97. Iwasaki, I., Cooke, S.R.B. and Colombo, A.F., Rep. Invest. U.S. Bur. Mines 5593, 1960, 25 p.

98. Dunsdale, J.D. and Berubé, Y., Can. Met. Quart. 11, 507 (1972).

99. Reference 20, Chap. 22.

100. Finch, J.A. and Smith, G.W., Paper presented at CIM Conference of Metallurgists, Halifax, N.S. 1972.

101. Fuerstenau, D.W., Trans AIME 208, 1365 (1957).

102. Shubert, H., Freiberger Forschungshefte A335, 51 (1965).

103. Gaudin, A.M. and Fuerstenau, D.W., Trans AIME 202 958 (1955).

104. Mahne, E.J. and Lovell, V.M., Nat. Inst. Met. (S. Afr.) Rep. No. 1026 (1970) 20 p.

105. Cooke, S.R.B. and Digrè, M., Trans AIME 184, 299 (1950).

106. Sun, S.C. and Troxell, R.C., Engng. Min. J. 158, 79 (1957).

107. Last, G.A. and Cook, M.A., J. Phys. and Coll. Chem. 56, 637 (1952).

108. Sagheer, M., Trans AIME 235, 60 (1966).

109. Parekh, B.K. and Aplan, F.F., Presented at 47th Colloid Symposium, Ottawa, Canada, June 1973.

110. Weast, R.C. Ed., Handbook of Chemistry and Physics Edn. 50 Chem. Rubber Co. Cleveland, 1970 F-28.

111. Marchandise, H., Trans IMM 68, 57 (1957).

112. Buckenham, M.H. and Rogers, J., ibid. 64, 11 (1954).

113. Schulman, J.H. and Leja, J., In "Surface Phenomena in Chemistry and Biology" Pergamon, 1958 Chap. 18.

114. Cassie, A.B.D., Dis. Faraday Soc. 3, 11 (1948).

115. Rhee, S.K., J. Am. Ceram. Soc. 55, 157 (1972).

116. Rhee, S.K., ibid 55, 300 (1972).

117. Shafrin, E.G. and Zisman, W.A., J. Phy. Chem. 76, 3259 (1972).

118. Olsen, D.A. and Osterhaas, A.J., ibid. 68, 2730 (1964).

119. Olsen, D.A., Moravec, R.W. and Osterhaas, A.J., ibid. 71, 4464 (1967).

120. Blake, T.D. and Kitchener, J.A., Trans. Faraday Soc., 1435 (1972).

121. Laskowski, J. and Iskra, J., Trans IMM 79, C6 (1970).

122. Rance, R.W., J. Coll. Interface Sci. 41, 588 (1972).

123. Dergaguin, B.V. and Dukhin, S.S., Trans. IMM 70, 221 (1960).

124. Lyman, G., Current research in Mining and Met. Engng., Dept., McGill University.

125. Hansen, R.S., J. Phys. Chem. 64, 637 (1960).

126. Hansen, R.S., J. Coll. Sci. 16, 549 (1961).

127. Ward, A.F.H. and Tordai, L., J. Chem. Phys. 14, 453 (1946).

128. Defay, R., In "Surface and Colloid Science" (ed. E. Matjevic) vol. 3, 1972.

129. Langmuir, I. and Shaefer, V., J. Am. Chem. Soc. 59, 2400 (1937).

130. Davies, J.T. and Rideal, E.K., "Interfacial Phenomena" Academic Press, N.Y., London, 1963 pp. 165-186.

131. Fowkes, F.M., J. Phys. Chem. 66, 385 (1962).

132. Addison, C.C., J. Chem. Soc. 579 (1946).

133. Sandvik, K.L., Lich. Techn. Thesis, Trondheim, Norway 1968.

134. Ruch, R.J. and Bartell, L.S., J. Phys. Chem. 64, 513 (1960).

135. Parker, R.A. and Wasik, S.P., ibid 63, 1921 (1959).

136. Owens, D.K., J. Coll. Interface Sci. 29, 496 (1969).

137. Netzel, D.A., Hoch, G. and Marx, T.I., J. Coll. Sci. 19, 774 (1964).

138. Vandegrift, A.E., J. Coll. Interface Sci. 23, 43 (1967).

139. De Witt, C.C. and Roper, E.E., J. Am. Chem. Soc. 54, 445 (1932).

140. De Witt, C.C. and Makens, R.F., ibid 54, 455 (1932).

141. De Witt, C.C., Makens, R.F. and Helz, A.W., ibid 57, 796 (1935).

142. Ref. 20 p. 80.

143. Elligani, D.A. and Fuerstenau, M.C., Trans AIME 241, 437 (1968).

144. Majima, H. and Takeda, M., ibid 241, 431 (1968).

145. Granville, A., Finkelstein, N.P. and Allison, S.A., Trans IMM 81, C1 (1972).

146. Fuerstenau, M.C., Huiatt, J.L. and Kuhn, M.C., Trans AIME 250, 227 (1971).

147. Cante, C.J., McDermott, J.E. and Saleeb, F.Z., Presented at 47th Colloid Symposium, Ottawa, June 1973.

148. Somasundaran, P. and Moudgil, B.M., ibid.

149. Gibbs, J.W., "Collected Works" 1, 301 N.Y. Longmans, Green and Co., 1928.

150. Marangoni, C., Nuovo cimento (3) 3, 97 (1878).

151. Bikerman, J.J., "Foams: Theory and Industrial Applications" Chap. 9, Reinhold Publ. Corp., N.Y. 1953.

152. Jones, T.G., Durham, K., Evans, W.P. and Camp, M., In "Gas/Liquid and Liquid/Liquid Interfaces", Proc. 2nd Int. Congress on Surface Activity I, Butterworths, London 1957, p. 225.

153. Dervichian, G., Bull. Soc. chim. Fr. 15 (1956).

154. Donnan, F.G., Chemistry and Industry 42, 902 (1923).

155. Hommelen, J.R., J. Coll. Sci. 14, 385 (1959).